THE JOURNAL
OF
CHEMICAL PHYSICS

VOLUME 3 OCTOBER, 1935 NUMBER 10

The Pressure-Volume-Temperature Relations of the Liquid, and the Phase Diagram of Heavy Water

P. W. BRIDGMAN, *Research Laboratory of Physics, Harvard University*

(Received July 11, 1935)

The pressure-volume-temperature relations of both liquid D_2O and H_2O are measured between $-20°$ and 95°C and up to 12,000 kg/cm², and the transition parameters of the liquid and solid modifications of D_2O in the range between $-60°$ and $+20°$C and up to about 9000 kg/cm². An unstable modification of solid D_2O, for which the designation IV is proposed, is found in the field of stability of V. Reference to the original work on H_2O shows that the corresponding modification of H_2O also exists. In general the properties of H_2O and D_2O covered by these measurements are very much alike, and differ in the direction suggested by the greater zero-point energy of H_2O: the molar volume of D_2O is always greater than that of H_2O at the same pressure and temperature, and the transition lines of D_2O always run at higher temperatures. In finer detail, however, the differences between the two waters do not vary regularly, and probably other considerations than of zero-point energy alone are necessary for a complete explanation.

THE following measurements of some of the simpler properties of heavy water under pressure were made on 99.9 percent heavy water which I obtained through the courtesy of Professor Urey. My conventional high pressure apparatus was used in the measurements; the pressure range was up to 12,000 kg/cm² and the temperature range from $-60°$ to $+95°$C.

PRESSURE-VOLUME-TEMPERATURE RELATIONS OF THE LIQUID

The measurements of the volume of the liquid as a function of pressure and temperature were made by the sylphon method fully described in other places.[1] A new sylphon was used, calibrated as usual. Since the principal interest of these measurements is in the difference between the properties of ordinary and heavy water rather than in the absolute values, the compressibility of ordinary water was redetermined in the same sylphon and with all other parts of the set-up unchanged. The order of the measurements was as follows: first, measurements with H_2O at $0°$, $-5°$, $-10°$, $-15°$, $-20°$, and check at $0°$; second, measurements with D_2O at $+30°$, $0°$, $-5°$, $-11°$, $-16°$, $+52.5°$, $+75°$, $+95°$ and check at $30°$; and third, measurements with H_2O again at $+52.5°$, $+95°$, and $0°$. The smoothness of functioning of the apparatus can be estimated from a comparison of the volumes of H_2O at $0°$ with the two fillings of the sylphon. The maximum discrepancy between the two determinations of the volume was at 4000 kg, where the first run gave 15.875 for the molar volume and the second run 15.892. At 6000 kg the difference between the two runs had dropped from 0.017 to 0.009. In calculating the volumes listed in the tables the first step was, in principle, to draw smooth curves through the experimental points at each constant temper-

[1] P. W. Bridgman, Proc. Am. Acad. **66**, 185 (1931); **68**, 1 (1933).

TABLE I. *Molecular volume of liquid D_2O.*

PRESSURE (kg/cm²)	−20°	−15°	−10°	−5°	0°	20°	40°	50°	60°	80°	100°
1					18.122	18.125	18.200	18.270	18.363	18.570	
500					17.692	17.739	17.835	17.904	17.985	18.174	18.400
1000				17.308	17.328	17.404	17.512	17.585	17.665	17.850	18.048
1500			16.974	16.994	17.014	17.110	17.235	17.306	17.385	17.562	17.753
2000		16.660	16.685	16.712	16.741	16.854	16.982	17.054	17.130	17.302	17.486
2500	16.380	16.410	16.440	16.468	16.501	16.620	16.751	16.827	16.905	17.067	17.250
3000	16.155	16.188	16.221	16.255	16.287	16.411	16.543	16.617	16.693	16.850	17.028
3500		15.987	16.025	16.061	16.094	16.215	16.353	16.428	16.503	16.657	16.824
4000		15.807	15.843	15.879	15.915	16.040	16.178	16.252	16.330	16.477	16.634
5000				15.567	15.600	15.730	15.870	15.949	16.015	16.150	16.310
6000					15.352	15.465	15.597	15.671	15.740	15.875	16.023
7000						15.215	15.358	15.427	15.494	15.625	15.763
8000						15.001	15.140	15.207	15.272	15.402	15.533
9000						14.803	14.944	15.010	15.074	15.198	15.328
10000							14.767	14.827	14.885	15.007	15.137
11000							14.606	14.663	14.718	14.835	14.961
12000							14.452	14.508	14.563	14.677	14.807

TABLE II. *Molecular volume of liquid H_2O.*

PRESSURE (kg/cm²)	−20°	−15°	−10°	−5°	0°	20°	40°	50°	60°	80°	100°
1					18.018	18.048	(18.157)	(18.233)	(18.323)	(18.539)	(18.800)
500					17.601	17.690	17.800	17.865	17.941	18.129	18.345
1000				17.234	17.251	17.352	17.485	17.554	17.630	17.805	18.002
1500		16.880	16.898	16.924	16.951	17.072	17.204	17.275	17.352	17.518	17.701
2000	16.579	16.600	16.624	16.658	16.684	16.805	16.949	17.025	17.100	17.262	17.437
2500	16.324	16.357	16.389	16.423	16.452	16.573	16.722	16.796	16.871	17.030	17.195
3000		16.140	16.173	16.213	16.241	16.366	16.514	16.587	16.661	16.816	16.977
3500		15.948	15.982	16.019	16.050	16.185	16.326	16.397	16.469	16.620	16.776
4000			15.802	15.843	15.875	16.012	16.152	16.224	16.294	16.440	16.589
5000			15.486	15.532	15.564	15.698	15.847	15.918	15.986	16.122	16.265
6000					15.293	15.430	15.575	15.645	15.712	15.842	15.982
7000							15.340	15.405	15.469	15.599	15.730
8000							15.125	15.188	15.249	15.374	15.501
9000							14.930	14.990	15.050	15.172	15.295
10000							14.748	14.807	14.866	14.985	15.106
11000							14.575	14.636	14.695	14.812	14.930
12000							14.422	14.480	14.538	14.653	14.771

ature, and then to compute and tabulate the volume at regular pressure intervals from each of these curves. The graphical representation used was on a very large scale. To give greater accuracy, not the actual observations were plotted, but the difference between the actual observations and points computed by a simple logarithmic formula with two constants that could be so adjusted as approximately to fit the experimental curve over the entire range. At each constant pressure of this first tabulation curves were then drawn, also on a very large scale, giving volume as a function of temperature, and from these curves were constructed the final Tables I and II, of volume at regular intervals of pressure and temperature.

The quantities of water used in filling the sylphon, which were of the order of 5 grams, were determined by weighing. The density of H_2O at atmospheric pressure was taken from *International Critical Tables*. The molecular volume of D_2O was based on the value of Taylor and Sherwood[2] for the molecular volume at 25°, 18.127. The values at other temperatures below this were obtained by combining this value with the values of Lewis and Macdonald[3] for the thermal expansion. The molecular volumes at higher temperatures at atmospheric pressure were obtained directly from the sylphon readings; these are not as accurate as the values under higher pressures, the sylphon not being particularly well adapted to readings at low pressures.

THE PHASE DIAGRAM OF THE SOLIDS

The method and the apparatus were very similar to those used for the corresponding measurements of H_2O in 1912.[4] The D_2O, about 13.5 grams in amount, was placed in a steel shell, completely surrounded by the pressure

[2] H. S. Taylor and P. W. Sherwood, J. Am. Chem. Soc. **56**, 998 (1934).
[3] G. N. Lewis and R. T. Macdonald, J. Am. Chem. Soc. **55**, 3057 (1933).
[4] P. W. Bridgman, Proc. Am. Acad. **47**, 441 (1912).

TABLE III. *Parameters of the transition lines of D_2O.*

Pressure (kg/cm²)	Temperature (°C)	$\frac{d\tau}{dp}$	Volume Change (cm³/mole)	Latent Heat (kg cm/mole)	Latent Heat (cal/mole)
		L–I			
0	+ 3.82	−.00665	1.56	−65,000	−1523
400	+ 0.82	823	1.79	59,600	1396
800	− 2.74	950	2.01	57,000	1335
1200	− 6.76	1055	2.23	56,300	1319
1600	−11.14	1135	2.45	56,600	1326
2000	−15.82	1195	2.64	56,800	1331
2400	−20.70	1238	2.77₄	56,600	1326
		III–L			
2200	−18.90	.00409	0.860	53,500	1253
2600	−17.37	356	.730	52,400	1228
3000	−16.04	310	.620	51,400	1204
3400	−14.90	268	.530	51,100	1197
3800	−13.96	230	.460	51,800	1214
		IV–L			
4000	−17.90	.00946	1.710	46,100	1080
4500	−13.40	856	1.633	49,600	1162
5000	− 9.30	790	1.556	52,000	1218
5500	− 5.50	736	1.478	53,700	1258
		V–L			
3000	−18.90	.00812	1.647	51,500	1206
3500	−14.98	.00754	1.498	51,300	1202
4000	−11.34	.00698	1.372	51,500	1206
4500	− 7.99	642	1.264	52,200	1223
5000	− 4.91	590	1.173	53,300	1249
5500	− 2.09	546	1.095	54,400	1274
6000	+ 0.57	514	1.026	54,600	1279
6500	+ 3.08	494	0.967	54,100	1267
		VI–L			
5000	−10.01	.00936	1.920	54,000	1265
5500	− 5.40	914	1.825	53,500	1253
6000	− 0.91	880	1.738	53,800	1260
6500	+ 3.41	848	1.659	54,100	1267
7000	7.57	812	1.589	54,900	1286
7500	11.53	769	1.528	56,500	1324
8000	15.26	721	1.475	59,000	1382
8500	18.74	668	1.430	62,500	1464
		I–III			
2250	−20.0	−.270	−3.553	3,330	78
2285	−30.0	−.270	3.503	3,150	74
2325	−40.0	−.270	3.453	2,980	70
2360	−50.0	−.270	3.403	2,810	66
		I–II			
2295	−30.0	.1815	−3.950	5,290	124
2240	−40.0	.1815	3.925	5,040	118
2185	−50.0	.1815	3.900	4,790	112
		II–III			
2400	−29.69	.01137	0.431	9,200	216
2800	−26.08	775	.380	12,100	283
3200	−23.40	605	.344	14,200	333
3600	−21.20	520	.313	15,200	356
		II–V			
3540	−21.5	−.0124	−0.712	14,500	340
3800	−24.7	−.0124	0.712	14,300	335
		III–V			
3555	−14.5	.468	− .985	−540	− 12.7
3540	−21.5	.468	−1.029	−560	− 13.1
		IV–VI			
5410	− 6.2	.94	0.352	−100	− 2.3
5402	−14.0	.94	0.310	−100	− 2.3
		V–VI			
6405	+ 2.6	1.90	0.696	100	2.3
6401	− 5.0	1.90	0.670	95	2.2

transmitting medium, in the lower cylinder, the temperature of which was thermostatically controlled, and which was varied for these measurements from +20° to −60°. The phase diagram was not followed beyond +20° and 8600 kg because I did not want to risk the loss of such a large quantity of D_2O; there is, however, no reason to think that there are any significant features beyond the range actually covered. The bath for temperatures below 0° was ethyl alcohol, about five gallons in amount, into which the temperature regulating arrangement admitted, when necessary, a stream of alcohol from a reservoir maintained at −75° by solid CO_2. The commercial availability of solid CO_2 made the low temperature manipulations very much more convenient than in 1912. The lower cylinder connected through a heavy pipe with the upper cylinder, maintained at room temperature, in which was situated the manganin gauge. The position of the piston by which pressure was generated in the upper cylinder was read to 0.0001 inch by two Ames dial gauges, so mounted as to compensate for any slight warping of the press. The position of the piston was determined at constant bath temperature as a function of pressure; a phase change is shown by a discontinuity in the position of the piston. The change of volume is determined at once by the amount of the discontinuity and the cross section of the piston. The cross section has to be corrected for the elastic stretch of the cylinder under pressure. This correction was calculated from the elastic constants; it is proportional to the pressure and at 10,000 kg is 1.35 percent. There is in addition a correction for the thermal expansion of the transmitting liquid, isopentane, on passing, during a phase change, from the temperature of the lower to that of the upper cylinder.

A few of the changes of volume, on the II–III

and the II–V curves, were determined by the method of varying bath temperature and plotting pressure against temperature at constant volume. This change in procedure was made necessary by the smallness of these volume changes; the method was essentially the same as followed in the previous work on H_2O.

A special apparatus was made for the determination of the points on the freezing curve of the ordinary ice between 0° and +3.82°, since the high pressure apparatus is not sensitive in this range. This special apparatus was constructed of mild steel and was the same in principle as the other. Pressure was read on a Bourdon gauge, calibrated against an absolute free piston gauge. Two independent determinations of the freezing pressure at 0.00° were 496 and 497 kg/cm². In computing the results, the slope of the upper end of L–I curve, between 0° and +3.82°, was so determined as to be consistent with this value, 496.5, for the melting pressure; the other two points at +2° and +3° were not quite so regular, perhaps because of inferior temperature control.

The measurements were completed without accident, with a single set-up of the apparatus for all the points above 500 kg, and with a single set-up of the special low pressure apparatus for all the points below 500 kg. There was no perceptible rounding of the corners of the melting curves, indicating adequate purity. The equilibrium points (temperature as a function of pressure) are shown in Fig. 1. In Fig. 2 are shown the corresponding changes of volume, in

TABLE IV. *Triple points of the system water-ices.*

	D_2O					H_2O				
PHASES	PRESSURE (kg/cm²)	TEMP. (°C)	VOLUME CHANGE (cm³/mole)	LATENT HEAT (kg cm/mole)	LATENT HEAT (cal/mole)	PRESSURE (kg/cm²)	TEMP. (°C)	VOLUME CHANGE (cm³/mole)	LATENT HEAT (kg cm/mole)	LATENT HEAT (cal/mole)
				L–I–III						
L–I	2245	−18.75°	2.713	−56,600	−1326	2115	−22.0°	2.434	−43,100	−1010
III–L			.847	53,300	1249			.839	39,100	916
III–I			3.560	− 3,300	− 77			3.273	− 4,000	− 94
				L–III–V						
III–L	3555	−14.5°	.498	50,900	1192	3530	−17.0°	.434	47,100	1103
V–III			.985	500	12			.985	700	17
V–L			1.483	51,400	1204			1.419	47,800	1120
				L–IV–VI						
IV–L	5410	− 6.2°	1.492	53,500	1253					
VI–IV			.352	100	2.3					
VI–L			1.844	53,600	1255					
				L–V–VI						
V–L	6405	+ 2.6°	.978	54,100	1267	6380	+ 0.16°	.949	53,800	1260
VI–V			.696	− 100	− 2.3			.700	150	4
VI–L			1.674	54,000	1265			1.649	53,950	1264
				I–II–III						
III–I	2290	−31.0°	3.498	− 3,100	− 73	2170	−34.7°	3.532	− 1,700	− 40
II–III			.449	8,400	197			.387	9,400	220
II–I			3.947	5,300	124			3.919	7,700	180
				II–III–V						
II–III	3540	−21.5°	.317	15,100	353	3510	−24.3°	.261	13,000	304
V–II			.712	−14,600	− 342			.721	−12,300	− 288
V–III			1.029	500	11			.982	700	16

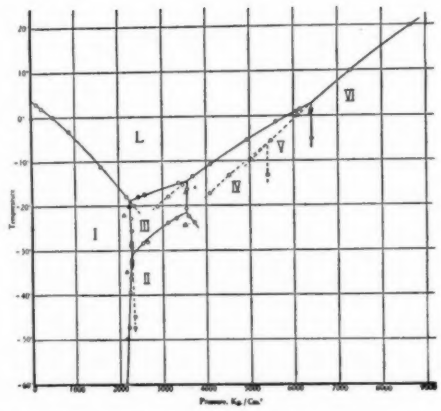

FIG. 1. The transition lines of the system D_2O. Prolongations of transition lines into regions of instability are dotted. Observed points are shown by circles. The triangles are the triple points in the H_2O system.

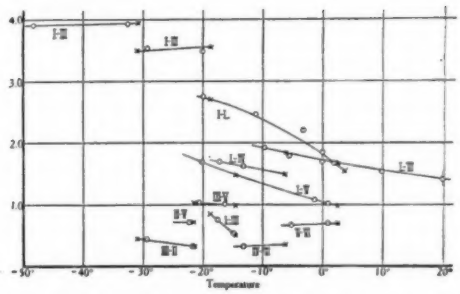

FIG. 2. The change of volume for the various transitions of the D_2O system, plotted as ordinates in cm^3 per mole, against temperature as abscissa. The observed values are shown as circles; the crosses are the values computed at the triple points.

cm^3 per mole, as a function of temperature on the transition lines. The smoothed results are given in Table III; this table gives the pressure-temperature coordinates, the volume difference, the slope $d\tau/dp$ of the transition line, the latent heat of the transition, the latter calculated by Clapeyron's equation and this latent heat in calories per mole calculated with the conversion factor, 1 kg cm = 0.02343 mean calorie. In finding the smoothed results there are several conditions that must be met at the triple points of which there are six: namely, the three independently determined transition lines must pass through a common point, the three independently determined changes of volume must satisfy the additive relation, and the calculated latent heats must also satisfy the additive relation. These three conditions are so interrelated as to leave very little freedom in drawing the best curves through the experimental points, the latent heats being determined by the slopes which are tied down by the conditions that the curves pass through a triple point. One may therefore feel considerable confidence in the results, since any important error would be expected to manifest itself in the impossibility of satisfying the triple point conditions. In Table IV are collected the triple points parameters, with the values for H_2O also given for comparison.

The qualitative characteristics of the transitions are very much like those of H_2O. Perhaps the most striking characteristic is the enormous velocity of the transitions between the solid phases I–III, III–V and V–VI at the upper end of the range, immediately below the triple points with the liquid, and the enormously rapid decrease of this velocity with falling temperature. The phenomena with regard to subcooling and prolongation of transition lines into regions of instability are essentially the same as for H_2O; as indicated in Fig. 1 the line L–I may be unstably prolonged into the region of instability of III, the line L–V into the region of III, the line L–VI into that of IV or V, and I–III into that of II. The reluctance of V to appear from the liquid phase is again noteworthy, making possible the very marked extension of the L–VI line into the region of V. But just as in the case of H_2O, if V had been recently present in the apparatus it was easy to make it appear again, even if in the meantime the system had been completely melted. The probable explanation is the persistence in the liquid phase of some sort of nuclei from which V is readily formed. A difference compared with the H_2O system is that the prolongation of the I–III line into the region of II apparently does not have a vertical tangent; in fact the I–III line is straight within the limits of error instead of being markedly curved toward the temperature axis as in the H_2O system.

In one important respect Fig. 1 differs from the phase diagram published for H_2O, namely, in the presence of the phase IV and the two transition lines L–IV and IV–VI. IV is totally unstable with respect to V, and once V has been produced, IV disappears. IV was found in the early part of these measurements, after the determination of points on the L–VI line at 0° and +10°, and before V had yet appeared. The

first point found involving IV was on the IV–VI line. Since there was no analog for this in the diagram of H_2O, it appeared at first as if the phase diagram of D_2O must be entirely different from that of H_2O, and for a while there was considerable confusion in identifying the transitions as they were found. The confusion was increased by the fact that the melting line L–IV is not greatly different from the unstable prolongation of L–VI. The decisive factor in fixing the identification was the volume changes, the change L–IV plus IV–VI adding to L–VI, as it should, and the change L–IV being markedly different from L–VI.

After the phase diagram of D_2O was completed it was found on consulting again the original work on H_2O that the phase IV had also been found in the H_2O system, and in fact on page 529 of my 1912 paper will be found an explicit statement of the probability of the existence of another unstable form. The existence of this form was made probable both by the location of the pressure-temperature points, and by the values of the change of volume. The reason that the existence of the phase was not regarded as a certainty and the phase listed in the final results was that the transition IV–VI was not found. With the discovery of this transition for D_2O, however, the whole situation is cleared up, and the phase diagrams of D_2O and H_2O appear very similar in all respects.

The designation IV is given to the new unstable phase, thus completing the sequence I to VI. When I chose the designations V and VI for the new high pressure ices beyond II and III, which had been previously found and named by Tammann, I left the designation IV blank because of uncertainty with regard to some unstable forms, the existence of which was suspected by Tammann. None of the suspected forms of Tammann have turned up, however, in the 40 years or more since he did his work, so that there seems no reason for holding this designation open any longer, and it is now employed to complete the scheme of nomenclature.

Discussion

Accuracy of the results

The absolute accuracy of the volumes of the liquid phase listed in Tables I and II is not as high as could be desired for a substance like water for which very slight departures from regularity are significant in disclosing conditions of varying association. Five different determination of the p–τ–v surface of liquid H_2O have now been made in this laboratory, either by myself or by others using my apparatus, utilizing three different methods: the Aimé piezometer, the piston displacement method, both in 1912,[4] and the sylphon method in 1931,[5] 1934,[6] and now again in 1935. The maximum discrepancy between any of these determinations at any pressure is about 0.002 on the relative volume; for example, for the relative volumes at 3000 kg and 0° the values 0.901 and 0.899 occur. The maximum discrepancy occurs at an intermediate pressure and tends to become less at the highest pressures. A great deal more work would be necessary before the p–τ–v surface of water is known with an accuracy corresponding to the accuracy of our knowledge of volume as a function of temperature at atmospheric pressure. With regard to the values below 0°, this is the first time since 1912 that the volume has been measured in this region. The results now found do not check in fine detail with those found before; in particular the minimum and maximum of volume as a function of temperature on the isobar at 1500 kg found in 1912 and shown in Fig. 40 of the 1912 paper, has not been found this time. Irregularities are now found suggesting the maximum and minimum, but not so pronounced. The sylphon method is not particularly accurate at the lower pressures, and in the present case suffers from the additional disadvantage that it is not safe to carry the liquid into the subcooled region because of danger of destroying the sylphon if freezing should occur. The measurements of 1912 represent considerable excursions into the subcooled regions, so that the chance of losing a maximum or minimum by the smoothing process at the end of the range was less. On the other hand, these new measurements, both on H_2O and D_2O, are the first in which the same apparatus and the same filling of the apparatus has been used to make measurements both above and below 0°. The present

[5] Second part of reference 1.
[6] P. W. Bridgman and R. B. Dow, J. Chem. Phys. 3, 35 (1935).

measurements should give a more reliable picture of the complete range of the phenomena than the former measurements. Further, the present measurements should give considerably greater accuracy for the comparative volumes of H_2O and D_2O than can be claimed for the absolute accuracy of either. In making any comparative study of the properties of D_2O and H_2O from the volumes of Tables I and II it must be remembered that the volumes of H_2O at 0°, 50°, and 100° are doubtless somewhat more accurate than the values at 20°, 40°, 60°, and 80°, since the observations were made only at 0°, 52.5°, and 95°, and the volumes at other temperatures were obtained by a graphical interpolation, which may have been subject in some cases to slight doubt because of lack of linearity. The measurements for D_2O on the other hand, were made at four temperatures above 0°, and so the interpolation is more certain.

The accuracy of the phase diagram is perhaps sufficiently indicated by the smoothness of the experimental points in Figs. 1 and 2. All the p–τ points obtained are shown, but not all the Δv points, since a perfectly satisfactory value of Δv cannot be obtained unless the transition is allowed to run to completion in both directions, and this was frequently inconvenient, either because of slowness of the transition, as on the lower end of the I–II and I–III lines, or because of the probability of completely losing one of the phases, as at some points on the melting curves of III and V. The measurements of the volume changes of the two transitions I–II and I–III were the most difficult, and are open to the greatest possibility of error. In the tables more significant figures are given for the temperatures, for $d\tau/dp$, and sometimes for Δv than are justified by the direct measurements. However, the differences of temperature and pressure could often be obtained with a greater accuracy than the absolute values themselves. Furthermore, the conditions at the triple points give a greater certainty than could be obtained from the absolute values; the values listed in the tables with a greater number of significant figures than apparently are justified have been smoothed and adjusted to satisfy the conditions at the triple points and give relative accuracy of the order suggested.

A word should be said about the normal melting parameters of D_2O. The melting temperature (triple point with the vapor) was taken as 3.82°, as given by Bartholomé und Clusius.[7] The latent heat given above, 64,950 kg cm per mole is equivalent to 1523 g cal. per mole, against 1522 recently determined by Bartholomé and Clusius. The agreement is in part fortuitous, since my measurements could hardly distinguish between a volume change at atmospheric pressure of 1.56 (the value used) and 1.57. Bartholomé and Clusius quote in their paper for the volume change 1.58, determined by Megaw from measurements of the lattice spacing in the crystals by x-rays.

Relative behavior of D_2O and H_2O

The molecular volume of liquid D_2O is greater at all pressures and temperatures than that of H_2O at the same pressure and temperature. This is consistent with the frequently expressed idea that "association" is greater in liquid D_2O than H_2O. The general tendency is for the volume excess to become less with both rising temperature and pressure, the maximum difference, 0.104, occurring at 0°C and atmospheric pressure. This again is what would be expected, because it is known that H_2O becomes more normal both with increasing temperature and pressure. However, the details of the variation of the volume excess are not altogether regular. If the excess is plotted as a function of pressure at constant temperature, a flat minimum will be found at the higher temperatures, the pressure of the minimum rising with increasing temperature. Thus at 40° the minimum is about 0.015 at 8000 kg, while at 100° the minimum is 0.030 at 10,000 or 11,000 kg. On the other hand, if the excess is plotted as a function of temperature at different constant pressures, a minimum will be found not far from 40° at all pressures up to about 8000, the depth of the minimum decreasing to about 0.015 at 8000, but beyond 8000 the temperature of the minimum increases to perhaps 70° at 12,000, where the depth of the minimum is of the order of 0.025. This complication in fine detail is doubtless indicative of slight differences

[7] E. Bartholomé and K. Clusius, Zeits. f. physik. Chemie **B28**, 167 (1935).

in the details of the "association." This is further indicated by the fact that the greatest departures from smoothness in the isotherms of H_2O are found in the general neighborhood of 0° and at low pressures, whereas the greatest irregularities in liquid D_2O are found at 5000 kg in the neighborhood of 50°.

Perhaps the most sweeping characterization that can be made with regard to the phase diagrams is that the triple points in the D_2O diagram all occur at higher temperatures, and the transition lines, except those running approximately vertical, all run at higher temperatures than in the H_2O diagram. This is what would be expected in view of the usual explanation of the higher melting point of D_2O in terms of its lower zero-point energy; the ν_0 of D_2O is less than that of H_2O in consequence of the greater mass of the D_2O molecule, so that a greater temperature energy must be added to shake the molecule of solid D_2O out of its trough into the liquid phase, the implication being that zero-point energies have largely disappeared in the liquid phase. This explanation demands the approximate equality of the specific heats of solid D_2O and H_2O, and this does seem to be the fact experimentally.

Going now to finer details of the phase diagrams, the differences at the triple points are not uniform, but in general the differences become less at higher pressures. Thus the excesses of the absolute temperatures of transition in the D_2O system over the H_2O system for the successive triple points L–I–Vap, L–I–III, L–III–V, and L–V–VI are, respectively, 1.40, 1.40, 1.02 and 0.86 percent. The variations of the ratio of pressures at the triple points are greater than the variations of temperature; the pressure in the D_2O system is always greater, the excess varying from 6.0 percent at the I–II–III triple point to only 0.31 percent at the L–V–VI triple point. The fact that the variations of pressure and temperature at the triple points are irregular shows that there can be no law of corresponding states for corresponding phases in the two systems. This is perhaps not surprising when the liquid phase is involved, but one might perhaps expect a closer approximation in the solid phases. The pressure in the D_2O system exceeds that in the H_2O system at the I–II–III triple point by 6 percent, whereas at the II–III–V triple point the excess is only 1.14 percent.

The latent heat of melting of all the ices at the low pressure end of the range is greater in the D_2O system than in the H_2O system. The sign of the difference is again what would be expected in view of the difference of zero-point energies discussed above; the magnitude of the difference is, however, somewhat surprising. The melting heat of I at the triple point with the vapor is 6 percent greater in the D_2O system than in H_2O. This difference rapidly increases with increasing pressure along the melting curve of I, and at the triple point L–I–III the excess of latent heat in the D_2O system has become 31 percent. At the same triple point the latent heat of L–III is 37 percent greater for D_2O than for H_2O. This marks the extreme—from here on with increasing pressure the differences become smaller, until at the L–V–VI triple point the latent heats in the two systems are the same within experimental error. Exact equality of the latent heats in the two systems would not be expected according to the simple zero-point energy explanation, for ice VI in the two systems must differ in the same direction with regard to zero-point energy as ice I. Another consideration also suggests that other factors besides zero-point energy must be of importance, because it is usual experience that those substances with the higher natural frequency (higher characteristic temperature) have the higher melting temperatures, whereas here it is the D_2O system, with the lower natural frequency, which has the higher melting temperature.

The relative volume changes in the two systems are significant. In general, the volume change on melting is greatest in the D_2O system; it is greater by about 4 percent at the atmospheric melting point, increases to about 12 percent at the L–I–III triple point, and from here decreases with increasing pressure, remaining 1.5 percent for VI–L at the L–V–VI triple point. In finer detail, the difference of volume between VI and the liquid in the H_2O system when plotted against temperature is concave toward the temperature axis up to 20°. This is abnormal. Above 20°, the curvature reverses, and H_2O becomes convex toward the temperature axis like other liquids. The abnormality does

not occur at all in the D_2O system, but the difference of volume between L and VI is convex toward the temperature axis over the entire measured range. The situation is reversed with regard to the phase I. In the H_2O system Δv is linear against temperature, whereas in the D_2O system it is abnormally concave toward the temperature axis. It is to be questioned, however, whether H_2O is not really more abnormal on its L–I line than D_2O, since the numerical magnitude of the variation of Δv is very much greater in H_2O. An accompaniment of this is a much greater variation of the latent heat along the L–I line for H_2O than for D_2O.

The greatest qualitative difference with regard to volume is shown by the phases I and III. At the triple point L–I–III the decrease of volume when I changes to III is 9 percent greater in the D_2O system, whereas at the I–II–III triple point, only 12° lower, it is 1 percent less. The variation is perhaps in small part due to experimental error, the volume determinations on the I–III line being the most uncertain of the measurements, but the triple point conditions did not seem to allow any important divergence from the values given, and the difference must be mostly real.

The conclusion seems forced, I believe, by this detailed examination of the differences in the two systems that abnormalities occur not only in the liquid but also in the solid phases, and particularly in the phases I and III. In fact, I have been of the opinion ever since making the original measurements in 1912 on the H_2O system that the p–τ–v surface of ice I would be found to deviate markedly from that of a normal solid, particularly in the neighborhood of the L–I–III triple point. This subject has never been investigated experimentally, and would, I believe, be well worth while. Measurements should be made if possible on single crystals. Not only is it highly probable that the ices I and III are abnormal, but the abnormalities must differ in the D_2O and the H_2O systems. More elaborate considerations than simply zero-point energy appear to be necessary to satisfactorily explain the situation.

I am indebted to my assistant, Mr. L. H. Abbot, for making all of the readings with the sylphon and many of the readings of the transitions. I am also indebted for financial assistance to the Joseph Barrett Daniels Fund of Harvard University and to the Rumford Fund of the American Academy of Arts and Sciences.

OCTOBER, 1935 JOURNAL OF CHEMICAL PHYSICS VOLUME 3

Precision Determination of Lattice Constants

ERIC R. JETTE AND FRANK FOOTE, *School of Mines, Columbia University*

(Received June 28, 1935)

In Part I the theoretical and experimental conditions which must be satisfied in order to determine lattice constants with a precision of a few parts per hundred thousand are discussed with particular application to the symmetrical focusing type of camera. Cohen's method of calculation of lattice constants for the elimination of "drift" and experimental errors is applied. Methods are developed for the evaluation of standard errors and fiduciary limits of results from a single film and from a set of films. The usefulness of x-ray targets made of alloys rather than pure elements for the purpose of securing a larger number and better distribution of lines is indicated. The influence of the number and Miller indices of diffraction lines on the values of lattice constants in noncubic systems is shown. The importance of the methods of sample preparation for precision work is emphasized. In Part II, precision measurements on Al, Ni, Ag, Au, Si, Fe, Mo, W, Mg, Zn, Cd, Sb, Bi and Sn are reported for materials of a high degree of purity. The fiduciary limits of these lattice constants vary between 2 and 7 parts per hundred thousand and are so chosen that the probability of the correct value lying between the stated limits is 19 out of 20.

Part I. Theoretical and Experimental Conditions

INTRODUCTION

DURING the last few years the determination of precise values of lattice constants has become more and more important. In many cases the problem consists mainly in determining comparatively small changes in lattice constants due to changes in the compositions or nature of the sample investigated. This is the case in one

of the most important fields of x-ray investigation, namely, the study of solid solutions and solubility limits in the solid state. Since the nature of the x-ray technique is such as to preclude the direct determination of these differences, it is necessary to obtain the individual values of the lattice constants with a precision of 0.01 percent or better.

The precision problem in this field may be divided into four distinct but equally important parts. (A) A theoretical study of the diffraction camera used to discover the sources of error inherent in it and their possible magnitude. (B) The development of an adequate method of calculating the experimental results. (C) The development of an experimental technique which in view of the preceding is capable of yielding results of high precision. (D) The development of a technique of preparing the samples to be measured so that it is worth while to apply the precision x-ray technique.

We shall confine our attention to measurements made on finely divided material by means of the so-called focusing type cameras of the symmetrical type which have the advantage of not requiring the use of a calibrating substance.[1]

A. Errors Inherent in the Symmetrical Focusing Camera

The principle on which the focusing camera depends[2] demands that the slit (or in some constructions the focal spot of the x-ray tube), the sample and the film be located on the same circumference and that the part of the sample exposed be very narrow in the direction parallel to the cylinder axis of the camera. These conditions can never be completely satisfied. In addition, the fact that photographic film must be used introduces an error due to film shrinkage which our experience indicates cannot be completely eliminated by the use of fiducial points. Further, if the camera is to be used as an absolute instrument and thus be free from the use of calibrating substances, the lattice constants will be subject to errors in measuring the camera radius. Finally, of course, errors of the ordinary accidental sort in determining the line positions will occur.

These errors just enumerated have been described in the articles by Saini[3] and Cohen[4] so that detailed discussion of them are unnecessary here. The systematic errors may be combined in the following equation

$$\Delta \sin^2\theta=\left(\frac{\Delta S}{L}+\frac{\Delta R_3-\Delta R_1}{R}\right)\phi \sin 2\phi+\left(\frac{\Delta R_2-\Delta R_3+k_4\Delta R_4}{4R}+\frac{1}{4}\left(\frac{h}{R}\right)^2\right)\tan 2\phi \sin 2\phi, \qquad (1)$$

where L = measured distance between reflections from the same plane on the opposite sides of the film;
R = camera radius
θ = glancing angle from a plane of indices hkl
$\phi=\pi/2-\theta=L/8R$
ΔS = error in shrinkage correction applied
ΔR_1 = error in measuring camera radius
ΔR_2 = error due to sample being off the circumference
ΔR_3 = error due to film being off the circumference
$k_4\Delta R_4$ = error due to thickness of sample, k_4 is not known
h = vertical divergence of beam.[4]

The accidental errors in determining the line position may be expressed by the equation

$$\Delta \sin^2\theta=(\Delta L/L)\phi \sin 2\phi. \qquad (2)$$

An exhaustive and laborious investigation in this laboratory has shown (1) that while some of the values for the individual errors may be estimated with a fair degree of assurance, others cannot, (2) that there is no way of predicting as to either quantity or sign the resultant effect of the errors on an individual film, (3) that with the technique as used in this laboratory and others the systematic error largely outweighs the accidental errors of measurement, (4) that while a fictitious value for the radius can be found for a single film which will make the resultant of all the terms in the above equation zero (assuming $\Delta S/L$ to be constant over the whole film) this radius will not serve for another film, (5) that the use of calibrating substances of known lattice constants mixed with the samples was in general unsatisfactory and no one such substance was suitable for the range of materials under investigation in this laboratory.

[1] W. F. De Jong, Physica **7**, 23 (1927); M. Gayler and G. D. Preston, J. Inst. Metals (Lond.) **41**, 191 (1929).

[2] H. Seeman, Ann. d. Physik **59**, 455 (1919); H. Bohlin, ibid. **61**, 421 (1920).

[3] H. Saini, Helv. Phys. Acta **6**, 597 (1933).

[4] M. U. Cohen, Rev. Sci. Inst. **6**, 68–74 (1935).

B. Calculation of Lattice Constants, the "Drift Constant" and Errors

The resultant effect of the errors included in Eq. (1) is to yield lattice constants which depend upon the angles used for calculating them. This is shown clearly for cubic substances where a value of the lattice constant can be secured for each diffraction line measured. The constants determined from the lines at lower angles differ from those from higher angles by amounts well beyond experimental error in the line positions. This "drift" arising from the systematic errors is the most serious source of error in the vast majority of lattice constant measurements available in the literature at present because not only the focusing methods but likewise Debye-Hull powder methods and back reflection methods of various types are subject to similar errors.

That the existence of this drift has been recognized is evidenced by the various graphical and analytical methods proposed to eliminate it among which may be mentioned those discussed by Bradley and Jay,[5] Stentzel and Weerts,[6] and Weigle.[7] While graphical methods involving plots of the lattice constant as a function of $\cos^2\theta$, $\phi\tan\phi$ or $\sin^2\theta$ with extrapolation to $\theta=90°$ or to $\phi=0$ are suitable for cubic substances, they become extremely complicated for other systems. During the course of our own investigations we developed graphical methods for hexagonal and tetragonal systems. All of these methods, however, are inexact and cumbersome in comparison with the analytical method by Cohen.[4]

For purpose of orientation, it may be mentioned at this point that what Cohen does is to assume that the errors in $\sin^2\theta$ will be proportional to $\phi\sin 2\phi$ and adds a term $D\phi\sin 2\phi$ to the quadratic form for the crystallographic system to which the substance belongs. Thus for the hexagonal system he uses the equation

$$\sin^2\theta=\frac{\lambda^2}{3a^2}(h^2+k^2+hk)+\frac{\lambda^2l^2}{4c^2}+D\phi\sin 2\phi \quad (3)$$

or $\sin^2\theta=A(h^2+k^2+hk)+Bl^2+D\phi\sin 2\phi$.

By knowing the values of the indices hkl and the angles θ and ϕ, the set of measured $\sin^2\theta$ values is solved by least squares methods to find A, B and the "drift constant" D. It is evident from Eq. (1) that setting $\Delta\sin^2\theta=D\phi\sin 2\phi$ involves an approximation. Cohen's experience, frequently confirmed in this laboratory, shows that any error arising from this source is unimportant in cameras of 10 and 15 centimeter diameter (cf. Table I). For larger cameras it may be necessary to use two correction terms as indicated by Eq. (1).

The method of calculation here used makes possible the evaluation of the errors of the lattice constants determined from an individual film. For the case of cubic crystals, the weight of $A(A=\lambda^2/4a_0^2)$ is given by $W_A=C/C_A$, where C is the determinant of the coefficients of the normal equation[4]

$$C=\begin{vmatrix}\Sigma(h^2+k^2+l^2)^2 & \Sigma(h^2+k^2+l^2)\,(\phi\sin 2\phi)\\ \Sigma(h^2+k^2+l^2)\,(\phi\sin 2\phi) & \Sigma(\phi\sin 2\phi)^2\end{vmatrix}$$

and C_A is the minor of the $\Sigma(h^2+k^2+l^2)^2$ element in the above determinant.

$$C_A=\Sigma(\phi\sin 2\phi)^2.$$

Back calculation yields a set of $\Delta\sin^2\theta$ terms and from these the variance, S^2, of $\sin^2\theta$ is obtained by:

$$S^2=(\Sigma(\Delta\sin^2\theta)^2)/(N-w),$$

where $N=$number of lines, $w=$number of constants to be determined, in the cubic case, $w=2$; $N-w=$degrees of freedom. The variance S_A^2 of the quadratic equation constant A, is given by $S_A^2=S^2\cdot C_A/C$ and the standard error, S_{a_0}, of the lattice constant (a_0) by

$$S_{a_0}=a_0S_A/2A. \quad (4)$$

The hexagonal case is a simple extension of the cubic case. The C determinant becomes

$$C=\begin{vmatrix}\Sigma(h^2+k^2+hk)^2 & \Sigma(h^2+k^2+hk)\,(l^2) & \Sigma(h^2+k^2+hk)\,(\phi\sin 2\phi)\\ \Sigma(h^2+k^2+hk)\,(l^2) & \Sigma(l^2)^2 & \Sigma(l^2)\,(\phi\sin 2\phi)\\ \Sigma(h^2+k^2+hk)\,(\phi\sin 2\phi) & \Sigma(l^2)\,(\phi\sin 2\phi) & \Sigma(\phi\sin 2\phi)^2\end{vmatrix}.$$

[5] A. J. Bradley and A. H. Jay, Proc. Phys. Soc. London **44**, 563 (1932).
[6] W. Stentzel and J. Weerts, Zeits. f. Krist. **A84**, 20 (1933).
[7] J. Weigle, Helv. Phys. Acta **7**, 46–50, 51–56 (1934).

C_A is the minor of the $\Sigma(h^2+k^2+hk)^2$ element in the C determinant

$$C_A=\begin{vmatrix} \Sigma(l^2)^2 & \Sigma(l^2)\ (\phi \sin 2\phi) \\ \Sigma(l^2)\ (\phi \sin 2\phi) & \Sigma(\phi \sin 2\phi)^2 \end{vmatrix}.$$

C_B is the minor of the $\Sigma(l^2)^2$ element in the C determinant.

$$C_B=\begin{vmatrix} \Sigma(h^2+k^2+hk)^2 & \Sigma(h^2+k^2+hk)\ (\phi \sin 2\phi) \\ \Sigma(h^2+k^2+hk)\ (\phi \sin 2\phi) & \Sigma(\phi \sin 2\phi)^2 \end{vmatrix}$$

the ratios C/C_A and C/C_B give the weights of A and B, respectively. As before the variance of $\sin^2\theta$, S^2, is given by

$$S^2=(\Sigma(\Delta \sin^2\theta))/(N-w)$$

and in the hexagonal case $w=3$. The variances of A and B are given by

$$S_A^2=S^2\ C_A/C, \quad S_B^2=S^2\ C_B/C$$

and the standard errors of the lattice constants a and c by

$$S_a=aS_A/2A, \quad S_c=cS_B/2B. \qquad (5)$$

The modifications necessary to treat tetragonal crystals and the extension to the orthorhombic case are obvious.

The standard errors as calculated above put rather narrow limits on the lattice constants since it corresponds to a probability of only 0.5 that the true values of the constants lie within these limits. To increase the probability that the true value of a calculated constant lies within the limits of error reported, use is made of fiduciary limits. Tables[8] have been set up giving the factor by which the standard error must be multiplied in order to obtain the desired limits. In our work we have taken a probability of 0.05 as our desired limit. This corresponds to the probability of 19 in 20 that the true value lies inside the limits thus set. The factor by which the standard error is multiplied varies with the number of degrees of freedom and is greater, the fewer the degrees of freedom.

When a series of films of the same material are taken the standard errors are, in general, not the same for the whole set. Further, if different radiations are used the degrees of freedom are often quite different for different films. Some method of averaging is desirable which takes account of these effects.

The most rigorous method is the following:

For cubic crystals, we obtain from quantities already computed the weight of a_0 for each film. $W_{a_0}=4\cdot(A^2/a_0^2)C/C_A$; a_0=lattice constant; $A=\lambda^2/4a_0^2$; C and C_A are the determinants defined above. The weighted average of a_0, namely $\bar{a}_0$, is

$$\bar{a}_0=\Sigma(W_{a_0}\cdot a_0)/\Sigma(W_{a_0}). \qquad (6)$$

To obtain the standard error in $\bar{a}_0$, we calculate the variance, $S_{\bar{a}}^2$, for the whole set of films

$$S_{\bar{a}}^2=\frac{\Sigma nS^2}{\Sigma n}=\frac{\Sigma(\Sigma(\Delta \sin^2\theta)^2)}{\Sigma n}. \qquad (7)$$

[8] R. A. Fisher, *Statistical Methods for Research Workers*, fourth edition (Oliver & Boyd, London, 1932), p. 151.

TABLE I.

Ag	Film VII-174		$\sin^2\theta$ Co-Ni rad.		$i=28.0°$ $\Delta \sin^2\theta\cdot10^6$			(1)–(2) to ΔL
LINE	(1)	(2)	(3)	(4)	(1)–(2)	(1)–(3)	(1)–(4)	(mm)
$19\alpha_2$Ni	0.781460	0.781413	0.781391	0.781422	+47	+69	+38	−0.02
$20\alpha_1$Ni	.822617	.822624	.822632	.822621	− 7	−15	− 4	0
$20\alpha_2$Ni	.822553	.822632	.822642	.822629	−79	−89	−76	+0.04
$19\alpha_1$Co	.781711	.781662	.781679	.781655	+48	+32	+56	−.04
$19\alpha_2$Co	.781690	.781669	.781686	.781662	+21	+ 4	+28	−.02
$20\alpha_1$Co	.822919	.822890	.822893	.822889	+29	+26	+30	−.03
$20\alpha_2$Co	.822849	.822897	.822898	.822896	−48	−49	−47	+.06
$24\alpha_1$Ni	.987509	.987529	.987516	.987534	−20	− 7	−25	+.02
$24\alpha_2$Ni	.987553	.987539	.987523	.987544	+14	+30	+ 9	−.03
	$S^2=(\Sigma(\Delta \sin^2\theta)^2)/(N-2)$				$S^2\cdot10^{12}=2140.7$	2567.6	2138.7	

(1) Experimental value from line measurements $\phi=(1/8R)\cdot L$, $1/8R=0.0024469$. Corrected for refraction and converted to Niα_1 as common wave-length.

(2) Calculated from the fitted equation:
$\sin^2\theta=0.04114809\ (h^2+k^2+l^2)-0.00101825\ (\phi \sin 2\phi)$
from which $a_0=4.0779_1\pm0.0000_6$ at 25°.

(3) Calculated from the fitted equation:
$\sin^2\theta=0.04114723\ (h^2+k^2+l^2)-0.00034556\ (\sin 2\phi \tan 2\phi)$
from which $a_{0_2}=4.0779_5\pm0.0000_6$ at 25°.

(4) Calculated from the fitted equation:
$\sin^2\theta=0.04114839\ (h^2+k^2+l^2)-0.00140727\ (\phi \sin 2\phi)+0.00013361\ (\sin 2\phi \tan 2\phi)$ from which $a_0=4.0778_9\pm0.0000_7$.

Then the variance of the mean $\bar{a}_0$ is

$$S^2_{\bar{a}_0} = S_t^2 / \Sigma W_{a_0}, \qquad (7a)$$

where n = degrees of freedom for each film; $\Sigma(\Delta \sin^2 \theta)^2$ = sum of the squares of the deviations for each film; W_{a_0} = weight of a_0.

The fiduciary limit of the average, $\bar{a}_0$, is obtained from the standard error $S_{\bar{a}_0}$ by using the factor for probability = 0.05 corresponding to Σn degrees of freedom.

For other systems the treatment is similar, the same set of operations merely being repeated for each of the lattice constants. Actually the calculations are rather less cumbersome than would appear at first sight because most of the required quantities have been determined previously.

C. The Experimental Technique

Concerning the main features of construction of the symmetrical focusing cameras there is little to be said. Cohen's method of calculation makes it unnecessary to use meticulous care in keeping slit, sample and film on the same circumference. It is obvious that large values of the drift constant are undesirable on general principles so that reasonable accuracy in keeping the camera a true cylinder is indicated.

It is necessary in practically all cases to keep the sample moving during the exposure, otherwise the diffraction lines are apt to be spotty which is a serious handicap to accurate measurement. Of the various constructions possible, the one adopted in this laboratory is to mount the sample on a segment of the cylinder supported by a conical bearing accurately centered with respect to the cylinder axis. The precaution was taken of mounting the entire structure in a lathe by means of a bar through the central axis and trueing the cylinder with the slit and movable segment in position by a grinding operation. The movable segment is oscillated over a path approximately 0.5 cm on the circumference by a cam device with a worm gear and pulley to reduce the speed of the motor drive. It was found that unless the entire oscillating mechanism was made to move quite freely, friction caused a steady increase in camera and sample temperature during the exposure with deleterious effects on the final results (see below).

Diaphragming the divergent beam is an important detail. Since the focal spot of the target is used either as a point or a line source, the beam diverges in both horizontal and vertical directions, the cylinder axis of the camera being almost perpendicular to the target face plane in multiple window x-ray tubes or to the main plane of the x-ray beam with tubes with 45° targets. In the horizontal direction the beam must be restricted so that it stays within the sample area at all positions of the sample holder. In the vertical direction it must be restricted so that the beam is symmetrical with respect to a plane bisecting the opening between the upper and lower plates of the camera. It must be further restricted so that the direct beam itself nowhere strikes the plates else excessive background darkening is produced on the film which may obscure some of the weaker lines. With a camera of 10 cm diameter and 1 cm opening between the plates we have found it satisfactory to use beams which covered a sample area of approximately 25–30 mm long and 4–6 mm high; the slit width is 0.1 mm.

We have found no completely satisfactory way of printing fiducial points on a film during the x-ray exposure but our investigation on this point was not exhaustive. While strictly speaking it is unnecessary to have such reference points on the film if Cohen's method of calculation is used, it is desirable to make an approximate correction to keep the value of D low. Since most of the change in film length occurs during and after development, we have adopted the scheme of printing reference lines on the film after exposure to the x-rays but prior to development. This is done by means of a heavily blackened photographic plate with very fine lines ruled on it at points just beyond the darkened portion of the film; a special printing frame is used for the purpose. When it is necessary to keep the camera evacuated or filled with a thoroughly dried gas during exposure some other means might be necessary to obtain an approximate shrinkage correction since the film length is particularly sensitive of changes in moisture content of the film.

Temperature affects the precision determination of lattice constants in several ways. It is necessary that the camera temperature be con-

stant within 1°C and that the sample be allowed time to reach the camera temperature. Correction to a standard temperature by one of the obvious methods must be made if precision work by various investigators is to be compared. Constancy of temperature during the exposure is very important. It may be shown that the effect of changes in camera dimensions is negligible for cameras made of brass, bronze or steel even with changes as great as 5° during exposure. The effect of changing sample temperature is more significant for the position of the diffraction lines shift according to the relation:

$$\Delta L = 8R\alpha\Delta t \cot\phi = 8R\alpha\Delta t \tan\theta$$

with an expansion coefficient $\alpha = 2\times10^{-5}$ and $\Delta t = 3$°C each line will be broadened (i.e., $\Delta L/2$) from 0.04 to 0.1 mm depending upon the angle. With varying temperature during exposure this broadening may be unsymmetrical and lead to false values for the lattice constants. It is for this reason that friction in the oscillating mechanism must be kept very low. We have occasionally observed temperature rises of 8 to 10°C when this detail was not cared for.

In this laboratory we have found it desirable to measure the line positions by means of a simple photometer. Light from a 6-volt, 108-watt Mazda ribbon filament lamp is passed through a lens system at the end of which is low power microscope. This is adjusted to give a very highly concentrated scanning beam of approximately 2.0×0.2 mm in area focused on the film. Light passing through the film strikes a Weston photronic cell. A portion of the light beam is split off ahead of the microscope and passes into a similar photronic cell. The two cells are opposed through a galvanometer. After the light has operated for 10 or 15 minutes, the deflections are virtually independent of variations in line voltage, etc. Intense lines produce galvanometer deflections of 20 to 30 cm. The film is firmly mounted on a carriage moved by a precision screw. A scale and drum is provided for making exact readings. Any systematic variation in the pitch of the screw is eliminated by the method of calculation. Irregular variations were found to be well within the other limits of error.

In our focusing cameras the range covered is from $\sin^2\theta = 0.78$ to 0.995. At the lower angles the two reflections of a $K\alpha_{1,2}$ doublet of iron radiation are separated about 0.5 mm; at the high angles by 6–7 mm. The high angle reflections, however, are rather broad while low angle reflections are sharp. Use of the photometer enables full use to be made of the sharpness of these low angle reflections as well as the high dispersion of the outer range of the camera. Lattice constants for a cubic substance calculated from the two lines of a doublet at low angles thus agree with each other quite as well as values from a doublet at high angles in spite of the difference in dispersion. The values obtained from the two doublets will not in general agree with each other because of the drift factor. The measurements over the entire film are, therefore, more consistent and if (for a cubic crystal) a graphical extrapolation such as a_0 *vs.* $\phi\tan\phi$ is used the scattering of the individual points about the best straight line representing them is nearly uniform over the entire range. The agreement between the measured and calculated line positions is shown by the last column of Table I. Similar results have been obtained for noncubic substances.

Cohen's method of calculating films is essentially an analytical extrapolation to $\phi=0$. As such, the films must satisfy two important conditions if full value of the method is to be obtained. In the first place the film must show diffraction lines from at least two sets of planes for a cubic crystal, from three sets for hexagonal and tetragonal crystals, and from four sets for orthorhombic crystals. In the second place, these reflections must be properly distributed over the range of angles covered and at least one set of reflections should occur at $\sin^2\theta > 0.90$ otherwise the extrapolation must be carried too far. With the more complicated structures it is usually not difficult to satisfy both conditions. The simpler metallic elements, however, yield relatively few lines and even when a number of different x-ray targets are available it is frequently impossible to obtain the necessary number and desired distribution of lines. Since the attainment of high precision is frequently required in these cases when solid solution limits are to be determined or deviations from some ideal law are to be studied, we have frequently

adopted the expedient of using a metallic alloy as a target, usually two elements in a 50 atomic percent mixture. Alloy targets of Fe-Mn, Fe-Ni, Fe-Cr, Cu-Ni, Fe-Co, Ni-Cr, Ni-Co and Cu-Mn all have been found to work satisfactorily. It is to be emphasized that one does not obtain the same result by exposing the same sample to the two different radiations on different films since the "drift constants" will not be the same except by chance.

The use of a refraction correction in lattice constant measurements has been discussed by several writers with the general conclusion that it was of uncertain validity and unnecessary in view of the attainable precision. The use of alloy targets and the attainment of higher precision makes it necessary to reconsider the matter. Without going into the theory of the subject, it may be said that in the few cases suitable for investigating the point, e.g., using radiation from a Ni-Cr target on a metal of high density, the results over the entire film were somewhat more consistent when a refraction correction was applied to each line measured. We have therefore applied such corrections in all the experimental work which follows in a later section. For convenience we have transformed Siegbahn's equation[9] and introduced a minor correction of 0.9 for anomalous dispersion as suggested by Weigle[7] which result in the following relation:

$$\Delta \sin^2\theta = -\frac{19.58\rho Z}{M}\cdot\frac{\lambda^2}{4}\cdot 10^{-6}, \qquad (8)$$

where ρ = density, Z = atomic number, M = atomic weight and λ = wave-length in Angstroms. Care must be used in comparing precision results of various investigators because there is as yet no complete agreement on this point.

In systems other than cubic, there is an important source of variation in lattice constant data which, to our knowledge, has not been adequately considered elsewhere. This is the choice of planes whose reflections are to be used in the calculation.

To find the conditions which must be satisfied if the relative errors in a and c are to be the same, we may start with the equation for the standard errors, Eq. (5). Since $S_a/a = S_A/2A$ and $S_c/c = S_B/2B$, we obtain by setting: $S_a/a = S_c/c = S_A/2A = S_B/2B$ the equation:

$$(16/9)(c/a)^4 = C_A/C_B. \qquad (9)$$

It will seldom be possible to satisfy this condition but excessive deviations from the equality can be avoided by proper choice of wave-lengths. The effect is illustrated by the results in zinc (see Table II). All of the films were taken with Fe-Co radiation. On film VIII-35 it was impossible to measure the reflections from the 104 planes which occur close to the low angle limit in the camera. On film VII-229 the reflections of $K\alpha_2$ radiation from the 104, 202, and 105 planes were too weak for measurement. Because of the distribution of the lines omitted in the second case, (VII-229) Eq. (9) is more closely satisfied than any of the other films tabulated while in the case of film VIII-35 the deviation from the equation is the largest although the lines dropped are those which have the least effect on the extrapolation.

TABLE II. *Zinc.*

FILM	C_A	C_B	ACTUAL $\left(\frac{C_A}{C_B}\right)$	$\left(\frac{C_A}{C_B}\text{(ACTUAL)}\right)$ / 21.11	$\frac{Sa/a}{Sc/c}$ MEAS.
VIII-35	279.37	1.7663	158.16	7.49	2.91
VIII-6	590.42	15.2077	38.82	1.84	1.36
VIII-8	590.45	15.2078	38.83	1.84	1.50
VII-229	227.90	6.9128	32.97	1.56	1.18

$c/a = 1.856$ $\quad (16/9)(c/a)^4 = 21.11 = C_A/C_B.$ $\qquad (9)$

While Eq. (9) appears cumbersome to use actually all the summations can be determined rather easily and the axial ratio c/a need not be known to more than three significant figures. Thus a preliminary value of the axial ratio and a knowledge of the reflection lines available from a given set of wave-lengths in a given camera are all that are needed to determine the best set of planes.

The application of this equation will frequently clear up otherwise puzzling discrepancies in the accuracies of results of different investigators and among different films obtained in a single investigation. Further it is occasionally important in solid solution investigations when, because of changing lattice parameters, certain lines move into or out of the range of the camera and the relative accuracy of several points on a lattice parameter *vs.* composition curve must be taken into consideration.

[9] M. Siegbahn, *Spectroscopie der Röntgenstrahlen* (Springer, Berlin, 1931), pp. 36–42.

D. Preparation of the Sample

With increasingly high dispersion in diffraction cameras and precision in measurement of lattice constants, the preparation of the material to be studied by the x-ray methods becomes a problem of major importance. A lattice constant measurement or a description of a phase in terms of its lattice structure is virtually useless unless the substance has been prepared with sufficient care and its composition and method of preparation adequately described. This fact, although obvious, has not received the attention it deserves and many x-ray results reported in the literature, particularly in the fields of alloy structures and phase diagram studies, are seriously marred by failure to consider this important feature of x-ray work.

While practically every substance presents its own problems on this matter of adequate sample preparation, a few guiding principles can be stated which generally, but by no means always, bring about satisfactory results. From the technical side, every effort must be made (1) to be certain that the diffraction lines found on the photographic film correspond to the phase or phases present under the conditions postulated and (2) to secure sharp diffraction lines from each phase. Essentially the problem is one of bringing the substance into equilibrium under a definite set of conditions and retaining it unchanged until after the x-ray exposure has been made. This means, of course, that the methods used to attain equilibrium in heterogeneous systems must be applied. The attainment of equilibrium may, however, be a very slow process. We have frequently found it necessary to anneal metallic alloys for a month at temperatures of 450°C or higher before equilibrium was reached and occasionally for 4–6 months. One case has been reported where the annealing time was a year at 100°C.[10] On the other hand, annealing for as little as one hour occasionally permits such excessive grain growth that the films contain discontinuous spots instead of uniform lines. Spotty films cannot be successfully measured by photometric measurements since the diffraction lines are generally curved and the spots are unsymmetrically distributed with respect to the median line of the films. For severely cold-worked specimens annealing for a few minutes at temperatures not far from their melting points is sufficient to secure equilibrium.

Most of the work in this laboratory concerns metallic alloys. The usual technique is to anneal the original ingot at the highest permissible temperature for 5–10 days to secure homogeneity of composition by eliminating "coring" and segregation. The ingot is then ground or filed to secure finely divided material for the x-ray work. These operations so frequently cause internal changes in the substance aside from the effect of the cold work that annealing of the powder is necessary. This final annealing is carried out at a definitely determined temperature and is followed by quenching so that the powder is brought to room temperature in a very short time, usually a small fraction of a second. Both annealing operations are usually carried out in vacuum but sometimes a hydrogen atmosphere is used. The latter has been found necessary if one of the elements is volatile in which case surprisingly small temperature gradients in the furnace may produce very marked effects. In the case of certain magnesium alloys, this element would distill out and partially react with the glass or quartz tube containing the powder. If sufficient time was allowed, a new equilibrium would be reached between the main portion of the powder and the material on the walls of the tube but, of course, the original analysis of the powder then became meaningless. By filling the tube with hydrogen so that at the annealing temperature the pressure inside would be approximately one atmosphere, distillation was hindered to such an extent that the powder remained unchanged in composition and the diffraction lines were quite sharp.

Variations in the composition of a phase produce variations in lattice parameter which will show up on the films either as a multiplicity of lines where only one line should occur or a broadening and blurring of the lines. The effect of small variations of lattice constant on line position is given by

$$\Delta L = 8R \cot \phi (\Delta a/a).$$

For a cubic substance with $a = 3.0$A in a camera

[10] E. A. Anderson, M. L. Fuller, R. L. Wilcox and J. L. Rodda, Trans. Am. Inst. Min. Met. Eng. **111**, 264 (1934).

of 50-mm radius ΔL varies from 0.075 at $\phi=28°$ to 0.75 at $\phi=3°$ when $\Delta a/a=0.0001$. There are many systems where such a variation in lattice constant is produced by relatively small composition changes.

Direct experimental test is the only way to determine whether a sample prepared under a given set of conditions can be retained without change under the conditions in the x-ray camera. In general there are three possibilities which must be considered. (1) The substance reacts with the atmosphere in the camera. This is comparatively rare and experimental means can usually be found to eliminate it. (2) The substance undergoes an allotropic change with greater or less rapidity, e.g., the transformation from γ to α iron which is exceedingly rapid or the transformation of sulfur from the monoclinic to the rhombic form which is comparatively slow. It is one of the serious disadvantages of the x-ray technique that in working with cameras at room temperature such transformations may be entirely missed. The $\gamma-\alpha$ transformation of pure iron could not have been found by ordinary x-ray methods. It was found by special cameras built for high temperature work.[11] No precision x-ray work has been done at temperature above 600°C and very little between 100° and 600°C.[12] Unfortunately very little can be done with x-ray methods alone to establish the existence or nonexistence of allotropic modifications when the investigation is restricted to pure substances at room temperatures. If a binary or more complex system involving such a substance is studied the chances of finding both modifications or of at least suspecting that there is more than one modification are greatly improved. For example, in a two-phase region where one of the modifications is in equilibrium with another phase it is very rare that both are pure compounds. In other words, one of the phases is a solid solution. That the equilibrium concentrations of each of the modifications with this other phase should be the same is also a rare occurrence. Thus, if the high temperature modification has been brought into equilibrium with the neighboring phase and transforms during cooling to room temperature, the diffraction lines of at least one of the phases will be badly blurred because of lack of chemical homogeneity. While such a criterion is by no means infallible, it has frequently proved to be exceedingly useful in this laboratory and has made it possible to locate certain phase boundary regions with a fair degree of correctness. The higher the cooling or quenching rates, the better this criterion can be applied. Slowly cooled samples yield untrustworthy indications because the time of cooling permits adjustments in composition which result in sharper lines. (3) During quenching the substance becomes strained due to unequal cooling rates in different directions. It has been shown by Phillips and Brick[13] that with powders, fine wires and very thin foils such strains do not arise on quenching to such an extent that lattice constants are measurably affected. With larger sized material including the small quenched ingots frequently used in back reflection cameras such as the Sachs type, the results may be in error by amounts far exceeding the experimental errors enumerated in Part A.

[11] A. Westgren and G. Phragmen, J. Iron and Steel Inst. **105**, 241 (1922).

[12] Cf. E. A. Owen and E. L. Yates, Phil. Mag. (7) **17**, 113 (1934).

[13] A. Phillips and R. M. Brick, Trans. Am. Inst. Min. Met. Eng. Inst. of Metals Division **111**, 94 (1934).

Part II. Experimental Results on Fourteen Metallic Elements

The theory and technique outlined in Part I have been applied to fourteen metallic elements of cubic, hexagonal and tetragonal symmetry. The cameras used were of the symmetrical focusing type of 10-cm diameter. Further details are concerned merely with the preparation and purity of the samples which will be given in connection with each element. Corrections for the temperature of the sample were made by the use of the ordinary expansion formula using expansion data given in *International Critical Tables*. In noncubic systems the coefficients appropriate to each axis were used. All lattice constants have been corrected to 25°C. It should be mentioned again that the values have been corrected for refraction.

It is interesting to note that for but one of the elements investigated (iron) does a very small

amount of impurity have a marked effect and the only reported impurity which has such an effect is carbon. Carbon enters the alpha-iron lattice in the interstices and expands the lattice. Further, since the atomic weight is low in comparison with iron the weight percentage is a misleading way of giving the amount of impurity. There seems to be good reasons to believe that of the impurities contained in readily available "pure" metals the only ones which need be feared in regard to their direct effect upon the lattice constants are those of low atomic weight which form the interstitial type of solid solution. While interstitial solid solution in lattices of metallic elements is a rather rare phenomenon the elements which are most likely to go into this form of solid solution are carbon, hydrogen,

TABLE III. *Aluminum—face-centered cubic.*

SAMPLE	a_0	$Sa_0 \cdot 10^5$	NO. OF LINES	RAD.
1	4.0417_0	10	5	Cr
1	4.0412_7	11	4	Cu
1	4.0412_2	11	4	Cu
2	4.0414_2	3	4	Cu
2	4.0414_0	7	4	Cu
2	4.0412_9	15	8	Cr-Ni
Mean	$a_0 = 4.0413_9 \pm 0.0000_8$			

Sample No. 1. 99.971%. Aluminum Co. of America. Analysis: Si—0.009; Fe—0.016; Cu—0.004.
Sample No. 2. Another sample of the above.

TABLE IV. *Nickel—face-centered cubic.*

SAMPLE	a_0	$Sa_0 \cdot 10^5$	NO. OF LINES	RAD.
1	3.5167_3	8	6	Fe-Mn
1	3.5168_1	7	6	"
2	3.5168_9	6	6	"
3	3.5168_9	11	6	"
4	3.5168_8	9	6	"
Mean	$a_0 = 3.5168_4 \pm 0.0000_8$			

Sample No. 1. Spectroscopic traces of Cu. Prepared by C. G. Fink and F. A. Rohrman (Trans. Electrochem. Soc. **59**, 359 (1931)). 16 hr.—525°.
Sample No. 2. Electrolytic. 51 hr.—525°. Fe = 0.013%; Co = 0.11%; Si and S, traces.
Sample No. 3. 99.99%. Obtained from E. Fetz. 1 hr.—700°.
Sample No. 4. Prepared from $NiCl_2 \cdot 6H_2O$ by reduction with pure, dry hydrogen. Analysis of $NiCl_2 \cdot 6H_2O$ (J. T. Baker & Co.) SO_4—0.001; Fe—0.000; N compds. (as N)—0.04; Zn—0.00; Pb—0.00; Earths & alkalis, 0.15; Cu—0.004; Co—0.00. 71 hr.—550°.

TABLE V. *Silver—face-centered cubic.*

SAMPLE	a_0	$Sa_0 \cdot 10^5$	NO. OF LINES	RAD.
1	4.0779_0	6	9	Co-Ni
1	4.0778_8	8	11	Co-Ni
1	4.0776_5	5	4	Cu
1	4.0777_5	20	4	Cu
1	4.0778_9	5	9	Cr-Ni
1	4.0779_6	13	9	Cu-Ni
Mean	$a_0 = 4.0778_7 \pm 0.0000_8$			

Sample No. 1. Proof silver—99.999+%. U. S. Metals Refining Co. Melted in an alundum crucible under vacuum in high frequency furnace. 24 hr.—600°.

TABLE VI. *Gold—face-centered cubic.*

SAMPLE	a_0	$Sa_0 \cdot 10^5$	NO. OF LINES	RAD.
1	4.0704_4	5	8	Cu-Ni
1	4.0703_5	5	9	Co-Ni
1	4.0703_3	8	9	Co-Ni
1a*	4.0705_2	7	8	Cr-Ni
1b*	4.0705_6	5	8	Cr-Ni
Mean	$a_0 = 4.0704_2 \pm 0.0000_8$			

* Two measurements on same film.
Sample No. 1. Prepared by double precipitation with SO_2. 15 hr.—500°.

TABLE VII. *Silicon—diamond type cubic.*

SAMPLE	a_0	$Sa_0 \cdot 10^5$	NO. OF LINES	RAD.
1	5.4199_5	23	6	Fe-Co
1	5.4196_8	4	4	Ni
Mean	$a_0 = 5.4198_2 \pm 0.0003_4$*			

* Silicon gives rather spotty films which accounts for the rather high value for the fiduciary limits.
Sample No. 1. 99.84%. Electro Metallurgical Co. Analysis: C—0.025; Mn—0.001; Fe—0.020; N_2—0.006; Al—0.016; O_2—0.034; Ca—0.005; H_2—0.006. 36 hr.—600°.

TABLE VIII. *α-Iron—body-centered cubic.*

SAMPLE	a_0	$Sa_0 \cdot 10^5$	a_0 (corr.)	FIDUCIARY LIMIT	NO. LINES	RAD.
1	2.8607_8	4	2.8604_2	$17 \cdot 10^{-5}$	4	Fe-Co
2	2.8607_1	5	—	22	4	"
3	2.8607_1	13	—	56	4	"
4	2.8607_6	11	2.8604_9	47	4	"
Mean			2.8604_6			

Powders of samples 1 and 2 were annealed for 71 hours at 550°C; samples 3 and 4 for 13 hours at 570°C.
Sample No. 1 was German carbonyl iron. Analyses by the Union Carbide and Carbon Research Laboratories gave C, 0.007; Mn, trace; Si, 0.004; S, 0.004; P, nil; O, 0.004. The oxygen was determined by the iodine extraction method and was therefore not dissolved oxygen.
Sample No. 2 was some of Merck's "Iron by hydrogen" lot #33400 which had been further treated by heating 15 hours in pure dry H_2 at 500°C. "Maximum impurities," as stated on the label, were: substances insoluble in sulphuric acid, 0.500%; water-soluble substances, 0.05%; nitrogen, 0.003%; sulphide, 0.030%; arsenic, 0.0015%. The "insoluble in sulphuric acid" material is probably mostly SiO_2 which would not affect the lattice constant.
Sample No. 3 was a small piece received from Dr. J. B. Austin of the U. S. Steel Corporation Research Laboratories. It was made by P. P. Cioffi of the Bell Telephone Laboratories by heating in pure dry hydrogen at 1490°C for 24 hours. This sample is now being analyzed by the Bureau of Standards.
Sample No. 4 was from the same original source (Cioffi) but had been heated in moist hydrogen at 1500°C for 18 hours. The American Rolling Mills Co. reported the following analysis: C, 0.005; Mn, 0.03; S, 0.003; P, 0.004; Si, 0.01; O, 0.002; N, 0.0001.
Corrections. The measured values of a_0 were corrected for the effects of the impurities present insofar as these effects are known. It is certain that carbon, manganese, silicon and nitrogen enter into the alpha-iron lattice and change its dimensions. To what extent oxygen, sulphur and phosphorus enter the lattice and how much they affect the dimensions is, as yet, unknown. No correction is possible for these last three elements at the present time.
Silicon decreases the lattice constant of iron at the rate of 6.5×10^{-4}A per atomic percent[14] when the silicon is less than 9 atomic percent. Manganese increases the lattice dimensions. For small amounts of Mn we may assume the additivity of atomic radii (Vegard's rule) which gives a change of 8×10^{-4}A per atomic percent Mn if the radius of the latter is taken as 1.27A. This change is roughly checked by the work of W. Schmidt[15] who used very impure manganese in making his alloys.
J. L. Burns[16] showed that carbon increases the iron lattice at the rate of 0.0515A per *weight* percent carbon.
It should be pointed out that the analyses of the samples are probably not complete. Because of the uncertainties in the corrections no fiduciary limits are given for this element.

[14] E. R. Jette and E. S. Greiner, Trans. Am. Inst. Min. Met. Eng. **105**, 259 (1933).
[15] W. Schmidt, Stahl and Eisen, **49**, 1696 (1929).
[16] J. L. Burns, Trans. Inst. Min. Met. Eng. **113**, 239 (1934).

TABLE IX. *Molybdenum—body-centered cubic.*

SAMPLE	a_0	$Sa_0 \cdot 10^5$	NO. OF LINES	RAD.
1	3.1409_0	3	5	Cu
1	3.1410_9	2	6	Cu
1	3.1410_5	2	6	Fe-Co
2	3.1410_8	6	6	Cu
2	3.1409_7	5	6	Cu
	Mean $a_0 = 3.1410_3 \pm 0.0000_4$			

Sample No. 1. MoO_3 reduced with pure dry hydrogen at about 500°. Analysis of MoO_3: Mo—99.5; insoluble in NH_4OH—0.01; SO_4—0.01; Heavy metals as Pb—0.002; Cl—0.001; NH_3—0.002; PO_4—0.0005; NO_3—0.003.

Sample No. 2. Sample prepared by a second reduction. Starting material same as above. No further heat treatment—material was x-rayed as taken from reduction furnace.

TABLE X. *Tungsten—body-centered cubic.*

SAMPLE	a_0	$Sa_0 \cdot 10^5$	NO. OF LINES	RAD.
1	3.1583_7	4	7	Fe-Co
	Mean $a_0 = 3.1583_7 \pm 0.0001_2$			

Sample No. 1. 99.95%—W. P. Sykes, General Electric Co., Euclid, O. Analysis: spectroscopic traces of Si, Mo, Fe, Cu. 68 hr.—980°. Air cooled.

TABLE XI. *Magnesium—hexagonal close packed.*

SAMPLE	a	$Sa \cdot 10^5$	c	$Sc \cdot 10^5$	NO. LINES	RAD.
1	3.2029_8	21	5.2001_0	18	8	Fe
1	3.2031_6	15	5.2001_2	13	8	Fe
1	3.2029_2	18	5.2003_2	16	8	Fe
2	3.2030_6	11	5.2001_2	9	8	Fe
3	3.2028_2	13	5.2003_9	11	8	Fe
4	3.2030_5	29	5.2002_0	25	8	Fe
	Mean: $a = 3.2030_0 \pm 0.0001_6$, $c = 5.2002_1 \pm 0.0001_4$, $c/a = 1.62354 \pm 0.0001_2$.					

Sample No. 1. 99.987%. Aluminum Co. of America. Analysis: Cu—nil; Pb—nil; Fe, Al—0.004; Zn—trace; Si—0.009. Sample prepared from original rods. 140 min.—405°.

Sample No. 2. Another sample prepared as above.

Sample No. 3. Same material as sample No. 1, but first melted in a magnesia lined alundum crucible in a high frequency induction furnace in an atmosphere of tank hydrogen. 140 min.—405°.

Sample No. 4. Same material as sample No. 1, but first melted in an electrical resistance furnace in an atmosphere of pure dry hydrogen. The hydrogen was purified by passing through heated tubes containing copper and magnesium and then through bottles of solid NaOH and calcium chloride. 140 min.—405°.

TABLE XII. *Zinc—hexagonal close packed.*

SAMPLE	a	$Sa \cdot 10^5$	c	$Sc \cdot 10^5$	NO. LINES	RAD.
1	2.6597_4	17	4.9367_4	11	8	Fe-Co
1	2.6593_7	6	4.9367_8	8	10	Fe-Co
2	2.6594_9	8	4.9370_3	11	10	Fe-Co
3	2.6596_1	7	4.9368_4	11	7	Fe-Co
	Mean: $a = 2.6594_9 \pm 0.0000_8$, $c = 4.9368_2 \pm 0.0001_1$, $c/a = 1.85631 \pm 0.0001_0$.					

Sample No. 1. Spectroscopic, N. J. Zinc Co. Analysis: Pb—0.0004; Fe—extremely faint; Cd—absent; Hg—extremely faint; Cu—extremely low; Mn—absent. 24 hr.—285°.

Sample No. 2. 99.936%. Eimer & Amend. Analysis: As—0.00005; Pb—0.05; Fe—0.01; Cd—0.001; sulfate (SO_4)—0.0019; chloride (Cl)—0.001. 36 hr.—285°.

Sample No. 3. 99.982%. Merck. Analysis: As—0.000025; Pb—0.010; substances oxidized by $KMnO_4$, such as Fe—0.0056; compds. of S & P = 0.0000. 24 hr.—285°.

nitrogen and perhaps boron and oxygen; these elements are seldom reported in the analyses.

The powders, prepared by grinding or filing, were sealed in glass or quartz tubes and gently heated during evacuation with a mercury diffusion pump, the evacuation system was provided with a condensation trap to prevent mercury or oil vapor reaching the metal.

The annealing data on the powders are given with the analysis and source of the material.

TABLE XIII. *Cadmium—hexagonal close packed.*

SAMPLE	a	$Sa \cdot 10^5$	c	$Sc \cdot 10^5$	NO. LINES	RAD.
1	2.97298	10	5.60681	33	10	Fe-Co
2	2.97324	8	5.60707	26	10	Fe-Co
	Mean: $a = 2.9731_1 \pm 0.0001_4$, $c = 5.6069_4 \pm 0.0004_5$, $c/a = 1.88588 \pm 0.0002_4$.					

Sample No. 1. Spectroscopic purity—N. J. Zinc Co. Analysis: Cu—extremely low; Mn—extremely faint; Fe—very faint; Zn, Pb, Hg—absent. 72 hr.—245°.

Sample No. 2. Baker—99.94%. Analysis on label: Zn—0.057; Pb—0.000; Fe—0.000; Cu—0.000. 72 hr.—245°.

TABLE XIV. *Antimony—hexagonal rhombohedral.*

SAMPLE	a	$Sa \cdot 10^5$	c	$Sc \cdot 10^5$	NO. LINES	RAD.
1	4.2995_7	9	11.2515_9	18	14	Fe
Mean	Hexagonal axes: $a = 4.2995_7 \pm 0.0002_0$, $c = 11.2515_9 \pm 0.0004_6$, $c/a = 2.6169_1 \pm 0.0002_1$. Rhombohedral axes: $a_{rh} = 4.4976_2 \pm 0.0001_8$, $\alpha = 0.9967_{11} \pm 0.00009_2$ radians, $\alpha = 57° 6' 27'' \pm 19''$.					

Sample No. 1. Kahlbaum "Zur analyse." No analysis. 18 hr.—475°.

TABLE XV. *Bismuth—hexagonal-rhombohedral.*

SAMPLE	a	$Sa \cdot 10^5$	c	$Sc \cdot 10^5$	NO. LINES	RAD.
1	4.53722	29	11.83708	105	9	Fe
2	4.53732	9	11.83883	35	12	Fe
3	4.53722	16	11.83800	65	12	Fe
Mean	Hexagonal axes: $a = 4.5372_6 \pm 0.0002_0$, $c = 11.8381 \pm 0.0008$, $c/a = 2.6091 \pm 0.0003$. Rhombohedral axes (calculated from the above means): $a_{rh} = 4.7364 \pm 0.0003$, $\alpha = .99898 \pm 0.00011$ radians, $\alpha = 57° 14' 13'' \pm 23''$.					

All samples were Merck's bismuth, minimum purity 99.95%. Impurities as reported on the label are: Sb—0.00; Fe—0.008; Sn—0.003; As—0.000; Pb—0.010; S—0.01; Cu—0.005; Ag—0.010.

1. 5 hr.—200°.
2. very finely ground, 5 hr.—200°.
3. 24 hr.—165°.

TABLE XVI. *Tin—tetragonal.*

SAMPLE	a	$Sa \cdot 10^5$	c	$Sc \cdot 10^5$	NO. LINES	RAD.
1	5.8195_0	14	3.1750_0	5	8	Fe
	Mean: $a = 5.8195_0 \pm 0.0003_5$, $c = 3.1750_0 \pm 0.0001_2$, $c/a = .54557_9 \pm 0.00005_7$.					

Sample No. 1. 99.995%. Baker. Analysis: As—0.0000; Zn—0.000; Pb—0.003; Cu—0.000; Fe—0.002. 117 hr.—151°.

TABLE XVII.

METAL			DENSITY 25°C X-RAY	DENSITY 25°C I.C.T. VOL. II
		Cubic		
	a_0			
Al	$4.0413_9 \pm 0.0000_8$		2.695	2.702 2.698
Ni	$3.5168_4 \pm .0000_8$		8.900	8.90±.05
Ag	$4.0778_7 \pm .0000_8$		10.494	10.489 10.483(1)
Au	$4.0704_2 \pm .0000_6$		19.287	19.264
Si	$5.4198_2 \pm .0003_4$		2.325	2.4
Fe	2.8604_6 (see text)		7.868	7.90
Mo	$3.1410_3 \pm .0000_4$		10.217	10.2*
W	$3.1583_7 \pm .0001_2$		19.261	19.3*
		Hexagonal		
METAL	a	c	DENSITY X-RAY	DENSITY I.C.T. VOL. II
Mg	$3.2030_0 \pm 0.0001_6$	$5.2002_1 \pm 0.0001_4$	1.736	1.738(2)
Zn	$2.6594_9 \pm .0000_8$	$4.9368_5 \pm .0001_1$	7.130	7.135
Cd	$2.9731_1 \pm .0001_4$	$5.6069_4 \pm .0004_5$	8.637	8.644
Sb	$4.2995_7 \pm .0002_6$	$11.2516 \pm .0004$	6.688	6.71 6.69
Bi	$4.5372_6 \pm .0002_0$	$11.8381 \pm .0008$	9.798	9.80
		Tetragonal		
Sn	$5.8195_0 \pm 0.0003_5$	$3.1750_0 \pm 0.0001_2$	7.281	7.30
		Rhombohedral		
METAL	a_{rh}	radians		
Sb	$4.4976_2 \pm 0.0001_8$	0.99671 ± 0.00009		57° 6′ 27″ ±19″
Bi	$4.7364 \pm .0003$	$.99898 \pm .00011$		57° 14′ 13″ ±23″

* No temperature given.
(1) Density determined in this laboratory = 10.492 at 25°C.
(2) " " " " " = 1.733 " "

The wave-lengths used in calculating these lattice constants were those given by M. Siegbahn.[17] Attention is called to the excellent agreement (cf. Table XVII) between densities calculated from x-ray measurements using these wave-lengths and the value of 6.0644×10^{23} for Avogadro's number.[18] Wave-lengths determined by means of ruled gratings and refraction phenomena[19] are on the average 0.25 percent higher than the crystal wave-lengths, and therefore the calculated (x-ray) densities would be nearly 0.75 percent lower than those given in Table XVII, unless Avogadro's number is changed in proportion.

It may be observed that the fiduciary limits range from ±2 to 7 parts per 100,000 and that from the way in which the fiduciary limits have been computed the chance that the correct value of the lattice constant falls within the respective limits is 19 out of 20.

The measurements on fourteen metallic elements are tabulated in Table XVII in text, together with densities calculated from the x-ray data and densities obtained by direct measurement. All measurements were corrected for refraction and temperature (to 25°). The limits given are the fiduciary limits for $P = 0.05$.

In conclusion, we wish to thank the various firms and individuals who have supplied pure materials and carried out analyses to assist in this work. We are indebted to Mr. Wm. Hurwitz for making a large proportion of the calculations included in this paper and for valuable suggestions as to the use of fiduciary limits. We are also indebted to the Federal Emergency Relief Administration for making available a number of student assistants who carried out the laborious routine of the photometric measurements of the x-ray films.

[17] M. Siegbahn, reference 9, p. 183, Table 46.
[18] R. T. Birge, Rev. Mod. Phys. **1**, 58 (1929).
[19] Cf. J. A. Bearden, Phys. Rev. **47**, 883 (1935).

The Green Flame of Phosphorus Hydride

E. B. LUDLAM, *Edinburgh University, Scotland*

(Received July 30, 1935)

The rotational structure of the bands in the green flame of phosphorus indicates that the emitting molecule is PH.

THE green flame associated with the burning of phosphorus has been known for many years. It had been examined by Salet and de Boisbaudran, but more in detail by Geuter[1] in 1907. Geuter also noticed that the same bands were produced in an electric discharge through a tube containing phosphorus if the air (moisture?) had not all been pumped out, the lines disappeared after passing the current for a short time; simultaneously with the green bands the many-lined spectrum of hydrogen appeared, then the Balmer lines and finally the green bands disappeared. He came to the conclusion that the spectrum was a hydride and suggested P_2H_4. He thought the same spectrum was emitted in the glow of phosphorus, but even with instruments of low dispersion the intensity of the emission from the glow is not sufficient to give a spectrum which can be measured.

Our own interest in the spectrum first arose from a study of the glow of phosphorus and the initiation of the chain reaction between phosphorus vapor and oxygen.[2] The vapor of white phosphorus consists of P_4 molecules and it had been suggested that the initial stage in the reaction between oxygen and phosphorus was the dissociation of P_4 into $2P_2$.

Recent work on the blue flame of sulphur had shown that the blue color was due to radiation emitted by the excited S_2 molecule, and it was thought possible that the green flame might be due to P_2 molecules; on the contrary, it turns out to be a hydride and most probably PH.

EXPERIMENTAL

After trying a number of different methods of producing the flame, it was found most satisfactory to burn air at a jet in a current of hydrogen which had been passed over white phosphorus. Oxygen was tried instead of air but was not quite so good. A current of air was regulated by means of a side tube dipping into water and was led upwards into a wide glass tube by a silica tube drawn out into a jet passing through a rubber bung in which it fitted rather loosely, so that it could be pushed easily up and down. Electrolytic hydrogen from a cylinder was passed through two bottles containing sticks of white phosphorus and entered the main tube through a side tube. The top of the main tube was slightly constricted and a short cylinder of mica inserted. The current of hydrogen was started and lighted at the top of the tube, then the air tube was pushed up until the jet was in the constriction, and a gentle stream of air was regulated so that, on pulling the air tube slowly down, the flame remained resting steadily on the jet. Several forms of jet were employed; there was not much to choose between them, but one which gave a fish-tail shape, placed edge-wise to the slit of the spectroscope was the best.

The spectroscope first used was one made by Bellingham and Stanley. It contained two dense glass prisms and the collimator and camera lenses were of six-foot focus. Its dispersion in the blue-green was about 10A per millimeter. Another instrument of about the same dispersion in the green but better in the yellow was fitted with a first quality Wallace one-meter concave replica grating of 25,000 lines to the inch. Neither of these were first-class instruments but they were the best available. As exposures lasting a whole week were necessary and no regulation of the temperature of the spectroscope was possible, the temperature variation would in itself account for some lack of definition; the gases were, of course, at atmospheric pressure and this also would cause broadening of the lines; the slit width used was a tenth of a millimeter. Attempts to get a brighter flame by raising the temperature of the bottles containing the phosphorus, to increase the amount of

[1] Geuter, Zeits. f. wiss. Phot. **5**, 1 (1907).
[2] Ludlam, Nature **128**, 271 (1931).

FIG. 1B. Low dispersion.

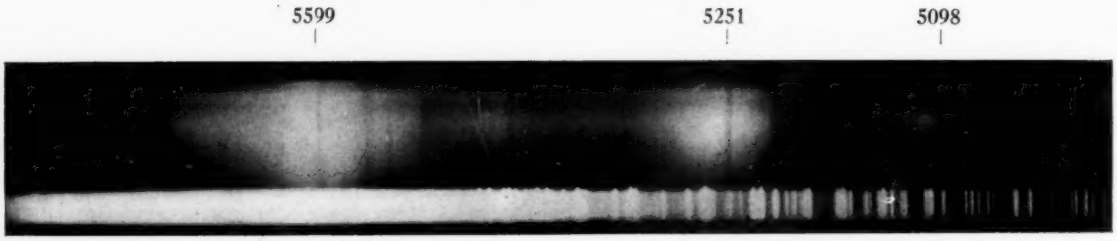

FIG. 1A. Photograph of system of bands from green to yellow. Ilford 'Chromatic' plate, 100-hour exposure, prism spectrograph, bromide enlargement.

phosphorus vapor in the flame, only led to the necessity for more frequent stoppage of the exposure to clean off the red phosphorus which deposits on the tube and cuts off the light from the slit. After trying a number of different brands of plate the fastest for the green region was found to be Ilford 'Chromatic.' These are plates of medium speed emulsion (HD 120) and fine grain, specially sensitized for the green. Later, in order to get the bands in the yellow, Ilford hypersensitive plates were used satisfactorily.

From the point of view of a thoroughgoing analysis of the spectrum the results are poor; the lines are very hazy and this is made much worse by overlapping of bands. They are, however, the best so far obtainable and settle the question quite definitely that the emitter is not P, but a hydride, probably PH.

Numerous attempts were made to photograph this spectrum excited by other methods. In the electric discharge using a tube containing P vapor over which hydrogen was passed (as in Pearse's work on PH in the ultraviolet[3]) the spectrum was easily *visible*; so, also, in a discharge through streaming PH_3; also when active hydrogen from a Wood's tube met vapor of phosphorus in a side tube; but in none of these cases was photography with a spectrograph possible. Any exposure that could have shown the least trace of the green bands in the electric discharge would have given many other lines of hydrogen and phosphorus heavily overexposed. It is one great advantage of the flame burning in excess of hydrogen that no lines due to any other spectrum appear on the plate.

The general appearance of the band system is shown in the plate (Fig. 1A). This is from a bromide enlargement of a photograph obtained with one hundred hours exposure, using the glass spectrograph. The band at 5098 is obtained conveniently free from overlapping, and the photo-micrograph (Fig. 2) brings out the intensity relations much more clearly than the enlargement. Another photograph (Fig. 1B) given eighty hours exposure in the first order of the meter grating, gave a negative which could be used for measuring the bands at 5251 and 5599 and although it was underexposed for the 5098 band, several of the faint and hazy lines were just measurable and they are included in the table for direct comparison with the others taken on the same plate (Tables I and II).

[3] Pearse, Proc. Roy. Soc. **A129**, 328 (1930).

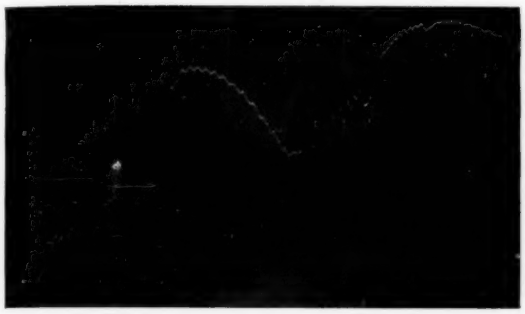

← *R* branch λ5098 *P* branch → λ5212 λ5251

FIG. 2. 100-hour exposure, Ilford 'Chromatic' plate, prism spectrograph. Shows complete bands at λλ5098 and 5257, and the *R* branch at λ5212, the *P* branch overlapping the tail of the *R* branch from λ5251.

← *P* branch λ5251 *R* branch →

FIG. 3. Grating; 80 hours, hypersensitive panchromatic plate. Enlargement 4.9 times.

TABLE I.

$R(J)-P(J)=B'(4J+2)$; $R(J-1)-P(J+1)=B''(4J+2)$

	λ5098 (PRISM), $\nu=19{,}615$				(GRATING)			
J	ΔR	ΔP	B'	B''	ΔR	ΔP	B'	B''
1	12.4	33.8(gap)	7.70	8.57	12.5	34.0(gap)	7.75	8.83
2	14.5	17.6	7.83	8.18	14.4	19	7.99	8.45
3	14.5	18.0	7.91	8.16	15.2	19	8.14	8.53
4	13.9	18.0	7.93	8.20	13.7	20.5	8.24	8.52
5	13.5	18.7	7.95	8.22	13.7	19	8.27	8.80
6	12.8	19.4	7.96	8.23				
7	12.1	19.8	7.97	8.18		too faint to measure		
8	11.4	21.6	8.0					
		mean	7.92	8.22		mean	8.08	8.62

TABLE II.

	λ5251 $\nu=19{,}044$ (GRATING)				λ5599 $\nu=17{,}860$ (GRATING)			
J	ΔR	ΔP	B'	B''	ΔR	ΔP	B'	B''
1	12.6	33.1(gap)	7.61	8.88	11.9	33.6(gap)	7.59	8.80
2	13.7	20.2	7.96	8.75	12.8	19.2	7.75	8.57
3	12.6	21.6	8.13	8.61	13.1	21.0	7.97	8.50
4	11.9	19.5	8.07	8.81	13.1	21.0	8.21	8.64
5	11.2	21.6	8.09	8.90	10.3	23.0	8.23	8.68
		mean	7.97	8.79		mean	7.95	8.64

ROTATIONAL STRUCTURE

As the general appearance of each band is that of a *P* and *R* branch, with one missing line between them, it is concluded that the emission is due to a $^1\Sigma-{}^1\Sigma$, or a $^1\Sigma-{}^3\Sigma$ transition. One cause of haziness of the lines may be due to the close triplet levels, if the transition is $^1\Sigma-{}^3\Sigma$.

Approximate values for B'' and B' are tabulated along with the separations between the lines in each branch. As the 5098 branch shows no sign of doubling back (though some of the other bands in the photograph exhibit an appearance rather as though the *R* branch went to a head) the moments of inertia in the upper and lower states are not very different. The standard of accuracy does not admit of any calculation of D, the term in B^2.

It will be noticed that the first line of the *R branch* is stronger than the second which is weaker also than would be expected from the average of the first and third. This is noticeable in all the bands that are sufficiently free from overlapping to show it.

Considering the lack of sharpness in the lines it is obvious from a glance at the tables for the values of B' and B'' for the three bands measured that they are in satisfactory agreement. The band at 5098 in the prism photograph was the clearest and was measured with the greatest care. Taking the value 8.2 as the mean of these values of B'', this may be compared with Pearse's value 8.4 for PH in the band at 3400 in the ultraviolet. The less accurate value obtained with the grating was 8.6, the mean of the two giving the value 8.4.

The corresponding values for the moment of inertia and radius are:

λ3400 $B''=8.411$ cm, $I=3.293\cdot10^{-40}$ g/cm,
$r''=1.43\cdot10^{-8}$ cm,

λ5098 $B''=8.2$ cm, $I=3.34\cdot10^{-40}$ g/cm,
$r''=1.41\cdot10^{-8}$ cm.

These results leave very little doubt that we are here dealing with the molecule PH. No other diatomic or polyatomic compound of phosphorus could have so small a moment of inertia.

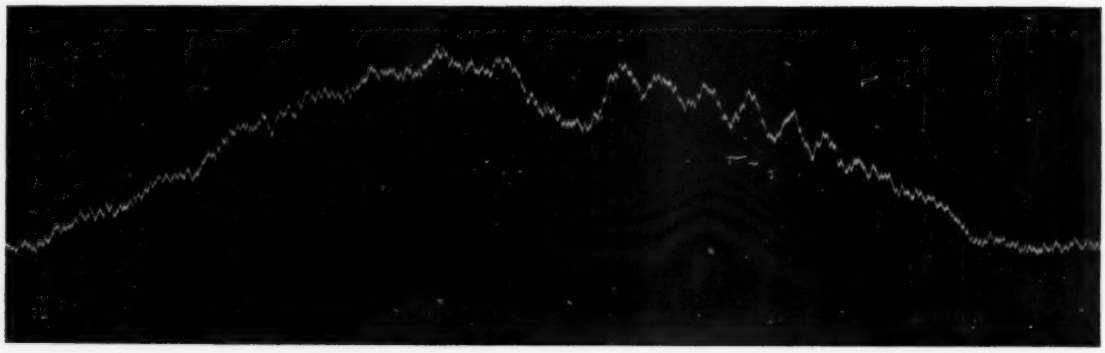

← *P* branch λ5599 *R* branch →

FIG. 4. Exposure 80 hours, grating, hypersensitive panchromatic plate, enlargement 14.8 times.

VIBRATION ANALYSIS

Many attempts have been made to arrive at some plausible analysis of the vibrational structure but nothing satisfactory has been obtained. Even with the longest exposures it was impossible to get measurements in the blue or red although there are faint bands in these regions. If it had not been for the decisive low moment of inertia the system might have been attributed to a polyatomic molecule such as P_2H_4 or P_2H_2.

The magnitude of the vibration quantum for PH is between 2300 and 2400 cm^{-1} and this is a range of wave-length from λ5098 (19,615 cm^{-1}) to, say, λ5800. There are faint bands, with apparent overlapping, in this region and even so far as about 6400, but they are hopeless for measurement. Rough visual measurements are given by the earlier workers. but they are of very little value, except for speculation.

The following points are noteworthy:

(a) The green bands in the flame are not accompanied by any other bands in the ultraviolet (except the OH bands) they are not a continuation of the $\Pi-\Sigma$ bands into the visible region.

(b) The rotational structure shows them to be $\Sigma-\Sigma$ bands.

(c) The moments of inertia in the upper and lower states are only slightly different, the equilibrium diameters are nearly the same, the potential energy curve for the higher state is almost symmetrically above that for the lower state and the Condon parabola will be a very narrow one. The result of this is to exclude transitions between vibration levels which are widely different in quantum number; e.g., 10→10 is much more probable than 0→10.

(d) The production of the PH and its spectrum in a flame may lead to the electronic excitation of molecules already possessing high energy of vibration, which, together with (c) would lead to a system of bands which would be sequences of high quantum number.

(e) Inter-combinations would have only a low probability and this would account for the difficulty in obtaining sufficient intensity. Consequently, although no exact vibrational analysis can be offered, it seems undesirable to leave the problem there without making a definite suggestion based on these considerations. As a tentative explanation of the spectrum it seems possible that the four brightest bands might be related in some such manner as the following:

	λ	ν	$v'-v''$
(a)	5098	19615	11−10
(b)	5251	19044	10−10
(c)	5435	18400	11−11
(d)	5599	17860	10−11

A further word of explanation is, perhaps, necessary. $(a-c)$ gives the value of the 11th vibrational quantum in the lower state, 1215 cm^{-1}; $(b-d)$ gives the 11th quantum in the upper state, 1184 cm^{-1}. There is nothing improbable in the reduction of the quantum from 2300 to 1200, but whether this would have happened at the tenth, or even the 15th, cannot be decided at present. Possibly work on the ultraviolet bands may lead to some definite decision.

I wish to express my thanks to Dr. R. W. B. Pearce and Dr. G. B. B. M. Sutherland for helpful advice, to the Carnegie Trustees for a Teaching Fellowship, and to Dr. Baker and Professor Sampson of the Royal Observatory for the photometer curves.

The Absorption Spectrum of Eu^{+++} in Crystalline $Eu_2(SO_4)_3 \cdot 8H_2O$

E. J. MEEHAN, *Department of Chemistry, University of California, Berkeley*

(Received July 29, 1935)

The absorption spectrum of $Eu_2(SO_4)_3 \cdot 8H_2O$ has been studied over the temperature range 14°K–290°K. Measurements of the absorption lines are given for five temperatures. Intensity variations caused by a change in temperature have been used to establish definitely the existence of levels 21 cm^{-1} and 41 cm^{-1} above the basic one, and to indicate the existence of 67 cm^{-1}, 86 cm^{-1}, and possible higher levels. An unusual feature of the spectrum is the constant energy difference occurring between many lines which are most intense at the lowest temperatures.

THE simple Hund theory predicted, with considerable accuracy, the magnetic susceptibilities of the ions of all the rare earths except Sm and Eu; Van Vleck and Miss Frank[1] have shown that no discrepancies exist if one uses the complete quantum-mechanical expression for calculating the susceptibilities, taking into account the "finite" width of the basic multiplet. These multiplet widths were unknown; Van Vleck and Frank have shown that agreement with experimental susceptibility measurements may be obtained by assuming the Goudsmit formula for calculating them; thus they calculated that the first excited state above the basic one occurs at about 930 cm^{-1} and 250 cm^{-1} for Sm^{+++} and Eu^{+++}, respectively.

Because of the action of the (generally asymmetric) crystalline fields, one expects, in general, a further splitting of the ground state of the ion.[2] It has been shown[3] that in many salts of Sm^{+++}, excited levels do exist far below 930 cm^{-1}, and that their positions depend on the nature of the crystalline fields to which the Sm^{+++} is subjected (determined by the crystal structure of the salt in question).

The present work was undertaken to determine the existence of similar low-lying levels in Eu^{+++}.

Experimental Part

The salt chosen for investigation was $Eu_2(SO_4)_3 \cdot 8H_2O$. Because of the difficulty of obtaining large single crystals, the work was carried out with conglomerates of small crystals. The material was of such purity that none of the strongest lines of Sm^{+++} (the most likely impurity) were observed. The crystal structure of the salt has not been determined; the crystallographic symmetry is presumably monoclinic.[4]

Photographs of 2–3 mm conglomerates were taken on a 3-meter concave grating (dispersion 5.5A per mm), over the temperature range 14°K (obtained with liquid hydrogen under reduced pressure), to room temperature. The apparatus has been described previously.[5] Measurements were made of the 14°, 20°, 77° (liquid N_2), 169° (liquid C_2H_4), and room temperature absorption. Additional photographs at the temperatures of liquid air and liquid methane (112°K) served confirmatory purposes.

Results

In Fig. 1 are shown reproductions of the spectra corresponding to the temperatures indicated.

Table I gives the frequencies (cm^{-1}) of absorption lines at five temperatures, and, for 14°K, wave-lengths (A). Very rough intensity estimates are given for 14°K and 77°K. Lines that increase in intensity with increasing temperature are marked *H*, those that decrease are marked *L*. The error in measurement is considered to be about 0.05A in most cases, although for faint or diffuse lines the error is greater.

Discussion of Results

As usual the lines increase markedly in sharpness as the temperature is lowered. The shift in position with temperature change is in most cases not much greater than the error in measure-

[1] See Van Vleck, *Electric and Magnetic Susceptibilities* (Oxford, 1932) pp. 239–249.
[2] H. Bethe, Ann. d. Physik **3**, 133 (1929).
[3] Spedding and Bear, Phys. Rev. **46**, 975 (1934); this paper contains references to earlier work.
[4] Zachariasen, J. Chem. Phys. **3**, 197 (1935) has found this symmetry in $Sm_2(SO_4)_3 \cdot 8H_2O$.
[5] Spedding and Bear, Phys. Rev. **42**, 58 (1932).

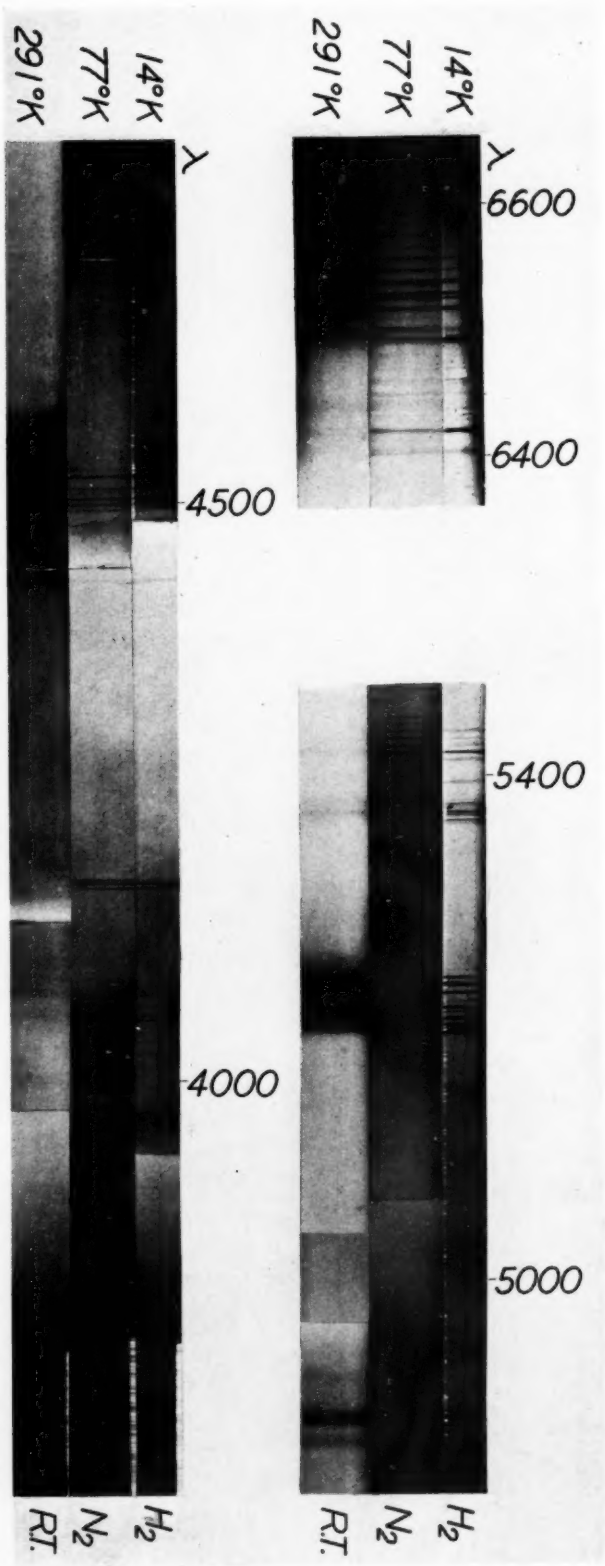

FIG. 1. Conglomerate absorption spectra of $Eu_2(SO_4)_3 \cdot 8H_2O$. On the right are given the substances used to obtain the temperatures given on the left.

TABLE I. *Conglomerate absorption lines of $Eu_2(SO_4)_3 \cdot 8H_2O$ in the visible region of the spectrum.*

Frequencies (cm^{-1}) are given for the temperature indicated; roughly estimated intensities, and characters, are given in the columns marked Int. Intensities are on the scale 0–10; the letters vd, d, nd, s, vs indicate increasing degrees of sharpness. 2? indicates that the line is probably double.

	ν, 291°K	ν, 169°K	ν, 77°K	Int.	ν, 20°K	ν, 14°K	λ, 14°K	Int.
	14886.0							
	14970.0							
	15010.0							
	15105.0							
					15121.0			
L			15131.8	4s	15131.8	15132.0	6606.69	4s
					15138.8			
					15140.2			
L	15166.0	15162.4	15162.7	7s	15161.5	15161.1	6594.03	5s
					15200.5			
H	15205.0	15205.9	15204.2	5s	15203.5	15203.9	6575.45	1
					15206.3			
		15220.9				15216.8	6569.86	0
		15222.7						
L		15225.1	15226.2	3vs	15225.8	15225.5	6566.11	5vs
	15229.0	15228.5						
		15234.2						
L	15246.0	15245.2	15244.7	6s	15245.3	15245.0	6557.70	7vs
	15260.2							
L	15267.6	15267.7	15266.1	8s	15266.2	15266.1	6548.67	6vs
H			15268.8	5s	15269.1	15269.1	6547.37	0
L			15285.4	8vs	15285.7	15285.5	6540.34	8vs
L	15289.8	15290.5	15290.7	8nd	15290.6	15290.6	6538.15	8vs
H			15297.5	1	15297.7	15297.4	6535.24	0
H	15305.5					15302.6	6533.02	0
L		15309.2	15309.8	9nd	15310.0	15310.2	6529.81	9s
L	15318.5	15318.8	15319.0	9nd	15318.6	15318.8	6526.07	8s
						15328.0	6522.21	0
L	15335.0	15336.9	15338.0	9nd	15338.2	15338.5	6517.76	9s
H		15356.5	15355.4	2d				
L	15380.0	15373.9	15376.2	8d	15377.2	15377.2	6501.35	5s
L		15397.3	15395.7	8d	15396.5(2?)	15395.6	6493.58	8s
L						15399.3	6492.01	5
	15409.2							
			15424.9	0				
			15440.5	0				
L			15445.6	0	15449.0	15450.7	6470.43	3vs
L		15451.5	15452.1	1		15452.5	6469.67	3vs
L						15468.1	6463.14	3vs
	15471.5		15472.4	3	15472.1			
L	15474.7				15474.6	15474.3	6460.56	3vs
		15476.5						
L	15478.8		15478.8	1	15478.8	15478.7	6458.69	3vs
L						15480.8	6457.82	3vs
	15484.4							
		15501.4	15498.9	3	15498.9	15497.9	6450.69	2vs
L			15510.6	2	15510.4	15510.8	6445.33	2vs
L	15515.2	15516.7	15515.3	1	15516.5	15516.0	6443.20	3vs
L			15521.2	2	15520.9	15520.3	6441.39	4vs
					15523.1			
L			15528.0	2	15528.4	15528.2	6438.14	4vs
L			15540.0	0	15540.3	15540.1	6433.18	3vs
L			15548.6	1	15548.4	15548.8	6429.59	3
						15560.3	6424.85	1
L	15568.4	15568.6	15569.7	9d	15570.0	15569.8	6420.90	9s
					15578.2			
H			15588.0	4d	15588.0	15589.0	6413.2	0
L	15601.0	15603.4	15607.9	6d	15610.7	15610.2	6404.30	6nd
	18094.0							
	18181.0							
	18240.0							
	18290.0							
			18302.8	2s				
		18344.5						
H	18346.7	18347.6	18346.9	4vs		18347.3	5448.87	0
		18364.5	18360.7	1s				
H	18367.2	18368.9	18369.1	4vs	18367.3	18368.4	5442.62	2vs
L	18388.3	18388.0	18388.5	5vs	18388.0	18388.2	5436.77	6vs
		18391.9						
		18397.5						
	18400.9					18402.5	5432.53	0
H		18406.3	18406.7	7s	18406.5	18407.0	5431.22	1
L	18422.8	18428.7	18428.7	6s	18428.8	18428.8	5424.79	5vs
H	18443.4	18442.0						
L		18447.5	18448.5	8s	18448.3	18448.4	5419.03	10s
						18455.3	5417.00	2vs
		18461.3				18458.8	5415.97	1vs
						18463.2	5414.68	1vs
						18467.5	5413.42	1vs
L		18471.4	18470.5	4vs	18469.5	18470.9	5412.43	4vs
L		18476.9	18476.7	0		18477.7	5410.43	2vs
						18483.6	5408.69	0
		18488.4						
		18496.0						
H	18499.7		18500.5	1				
		18503.0						
		18510.9						
		18513.3						
			18518.8	1		18517.6	5398.77	1vs

	ν, 291°K	ν, 169°K	ν, 77°K	Int.	ν, 20°K	ν, 14°K	λ, 14°K	Int.
		18521.8	18525.2	1	18525.2	18525.3	5396.53	3vs
	18527.8	18528.3						
		18531.2	18532.3	2	18532.2	18532.4	5394.47	4vs
		18534.4						
			18566.1	2		18565.6	5384.97	1
					18572.5	18572.6	5382.79	1
H	18577.9	18577.0	18575.6(2?)	3		18577.0	5381.51	2vs
						18580.4	5380.51	1
L			18585.2	2s	18583.1	18583.8	5379.54	4vs
L		18590.1			18592.1	18592.7	5376.96	4vs
H		18597.2	18596.3	4	18596.5	18596.9	5375.75	3vs
					18600.4	18600.7	5374.66	3vs
L		18606.8	18607.8	3s	18606.6	18606.9	5372.87	3vs
L	18612.2		18615.0(2?)	3	18615.3	18615.7	5370.32	8s
		18618.2						
L	18629.6		18625.3	2	18624.5	18624.7	5367.72	8s
		18634.4						
L		18638.5	18639.7	6	18639.1	18639.4	5363.48	8s
		18644.9						
L		18649.1	18648.4	6	18647.5	18648.1	5361.00	7s
		18656.4						
		18661.0	18660.9	2				
		18665.9						
		18672.2	18670.1	1				
		18675.0						
		18677.5						
		18683.3						
		18688.1						
		18693.2						
		18720.6						
		18735.6						
	18784.0							
	18957.0							
		18964.5						
		18967.5						
	18979.0							
		18998.0						
H		19013.3						
H	19035.4	19033.3	19029.4	4nd				
H		19046.1						
H		19057.6	19055.7	3nd	19057.7	19056.7	5246.03	1vs
H	19075.8	19075.4	19074.4	5vs	19074.2	19074.4	5241.17	2vs
L	19098.1	19098.3	19096.4	8s	19096.1	19095.8	5235.31	9vs
H			19101.5	8s	19101.0	19101.6	5233.72	2vs
					19104.4			
		19108.0			19107.6			
L	19118.5	19116.2	19115.4	9s	19115.5	19116.0	5229.76	10s
L, H		19124.1	19122.6	5vs	19122.2	19123.0	5227.85	5vs
H		19131.2	19132.0	2	19131.0			
		19137.8						
L	19142.7	19144.0	19143.0(2?)	6d	19142.1	19142.5	5222.56	10vs
H		19160.6	19155.8	2nd				
L, H	19168.2	19168.2	19167.3	5vs	19166.8	19167.3	5215.78	4vs
H		19177.7	19176.6	4s	19176.8	19176.6	5213.25	1
L	19184.0	19186.7	19186.5	9s	19186.6	19186.9	5210.45	10s
L, H	19200.7	19200.7	19200.1	9s	19199.0	19199.5	5207.03	4vs
L	19220.0	19219.9	19218.2	8s	19217.5	19217.9	5202.05	10vs
H			19222.1	7s	19222.3	19222.6	5200.77	3vs
L	19240.0	19242.0	19241.9	9s	19241.6	19241.7	5195.61	10s
L	19259.2	19260.2	19261.1	9s	19261.3	19261.2	5190.34	10s
					19269.8			
	20252.4							
	20292.6							
	20374.0		20362.3	1				
			20391.3	1				
	20430.0		20424.4	1				
					20434.5			
		20448.5						
		20451.9	20455.3	1	20450.4			
H	20471.9	20469.3	20468.1	5s	20467.4			
		20475.8						
		20480.0				20481.9	4881.01	2
		20484.7						
L		20490.8	20490.3	7s	20489.5	20489.6	4879.18	5vs
H	20494.2	20499.1	20498.6	6s	20498.7	20498.5	4877.05	2
L		20509.6	20509.2	7vs	20509.3	20509.0	4874.55	6vs
L	20524.4	20521.0	20520.2	8s	20520.5	20520.7	4871.78	6vs
L	20542.0	20540.0	20540.1	8s	20540.1	20539.9	4867.22	6vs
L		20561.9	20560.4	3s	20560.8	20560.8	4862.27	4vs
					20567.3			
		20571.0			20570.8			
			20576.8	3s	20576.6	20577.2	4858.40	3vs
	20579.0	20582.3	20585.7	3s	20586.3	20587.1	4856.06	3vs
		20592.4	20595.6	4s	20594.9	20594.7	4854.27	4vs
		20598.3	20601.6	3s				
	20603.1					20603.7	4852.14	3vs
		20606.2	20607.2	3s	20606.2(2?)	20608.5	4851.02	3vs
	20616.6		20614.5	3s	20614.1	20614.2	4849.68	4vs
		20624.3	20625.6	3s	20624.7	20625.5	4847.03	4s

TABLE I. (*Continued.*) *Conglomerate absorption lines of* $Eu_2(SO_4)_3 \cdot 8H_2O$ *in the visible region of the spectrum.*

	ν, 291°K	ν, 169°K	ν, 77°K	Int.	ν, 20°K	ν, 14°K	λ, 14°K	Int.
	20674.9		20678.7	2s	20678.2	20678.6	4834.57	3vs
					20684.0	20686.0	4832.9	1
		20690.6						
		20695.9	20694.6	1nd	20694.3	20695.5	4830.63	2s
		20700.8						
		20707.7						
		20715.0						
	20759.0							
	20842.0							
	20909.0					20967.7	4767.92	1
					21040.5			
						21049.3	4749.43	1
		21055.4						
		21059.9						
		21065.5	21065.0	1s				
		21073.9						
		21080.7	21078.2	2s				
					21086.8			
		21089.9	21089.0	1s		21089.5	4740.38	1
					21096.2			
		21104.4	21104.7	2s	21108.5	21106.4	4736.58	3s
		21116.6			21117.9			
					21122.9			
			21131.2	2s	21132.4	21132.1	4730.81	2s
		21137.9						
					21142.5	21142.2	4728.56	0
					21146.6			
		21157.4			21152.6	21152.7	4726.22	2
		21296.7			21302.4			
					21315.7			
					21323.7			
			21327.8	1vs				
					21338.6	21338.9	4684.98	0
	21345.6		21348.7(2?)	2	21349.0	21348.3	4682.91	2
					21356.0	21354.8	4681.49	1
			21365.5(2?)	1	21366.2	21365.7	4679.10	1
					21377.7			
					21384.0			
					21391.7			
					21407.2			
		21413.7						
		21418.6						
		21422.4						
		21425.6						
		21434.7						
		21443.0						
		21450.6						
		21457.2						
		21475.9						
		21490.4						
			21509.1	1nd		21511.3	4647.42	1
	21539.9		21534.6	1nd		21535.1	4642.29	1
H	21717.1							
H	21842.3							
H	21898.6							
H	21959.0							
			21992.3	0				
H	22015.3		22015.0	1nd				
						22040.5	4535.83	2
			22048.5	1nd	22046.3			
			22060.3	1nd	22057.3	22055.1	4532.83	2
						22077.2	4528.27	2
	22078.0	22081.2	22079.9	2nd	22079.7			
		22092.6	22087.3	1nd	22088.9	22087.0	4526.29	1
					22098.6	22097.5	4524.14	1
		22104.7						
L		22105.7	22107.3	5s	22108.8	22108.9	4521.80	5s
L	22112.5		22114.3	3s	22115.6	22114.8	4520.59	4s
H		22132.8	22128.0	2s				
		22141.7						
					22145.0	22147.0	4514.0	0
L	22153.7	22156.1	22155.4	6s	22155.6	22155.7	4512.24	5vs
L		22166.9	22167.4	2	22167.5	22167.1	4509.93	5vs
L	22177.1	22176.9	22177.0	4s	22176.1	22176.3	4508.05	5vs
					22183.5			
					22187.7			
					22191.2			
L	22196.3	22195.1	22196.7	6s	22196.6	22196.1	4504.03	6vs
		22200.9						
		22207.8	22209.1	1				
L		22215.8	22215.1	4s	22216.0	22215.6	4500.08	5vs
L	22220.7	22220.9	22221.7	6s	22221.4	22221.3	4498.93	5vs
L	22241.4	22237.0	22241.1	6vs	22241.3	22241.0	4494.95	6vs
			22297.0	3d	22297.0			
	22305.0							
			22319.8	3d				
					22326.0			
		22485.0						
		22492.0						
		22500.9						
		22508.2						
		22513.7						

	ν, 291°K	ν, 169°K	ν, 77°K	Int.	ν, 20°K	ν, 14°K	λ, 14°K	Int.
		22519.0	22520.5	2nd				
		22529.2						
		22535.5	22535.5	2nd				
		22541.2				22539.6	4435.39	1vs
	22549.1	22546.9	22546.6	2nd				
		22551.8						
	22573.0	22570.1	22569.2	2nd		22569.4	4429.53	1
						22577.8	4427.90	1
			22588.6	5vs	22590.4	22590.6	4425.39	5vs
		22592.7						
	22597.5		22597.4	1s	22595.8			
					22599.7	22598.5	4423.84	3vs
						23368.2	4278.12	1
						23449.3	4268.33	1
	23717.0							
H	23855.0		23875.9	1		23881.4	4257.49	1
H			23897.5	1				
H			23922.5	1		23921.1	4179.23	1
H			23947.2	1	23946.8			
H			23955.0	1	23957.7			
L		23965.5	23964.1	6vs	23965.2	23964.6	4171.66	4vs
L		23973.2	23973.4	4vs	23974.0	23973.3	4170.14	4vs
L	23978.0	23981.8	23983.1	6s	23983.9	23983.4	4168.38	5vs
		23990.3				23995.8	4166.23	2nd
L		24009.9	24005.5	6s	24007.8	24007.8	4164.14	4vs
			24013.9	2				
		24018.8						
	24029.0	24025.1	24032.8	1		24033.4	4159.71	1
		24041.1	24046.9	1				
						24064.9	4154.26	1
			24108.2	1		24103.3	4167.65	1
	24184.0							
	24268.0							
			24416.8	0				
H		24422.9	24423.6	0				
			24429.0	0				
H			24452.7	1				
H			24470.7	1				
	24477.0	24478.9						
			24486.2	0				
			24498.0	0				
		24502.6	24505.2	1				
H	24512.2	24513.1	24514.8	3s				
		24518.0						
H	24521.7		24521.0	2s				
		24528.9	24528.5	0	24528.0			
					24532.0			
H		24537.4	24537.3	5s	24536.2	24536.2	4074.47	1vs
	24542.4				24541.1	24540.5	4073.75	1vs
			24546.8	2	24548.0	24547.7	4072.56	1vs
L	24555.1	24555.9	24556.0	6s	24556.3	24555.8	4071.22	4vs
		24564.6						
H			24578.2	3s	24577.2			
			24585.7	0				
L	24595.3	24595.0	24597.2	4s	24598.5	24598.5	4064.14	4vs
					24602.9			
		24614.1			24611.5			
			24617.9	1	24618.9			
			24624.7	0	24626.6			
		24630.2	24629.9	1				
L			24637.1	4s	24637.6	24637.0	4057.80	5vs
L	24649.2	24651.3	24651.4	5s	24652.1	24651.6	4055.39	4vs
	24666.0							
L		24671.7	24670.8	5s	24671.8	24670.7	4052.25	6vs
		24685.1						
		24704.5						
		24715.2						
		24724.9						
H	24790.0	24808.3						
					24834.2			
		24843.8						
L	24856.0	24855.8	24852.8	4s	24851.9	24851.9	4022.67	4s
		24868.4						
		24881.4			24878.5			
		24889.8						
		24897.5			24899.3			
		24904.9						
		24914.3	24911.5	2nd				
						24916.6	4012.26	1
			24934.5	2nd	24934.0	24937.0	4009.0	1
		24941.7						
	24946.0	24949.0						
		24956.6	24956.7	2nd		24956.0	4005.92	1
			24969.9	1s		24967.7	4004.04	1
		25004.3				25004.5	3998.16	1
		25017.1	25020.0	0	25017.0			
		25025.5						
		25048.8						
		25064.8			25057.0			
					25114.0			
L			25157.2	1s	25158.2	25157.2	3973.89	3vs
	25280.0		25286.6	0				

TABLE I. (*Continued.*) *Conglomerate absorption lines of* $Eu_2(SO_4)_3 \cdot 8H_2O$ *in the visible region of the spectrum.*

	ν, 291°K	ν, 169°K	ν, 77°K	Int.	ν, 20°K	ν, 14°K	λ, 14°K	Int.
L			25306.1	0	25309.1	25309.8	3949.93	3s
	25361.0							
			25520.1	0	25523.2			
					25531.5			
			25541.5	1s	25541.3	25541.7	3914.06	0
L			25563.1	2s	25563.5	25563.5	3910.72	4vs
					25573.4			
			25580.7	1s	25581.1	25581.6	3907.96	1
L			25602.8	2s	25602.0	25602.9	3904.70	3vs
L			25627.1	2s	25627.7	25626.8	3901.07	3vs
					25634.4			
					25641.3			
					25666.4	25663.7	3895.45	1s
			25706.6	1nd	25706.9	25707.0	3888.89	2s
			25743.8	1s	25747.1			
L			25767.2	1s	25766.8	25766.5	3879.92	2s
			25783.1	0	25780.5			
	25795.0		25793.7	0	25792.6			
			25814.8	1	25812.0	25813.0	3872.9	2
			25832.1	0				
			25839.8	0	25838.0	25840.0	3868.9	2
			25844.6	0				
			25851.4	0	25850.9			
					25857.8			
			25865.4	0	25868.0	25869.0	3864.6	1
			25879.4	0	25885.0	25883.0	3862.4	1
					25887.0			
						25896.0	3860.6	1
					25900.0			
			25903.8	0	25908.0	25905.0	3859.2	1
			25913.1	0	25913.9	25914.4	3857.77	0
			25922.1	0	25924.0	25921.0	3856.8	0
					25934.0			
			25940.3	0				
	26198.0							
H		26247.2						
H		26278.2	26271.0	2s				
			26286.7	1s				
H		26297.9	26296.7	0				
		26306.5	26303.2	0				
		26309.3			26308.6			
H		26316.8	26316.7	2s	26317.0	26317.9	3798.62	1
		26324.5			26324.4			
H		26330.3	26328.9	2s	26330.0	26330.8	3796.76	0
L		26339.0	26338.6	2s	26339.1	26339.1	3795.57	3vs
					26346.1	26345.9	3794.58	0
H		26356.8	26355.4	2d	26352.2	26351.8	3793.73	1vs
L					26359.0	26358.2	3792.81	4vs
L	26365.0				26372.2	26371.6	3790.89	4vs
		26376.4	26377.8	2d	26378.7			

	ν, 291°K	ν, 169°K	ν, 77°K	Int.	ν, 20°K	ν, 14°K	λ, 14°K	Int.
		26400.3	26400.3	2s	26399.9	26399.5	3786.88*	2vs
					26407.4			
L		26420.4	26421.5	2d	26419.2	26418.8	3784.11	4s
					26434.3			
		26448.7	26446.5	1s	26447.3	26446.7	3780.12	1s
					26456.2			
L		26464.7	26462.0	2d	26467.6	26467.8	3777.11	4s
		26482.3	26481.3	1	26483.1	26484.5	3774.73	0
L		26502.2	26500.8	2nd	26501.9	26502.7	3772.13	4s
L		26522.1	26522.7	2nd	26522.3	26522.3	3769.35	3s
L	26534.0	26543.0	26541.5	2d	26543.1	26542.8	3766.43	4s
			26672.4	0				
			26705.0	0		26706.3	3743.39	0
					26774.5			
					27272.3			
					27288.0			
					27301.3			
		27318.5	27312.3	1s	27314.9	27314.1	3660.07	1
					27323.8			
L		27340.8	27334.2	1s	27335.7	27335.3	3657.24	2vs
					27345.2			
L		27357.7	27353.1	1s	27356.0	27356.1	3654.45	2vs
L		27377.1	27377.7	1s	27377.7	27377.0	3651.66	3vs
			27388.7	1s	27384.0	27386.0	3650.5	0
		27393.4			27392.4	27392.5	3649.60	0
		27401.0	27400.0	1	27401.0	27402.0	3648.3	1
			27410.0	0	27411.0	27412.0	3647.0	1
		27420.0	27421.0	0	27419.0	27420.0	3645.9	1
		27432.0	27433.0	0	27431.0			
		27440.5			27440.7	27440.9	3643.16	2
					27444.1			
		27454.6	27451.5	1s	27452.4	27451.4	3641.77	2s
					27457.4	27456.9	3641.04	2s
			27464.0	0	27463.0			
		27470.0	27470.0	0	27474.0	27472.0	3639.1	2
			27477.0	0		27476.5	3638.44	2s
			27485.0	0	27488.8			
		27493.0	27504.0	0				
					27510.0	27510.3	3633.97	2s
					27600.1			
					27609.0	27610.0	3620.8	1
					27618.0			
					27629.0	27629.0	3618.3	0
					27638.0			
					27649.0	27649.0	3615.8	0
			27661.0	0	27653.0			
			27673.0	0				
			27694.0	0				
					27926.0			
					27971.0			
					28090.0			

ment (0.2–0.3 cm^{-1}). Although in many salts of Sm^{+++} and Gd^{+++}, there seems to be a real shift to longer wave-lengths at lower temperatures, there appears to be no such marked shift in this salt of Eu^{+++}.

Variations in intensity with change of temperature may be noted in every group of lines, the most striking result being the pronounced increase in intensity of the red-most side of the group as the temperature is raised. In explaining this behavior one assumes that lines intense at the lowest temperature ("L.T.") originate in transitions between the basic level and excited upper levels, since at 14°K any excited state (except one very close to the basic one) must have a very small population. Those lines which are very faint or entirely absent at 14°K, and which increase in intensity with the temperature ("H.T.") may be interpreted as originating in transitions from levels close to the basic one, to the same excited upper levels. Evidently one must expect to find constant energy differences (corresponding to the separations of the low-lying levels from the basic one) between "L.T." and "H.T." lines.

Evidence for levels at 21 cm^{-1} and 41 cm^{-1} above the basic one is given in Table II (for hydrogen temperatures) and in Table III (for nitrogen temperature); it is reasonably certain that levels also exist at 67 cm^{-1} and at 86 cm^{-1}, although the evidence is less satisfactory. In addition, higher levels at 100–200 cm^{-1} seem to be indicated; and two very diffuse lines appearing at room temperature are over 350 cm^{-1} from the nearest low temperature line. It is, however, not possible to determine definitely these higher levels.

The occurrence (described later in more detail) of a separation, in a number of pairs of L.T. lines, approximately equal to the difference of

TABLE II. *Averages of values at 14°K and 20°K.*

L.T.	H.T.	$\Delta\nu_1$	L.T.	H.T.	$\Delta\nu_2$
			15161.3	15121.0	40.3
15225.7	15203.7	22.0			
			15245.2	15206.3	38.9
15290.6	15269.1	21.5			
15318.7	15297.6	21.1			
15520.6	15498.4	22.2			
15610.5	15588.5	22.0			
18388.1	18367.9	20.2	18388.1	18347.3	40.8
18428.8	18406.8	22.0			
18592.4	18572.6	19.8			
18615.5	18596.7	18.8	18615.5	18577.0	38.5
19096.0	19074.3	21.7	19096.0	19057.2	38.8
			19142.3	19101.3	41.0
19186.8	19167.1	19.7			
19199.3	19176.7	22.6			
19241.7	19222.5	19.2			
			20489.6	20450.4	39.2
			20509.2	20467.4	41.8
20520.6	20498.6	22.0			
			20625.1	20586.3	38.8
22599.1	22577.8	21.3			
			23964.9	23921.1	43.8
24556.1	24536.2	19.9			
24598.5	24577.2	21.3			
25563.5	25541.5	22.0	25563.5	25523.2	40.3
25602.5	25581.4	21.1			
26339.1	26317.5	21.6			
26371.9	26352.0	19.9	26371.9	26330.4	41.5
26399.7	26378.7	21.0			
26467.7	26446.7	21.0			
27335.5	27314.5	21.0			
Average = 21.0 cm^{-1}			Average = 40.3 cm^{-1}		

TABLE III. *Values at 77°K.*

L.T.	H.T.	$\Delta\nu_1$	L.T.	H.T.	$\Delta\nu_2$
15226.2	15204.2	22.0			
15290.7	15268.8	21.9			
15319.0	15297.5	21.5			
			15395.7	15355.4	40.3
15521.2	15498.9	22.3			
15607.9	15588.0	19.9			
18388.5	18369.1	19.4	18388.5	18346.9	41.6
18428.7	18406.7	22.0			
18615.0	18596.3	18.7			
19096.4	19074.4	22.0	19096.4	19055.7	40.7
			19143.0	19101.5	41.5
19186.5	19167.3	19.2			
19200.1	19176.6	23.5			
19241.9	19222.1	19.8			
			20509.2	20468.1	41.1
20520.2	20498.6	21.6			
			20625.6	20585.7	39.9
			22167.4	22128.0	39.4
			23964.1	23922.5	41.6
24556.0	24537.3	18.7	24556.0	24514.8	41.2
24597.2	24578.2	19.0			
			24670.8	24629.9	40.9
25563.1	25541.5	21.6	25563.1	25520.1	43.0
25602.8	25580.7	22.1			
26338.6	26316.7	21.9			
27334.2	27312.3	21.9			
Average = 21.0 cm^{-1}			Average = 41.0 cm^{-1}		

the 21 and 41 cm^{-1} levels, in some cases has made difficult the decision as to with which member of the pair a given H.T. line should be associated. It is believed, however, that a reasonably certain choice may be made by the comparison of calculated populations and observed intensities by using especially the data for 14°K and 20°K.[6]

[6] It is perhaps noteworthy that, when one plots the frequencies of occurrence of residuals from the average of the 21.0 cm^{-1} level, one does not find a true error curve; the lines seem to fall into two groups separated by about 2 cm^{-1} at 20°K. This is a quite unexpected result; but the splitting cannot be regarded as definitely proven. It seems not to exist in the 41 cm^{-1} level.

An unusual feature of the spectrum appears in the separation of certain L.T. lines. One expects these lines to give essentially the energy level diagram of the excited states, assuming that they originate at a common basic level. In this case, in the 15,000 cm^{-1} group, one finds 4 pairs of L.T. lines separated by very nearly the same interval, and in every other group but one, one or more similar pairs. Table IV gives the evidence.

TABLE IV. *Constant separation of low temperature lines.*

(Frequencies are the averages of 14°K and 20°K measurements; intensities are those for 14°K.)

L.T.$_1$	Int.	L.T.$_2$	Int.	$\Delta\nu$
15245.2	7	15225.7	5	19.5
15285.6	8	15266.2	6	19.4
15310.1	9	15290.6	8	19.5
15338.4	9	15318.7	8	19.7
18448.4	10	18428.8	5	19.6
19115.8	10	19096.0	9	19.8
19261.3	10	19241.7	10	19.6
20509.2	6	20489.6	5	19.6
20540.0	6	20520.6	6	19.4
22215.8	5	22196.4	6	19.4
22241.2	6	22221.4	5	19.8
23983.7	5	23964.9	4	18.8
24671.3	6	24651.9	4	19.4
26358.6	4	26339.1	3	19.5
26522.3	3	26502.3	4	20.0
27356.1	2	27335.5	2	20.6
			Average = 19.6 cm^{-1}	

This effect was not found in the Sm^{+++} salts.

One may assume (in the 15,000 cm^{-1} group for example) that the levels in the excited state are separated by exactly the same amount, and that the same interval occurs elsewhere; it seems much more reasonable to ascribe the existence of this constant difference to the basic level. The troublesome feature is that in every case the members of the pair are of about the same intensity, so that, if the upper level of the assumed doublet has at 14°K the population determined by the Boltzmann distribution, its statistical weight must be 5 or 10 times greater than that of the lower level; if the statistical weights are of the same order of magnitude, then the upper level cannot have an equilibrium population. Because of the relatively low intensities of some of the pairs (4 or 5 on the scale 0–10), one cannot escape the fact of approxi-

mately equal intensities (and say that one member is really much stronger) by assuming that the transition probabilities are so high, that each line is completely absorbed in the light path in the conglomerate.

Because of this uncertainty, it has not been considered advisable at present to draw an energy level diagram.

Conclusions

The existence of levels at 21 cm^{-1} and 41 cm^{-1} above the basic one has been proven; the probable existence of higher levels is indicated. These levels must yet be regarded as of uncertain origin. The existence of a constant energy difference between "low temperature" lines is described.

OCTOBER, 1935 JOURNAL OF CHEMICAL PHYSICS VOLUME 3

The Vapor Pressure of Barium

Erik Rudberg and Joseph Lempert, *Massachusetts Institute of Technology*

(Received July 1, 1935)

The vapor pressure of barium has been determined for temperatures from 525 to 750°C by a method based on molecular effusion. The metal was obtained by decomposition of barium azide in vacuum. The evaporated deposits were determined by microtitration to about 10^{-8} mole. The values obtained for the pressure range from 5×10^{-5} to 2×10^{-2} mm. They are well represented by the equation: $\log p$ (in mm) $=6.99-8980/T$. This corresponds to a latent heat of evaporation of 4.09×10^{4} cal. mole.

Introduction

DATA on the vapor pressure of metals are very useful in work on thin metal films, since one of the simplest methods of obtaining such films is that of evaporation in vacuum. If a knowledge of the thickness of the deposit is required, it is mostly necessary to know the rate of evaporation from the source as a function of the temperature. For relatively volatile metals of low ionization potential such as the alkali metals, the ionization method of Langmuir and Kingdon[1] has been used down to very low values of pressure. Accurate measurements have been made for Hg, Cd, Zn and some others, including alkali metals, by using the Knudsen method[2] of molecular effusion. In these cases the temperatures are so low, that the metal can be placed in direct contact with the glass wall of the tube and its temperature controlled from the outside by a suitable furnace. Vapor pressure values for a number of the less volatile metals, have been computed by Langmuir[3] and his collaborators[4] from measurements of the rate of evaporation from filaments. To obtain the vapor pressure from such data, one must know the reflection coefficient r of the emitting surface for atoms of the vapor in equilibrium with the metal. This quantity has not, in general, been determined by direct experiments. In the work referred to, r was assumed to be negligible compared with unity. In the effusion method the uncertainty about r is eliminated, since here the rate of evaporation is measured from a hole in the wall of an enclosure containing the metal. The relation between such a source and a filament source is clearly similar to that between a "hohlraum" black body emitter and a plane surface of the same temperature in thermal radiation: the emissivity of the surface corresponds to the quantity $1-r$, the accommodation coefficient, in the case of evaporation. Recently one of us has reported some new vapor pressure determinations for calcium, using a method based on molecular effusion.[5] In continuation of this work, we have now measured vapor pressures for barium by the same method but with a new, improved apparatus.

[1] Langmuir and Kingdon, Proc. Roy. Soc. **A107**, 61 (1925).
[2] Knudsen, Ann. d. Physik **29**, 179 (1909).
[3] Langmuir, Phys. Rev. **2**, 329 (1913).
[4] Jones, Langmuir and Mackay, Phys. Rev. **30**, 201 (1927).
[5] Rudberg, Phys. Rev. **46**, 763 (1934).

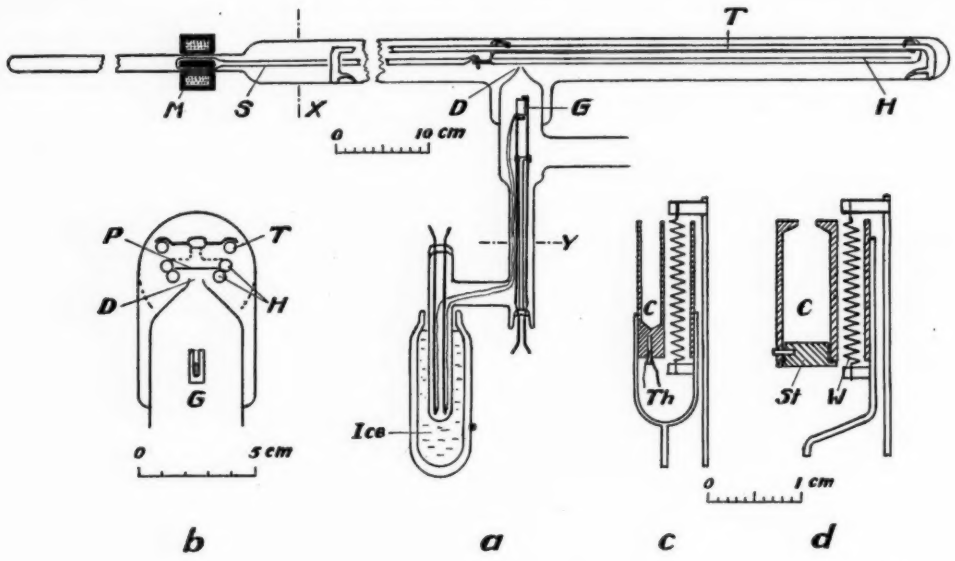

FIG. 1.

APPARATUS

Fig. 1 is a diagram of the essential parts of the apparatus. It consists of a big T-tube, shown from the side in *a*; *b* is an enlarged section through the central part of the T. The metal evaporates from a hole in the top of the heated gun *G*, and a well-defined beam of atoms, limited by the diaphragm *D*, enters the horizontal part of the tube. This part has a long plateholder *H*, made of glass rod, which can be loaded with some twenty microscope cover glass plates *P*. The plateholder rests on two glass tracks *T*, sealed to the main tube; by means of the slider *S*, operated from the outside by the magnetic coil *M*, the plateholder can be moved along the tracks and any one of the plates exposed to the beam emerging from *D*. The tube can be cut open at *X* and *Y* for removal of the plates and reloading of the gun.

Two different constructions have been used for the barium gun. Vertical sections of these are shown in *c* and *d*. In each case the gun is made of a piece of molybdenum rod (shaded in the figure), heated by radiation from a tungsten spiral *W*. The barium is contained in *C*. The thermocouple *Th* of chromel/platinum wire, 6 and 5 mils, respectively, is shown with the smaller gun, which is practically identical with the one previously used in the work on calcium. In the larger gun the thermocouple was introduced in a similar fashion, but from the side. This gun has a larger container with a stopper *St* at the bottom to facilitate loading.

EXPERIMENTAL PROCEDURE

It was impractical to load the gun directly with metallic barium, because of the rapidity with which the metal reacted with the air. Instead the gun was filled with barium azide BaN_6, which was subsequently decomposed by heating in vacuum into barium and nitrogen. The azide was made by passing gaseous HN_3, obtained from sodium azide and sulfuric acid, through a suspension of barium hydroxide in water under reduced pressure, as recommended by Hoth and Pyl.[6] The crystallized product was washed with alcohol on the filter and kept in a vacuum desiccator.

After the tube had been assembled and a vacuum of the order of 10^{-6} mm obtained, the temperature of the gun was raised very slowly, while the ionization gauge was closely watched for a rise in pressure. As soon as the decomposition started, the heating current was lowered or turned off. The speed of the reaction could be followed from the gauge indications and con-

[6] Hoth and Pyl, Zeits. f. angew. Chem. **42**, 888 (1929).

trolled by varying the heating current. In order to get a good yield of barium it was found necessary to control the reaction rate rather carefully, since a sudden local rise in pressure at the bottom of the container C would easily blow the fluffy powder of azide out of the gun. The danger of this is greatest at the start of the reaction. The time required for the decomposition of an azide charge was usually of the order of 1 to 2 hours. At the end of this time the temperature was gradually raised to values above 500°C. The entire tube was then baked at 400°C after which the pressure was of the order of 10^{-7} mm. The gun was now heated and some barium allowed to distil. This should have removed any small amounts of more volatile impurities that might have been present. For this first evaporation it was usually found necessary to bring the temperature up to the melting point of barium, before the metal would start to evaporate. Once this had been done, however, barium could be distilled at any time and at any temperature, without further melting. It thus appears as if the powdered metal resulting from the decomposition of the azide were covered with some impervious skin, which is removed by melting the metal. It was found that the capacity of the small gun was not large enough to allow all the plates P to be utilized with a single charge of the gun. The larger gun was designed to provide a greater capacity. However, tests showed that there was a considerable loss of barium with this gun, due to leakage at the stopper when the metal was melted, so that the number of exposures obtained from a single charge was about the same as with the smaller gun.

When an exposure was to be made, the gun was first heated until the steady temperature required had been attained. The plateholder was then moved so as to expose the desired plate to the beam. After a measured length of time, during which the temperature was kept sensibly constant, the plate was removed from the beam in the same manner.

The temperature of the gun could be kept constant to about 0.3°C. The chromel/platinum thermocouple was calibrated before assembly, with the freezing points of Cu, Al and Zn as standards. During the calibration the thermocouple was protected by a sealed quartz tube, containing hydrogen at a pressure of about 5 cm; the tube had been drawn into a thin-walled capillary at the hot junction end.

The barium deposits on the plates appeared with very sharp defining edges, except for the one at 750°C, which showed a slightly diffuse edge. No deposits could be detected on neighboring parts of the tube not directly exposed to the beam. This indicates that there was no appreciable reflection of atoms from the plates. In transparent light the deposits showed a deep black color, in contrast to the films of calcium which are blue. At a thickness of some 50 atom layers the barium deposits became visible. Through a completed exposure, which in general had about 1000 layers, the lighted filament of the gun could still be seen. When air was admitted to the tube, the deposits turned white almost instantaneously. To determine the amount of barium on a plate the method already used with calcium was adopted. The plate was placed in 2 cc of $0.001n$ HCl, which was then heated to boiling. In this way all the barium, whether present as metal, BaO, $Ba(OH)_2$ or $BaCO_3$, was dissolved, and an equivalent amount of HCl neutralized. This was determined after cooling by titrating the excess acid in the solution with $0.002n$ NaOH. The plates as well as all other glassware had been aged by boiling in HCl before use, in order to avoid errors due to alkali dissolved from the glass. As a further precaution several unexposed plates were taken from the plateholder and treated in the same way as the others, each time that deposits were analyzed. The mean value obtained from these blanks was actually used to find the number of Ba-equivalents in any particular sample for which the excess acid had been determined.

Results

The quantity measured in these experiments is dN/dt, the number of moles emitted per second from the opening δs in the gun, at temperature T, into a solid angle δo (defined by the size and position of D with respect to G) in a direction making an angle θ with the normal to δs. From this the pressure p of the vapor in G can be computed:

TABLE I.

No.	°C	SEC.	cc NaOH	NORMALITY	MOLE Ba ($\times 10^7$)	MOLE Ba/sec. $=dN/dt$
2.08	525	45000	0.071	0.00182	0.65	1.43×10^{-12}
1.06	550	37800	0.175	0.00190	1.66	4.40×10^{-12}
3.10	550	28800	0.179	0.00172	1.54	5.34×10^{-12}
2.10	575	18000	0.119	0.00182	1.08	6.01×10^{-12}
1.02	600	9000	0.161	0.00190	1.53	1.70×10^{-11}
3.16	610	5400	0.184	0.00172	1.58	2.93×10^{-11}
2.14	625	7200	0.191	0.00182	1.74	2.43×10^{-11}
4.13	650	3600	0.108	0.00187	1.01	2.81×10^{-11}
3.13	650	4500	0.250	0.00172	2.85	4.78×10^{-11}
1.15	650	2760	0.145	0.00190	1.38	5.00×10^{-11}
2.15	675	1500	0.120	0.00182	1.09	7.27×10^{-11}
4.14	700	900	0.129	0.00187	1.21	1.34×10^{-10}
4.16	700	900	0.149	0.00187	1.39	1.55×10^{-10}
2.18	725	480	0.112	0.00182	1.02	2.12×10^{-10}
1.19	750	240	0.138	0.00190	1.31	5.47×10^{-10}

TABLE II.

No.	°C	T	$10^{-6}\times A$	p (mm)	log p	$10^3\times 1/T$
2.08	525	798	1.323	5.34×10^{-5}	0.728−5	1.253
1.06	550	823	1.035	1.31×10^{-4}	0.117−4	1.215
3.10	550	823	0.991	1.52×10^{-4}	0.182−4	1.215
2.10	575	848	1.323	2.32×10^{-4}	0.366−4	1.176
1.02	600	873	1.035	5.22×10^{-4}	0.718−4	1.145
3.16	610	883	0.991	8.65×10^{-4}	0.937−4	1.131
2.14	625	898	1.323	9.65×10^{-4}	0.985−4	1.111
4.13	650	923	1.653	1.22×10^{-3}	0.088−3	1.084
3.13	650	923	0.991	1.44×10^{-3}	0.158−3	1.084
1.15	650	923	1.035	1.57×10^{-3}	0.196−3	1.084
2.15	675	948	1.323	2.97×10^{-3}	0.473−3	1.059
4.14	700	973	1.437	6.01×10^{-3}	0.779−3	1.028
4.16	700	973	1.437	6.94×10^{-3}	0.841−3	1.028
2.18	725	998	1.323	8.86×10^{-3}	0.947−3	1.002
1.19	750	1023	1.035	1.81×10^{-2}	0.258−2	0.978

$$p=(dN/dt)(2\pi MRT)^{\frac{1}{2}}\pi/\delta s\delta o\cos\theta$$

or $$p\text{ (in mm)}=AT^{\frac{1}{2}}dN/dt,$$

where

$$A=7.501\times10^{-4}(2\pi MR)^{\frac{1}{2}}\pi/\delta s\delta o\cos\theta.$$

Here M is the molecular weight for the vapor and R the gas constant pro mole. This equation holds provided the dimensions of the hole in the gun are small compared to the mean free path in the vapor, so that the process is one of molecular effusion.

The results of the analysis are given in Table I; the pressures calculated from these data are listed in Table II. Four different sets of exposures were taken. Of these the last one was obtained with the larger gun. In each case the first figure in the plate number stands for the particular set to which the plate belongs; the remaining two give the position of the plate on the holder. The different sets have somewhat different A-values as listed in Table II, mainly because the vertical distance between G and D, which enters in δo, varied. This distance was determined with a cathetometer; the values found were 2.77, 2.75, 2.71 and 3.17 cm for the four sets. The opening D had a diameter of 0.421 cm. The angles, which were only estimated, were usually negligible, never exceeding 8°. The diameter of the circular hole δs was 0.207 cm for the small gun, and 0.202 cm for the large one. In the second set the area of the hole was reduced 25 percent by a speck of oxide, resulting from an accident when the barium azide was decomposed. The high A value for No. 4.13 is due to a lateral shift of the plateholder, which reduced the effective solid angle for this exposure.

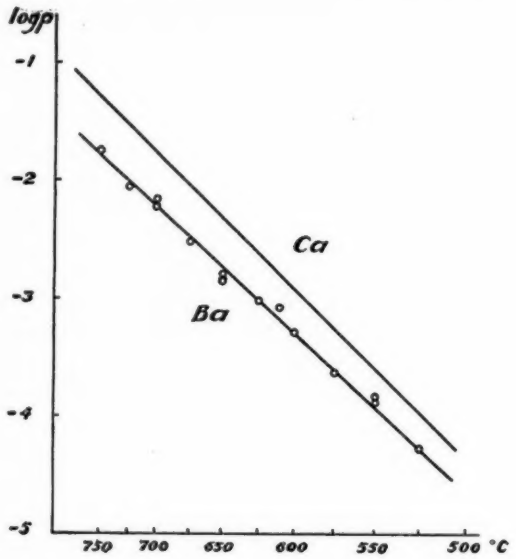

FIG. 2.

DISCUSSION

From the magnitude of the pressures listed in Table II it is evident that the condition that the mean free path be large compared with the dimensions of the hole is fulfilled over this range, except perhaps for the highest point. The mean free path in the vapor at 750°C is about 0.6 cm. The fact that the edge of the deposit was slightly diffuse in this exposure may thus be an indication of collisions between atoms in the beam. It could, however, also be due to a very small amount of reflection of atoms from D at this temperature.

In Fig. 2 the values of log p from Table II have been plotted in the usual manner against an abscissa proportional to $1/T$. The straight line drawn was computed from the same data, assuming a linear relationship. Its equation is: $\log p = 6.99 - 8980/T$. The points obtained fit this line fairly well; the mean deviation from the line corresponds to an error of about 10 percent in the value of p. In computing this equation the values at 750 and 725°C, which will be seen to fit the line quite well, were also included. Actually these temperatures are above the melting point of barium, 710°C.[7] Hence these points correspond to the vapor pressure over liquid barium and should therefore, strictly speaking, fall on a different line, intersecting the one for the solid at the melting point. Evidently the heat of fusion is so small compared to the heat of evaporation, that the change of slope is far beyond detection with the limited accuracy of these measurements.

[7] Rinck, Comptes rendus **193**, 1328 (1931).

We have also included in Fig. 2 a line representing the vapor pressure of calcium obtained in the previous work by one of us.[5] It will be seen that the calcium pressures are 2 to 3 times higher than those of barium for the same temperature in this range. From the slope of the barium curve the latent heat of evaporation is 4.09×10^4 cal./mole, a value somewhat smaller than that for calcium, *viz.*, 4.31×10^4 cal./mole. As in the case of calcium the vapor pressures for barium of from 12.5 to 26.5 mm in a small range near 1100°C, obtained by Hartmann and Schneider,[8] using the boiling point method, are higher than one would expect from these low pressure measurements by the method of molecular effusion. Unfortunately there are no reliable data for the specific heat of barium. It is therefore not possible to compute the heat of evaporation at $T=0$ and the vapor pressure constant from these measurements at present.

[8] Hartmann and Schneider, Zeits. f. anorg. u. allg. Chem. **180**, 275 (1929).

OCTOBER, 1935 JOURNAL OF CHEMICAL PHYSICS VOLUME 3

The Thermal Equilibrium Between Ethylene Iodide, Ethylene and Iodine

G. R. CUTHBERTSON AND G. B. KISTIAKOWSKY, *Mallinckrodt Chemical Laboratory, Harvard University*

(Received July 26, 1935)

The thermal equilibrium between ethylene iodide, ethylene and iodine in the vapor state has been studied in the temperature range 50 to 125°C. The method devised involved measurements of the iodine vapor pressure by a photometric device utilizing photronic cells in a null-point arrangement. Iodine and ethylene iodide were both present as unsaturated vapors. The measurements gave results which were found to agree with the extrapolation of Mooney and Ludlam's data for lower temperatures, but to disagree with the same authors' higher temperature determinations. The heat of dissociation of ethylene iodide is 13.4±0.5 kcal. The position of equilibrium is given by: $\log K = -13{,}400/4.58T + 8.17$, where the equilibrium constant is expressed in atmospheres as units.

STUDY of this equilibrium has already been described in the literature. Mooney and Ludlam[1] investigated the gaseous equilibrium in the presence of solid iodine and ethylene iodide at temperatures from 10 to 65°C. The plot of the logarithm of the equilibrium constant against inverse temperature gave a curve which they chose to interpret as two straight lines. One, with a slope corresponding to a heat of reaction of 13.4 kcal., was drawn in the temperature range 10 to 45°; the other, with 22.3 kcal. as the heat of reaction, represented the points from 45 to 65°. This second value they considered the more reliable of the two.

Polissar[2] studied the equilibrium in solution with carbon tetrachloride as the solvent. Between 122 and 152°C he obtained 11.3 kcal. as the heat of reaction. He interpreted the mechanism of the reaction with the aid of chains

[1] Mooney and Ludlam, Proc. Roy. Soc. Edin. **49**, 160 (1929).

[2] Polissar, J. Am. Chem. Soc. **52**, 956 (1930).

involving free iodine atoms and from this mechanism deduced an independent value for the heat of reaction equal to 13 kcal.

Combustion data of Berthelot[3] alone give 16 kcal. for the reaction between solid ethylene iodide and iodine and gaseous ethylene. Combined data of Berthelot and of Mixter[4] give 20.4 kcal. for the same quantity.

There is thus a considerable uncertainty about the heat of this reaction, which cannot be accounted for by the different physical state of the components in the several determinations cited. The same uncertainty exists concerning other organic iodine compounds and it seemed to us worth while to redetermine the heat of dissociation of ethylene iodide since this value may be used, at least as a crude approximation, for other iodine compounds also.

Apparatus and Method

It was intended to study the homogeneous gaseous equilibrium in the absence of solid or liquid condensates since it was their presence which must have caused the uncertainty of Mooney and Ludlam's results. The system chosen was a static one and three determinations were needed to calculate the position of equilibrium. They involved the measurement of the total pressure—with the aid of a quartz spiral gauge as a null instrument; the measurement of the total amount of iodine present (as free iodine or as ethylene iodide), which was accomplished by weighing the amount of iodine or ethylene iodide introduced into the apparatus; and the measurement of free iodine vapor by a photometric method.

The all-glass apparatus, placed into an air thermostat with automatic temperature regulation, consisted of the photometer tube, with plane-parallel windows, 40 cm long; a magnetically operated all-glass pump for circulation of the gases; the quartz manometer; a magnetic hammer for breaking the glass ampules containing weighed amounts of iodine or ethylene iodide and a system for introducing ethylene, which was sealed off from the rest during the runs.

The pump, of the Lind[5] design with some minor improvements, was found necessary because otherwise, even after twenty-four hours, the diffusion of iodine throughout the apparatus was not completed and no consistent readings could be obtained.

The photometer utilized two photronic cells and worked by the null method. Light from a small projection lamp was made parallel by two short-focus lenses. One beam passed through the absorption tube in the thermostat and on to one cell; the other passed through two Nicol prisms and on to the other cell. The cells were opposed and connected to a L & N high sensitivity galvanometer. One of the Nicol prisms could be rotated and was provided with the usual circular scale. It was adjusted, in taking readings, until the galvanometer gave a zero deflection; the lamp was turned on several minutes before taking the readings, to age the photronic cells. We found it most essential to keep the temperature of the cells constant and equal as otherwise considerable variation of the zero point was the result. It is well known[6] that the absorption of iodine depends to some extent on the presence of foreign gases. This is true of the banded region of absorption and therefore light filters were used to cut off all light above *ca.* 5000A in both light beams. They consisted of a 5 mm Corning lantern blue glass and of 2 mm medium cobalt glass. It was found that with the filters in place (but not without them) an addition of a full atmosphere of air made no measurable change in the absorption of iodine vapor. Since the effect on absorption of iodine is due chiefly to paramagnetic molecules, such as oxygen, while ethylene is diamagnetic, we feel justified in concluding that ethylene also has no effect on iodine absorption, under our experimental conditions, although such an experiment was not performed.

The calibration of the photometer was obtained by measuring the light absorption of iodine vapor of known pressure, in the presence of solid iodine in an otherwise evacuated apparatus; the temperature of the thermostat was carefully measured and the Giauque[7] data on

[3] Berthelot, Ann. Chim. Phys. (7) **21**, 296 (1900).
[4] Mixter, Am. J. Sci. (4) **12**, 347 (1901).
[5] Porter, Bardwell and Lind, Ind. Eng. Chem. **18**, 1086 (1926).
[6] Loomis and Fuller, Phys. Rev. **39**, 180 (1932).
[7] Giauque, J. Am. Chem. Soc. **53**, 507 (1931).

the vapor pressure of iodine used. Such calibrations were made over the entire range of iodine pressures used in the present investigation. An objection may be raised against this procedure because the calibration and the observations in the several runs were made at different temperatures. We have found, however, that the change in absorption of a fixed amount of iodine vapor over the small temperature range covered in these experiments is well within our experimental errors which amounted to about 0.3 percent of the maximum light transmitted.

The zero point of the photometer did not remain sufficiently constant over the periods of several days needed for a run, and therefore the absorption tube was attached to the rest of the apparatus by means of flexible glass tubing spirals so that it could be swung out of the light path. Thus a zero point of the photometer could be determined at frequent intervals.

To calculate the pressure of iodine from the weighed amounts introduced the volume of the apparatus had to be determined. This was done with the aid of a gas burette and pressure readings. A determination of the iodine pressure by the photometer, after a known weight of iodine, not enough to give saturation pressure, was introduced into the evacuated system, showed the correctness of this determination and also the absence of more than negligible adsorption on the glass walls.

In the temperature range covered in this work, 50 to 125°C, the equilibrium is very far on the side of dissociation and when approximately equal pressures of iodine and ethylene iodide, not too far from saturation, are desired, a large excess of ethylene is needed. This was introduced by decomposing purified ethylene iodide made by the method of Semenov.[8] Vapor of ethylene iodide, from a heated trap, was passed through a tube heated electrically to about 300°C, where it decomposed to more than 75 percent, then through two traps filled with glass wool and cooled by solid carbon dioxide and into the apparatus. When sufficient pressure was built up, the preparative unit was sealed off. Previously, of course, the entire system was thoroughly evacuated with a high vacuum pump and then sealed off from it, while the ethylene iodide for generation of ethylene was kept cold. No iodine or ethylene iodide passed through the traps as tested by the absorption measurements. After ethylene was introduced into the system, one of the ampules containing the iodine was broken magnetically and the temperature of the thermostat adjusted a few degrees above or below that one at which it was desired to determine the equilibrium. After allowing the equilibrium to establish itself approximately, the temperature was changed to the final setting and accurate readings were begun.

[8] Semenov, Jahr. Fort. Chem., 483 (1864).

Results

Table I gives the results of all experiments performed with the final form of apparatus. It was found to be more convenient to use iodine in the weighed tubes and in order to be certain that true equilibrium was reached, it was approached both from the side of higher and the side of lower temperatures of the thermostat. The first procedure means an initial excess of iodine, the latter an excess of ethylene iodide. The adjustment of the temperature of the thermostat took several hours as a rule and in that time the equilibrium was usually established. However, it was followed for a whole day. Several temperatures were studied with the same sample of iodine and ethylene and then more iodine from another tube added and higher temperatures investigated before the apparatus was opened and an entirely new filling made. In the first column of the table the capital letters

Table I.

	$T°$ Furnace	P (mm) (C_2H_4)	P (mm) (sample)	P (mm) I_2	K
C i	50.3	107.3	2.31	1.17	110.1
C e	50.2	107.9	2.31	1.17	110.7
A e	70.0	384.5	7.17	3.39	345
A i	69.7	385.3	7.17	3.39	345
C+De	76.1	120.4	10.38	8.19	449
A+Bi	88.0	406.3	17.38	11.72	841
A+Be	90.6	410.0	17.52	12.20	940
A e	90.8	401.2	7.60	5.84	1331
A+Be	99.6	421.5	17.94	14.07	1532
E i	107.6	672.0	52.70	40.08	2134
E e	125.0	709.0	55.11	49.20	5902

indicate the sample of iodine, while the letters *e* and *i* show whether the approach to equilibrium was made from the side of lower temperatures (and excess of ethylene iodide) or from the side of higher ones (and excess of iodine). The next column gives the temperature of the thermostat, the following one the pressure of ethylene calculated as the difference of the total pressure and that of the other two constituents of the mixture. The fourth column gives the total pressure (as free iodine plus ethylene iodide) of iodine and ethylene iodide introduced, while in the fifth are recorded the pressures of free iodine from the photometric measurements. The difference of these two columns gives the calculated pressure of ethylene iodide. The last column gives the equilibrium constant of the reaction in mm mercury as units:

$$K = P_{C_2H_4} \cdot P_{I_2} / P_{C_2H_4I_2}.$$

In Fig. 1 the logarithms of the equilibrium constants of Table I have been plotted against inverse temperature. It will be observed that the points fall on a straight line with the exception of the value at 90.8°C. In this experiment very little ethylene iodide was present and a relatively small error in iodine pressure will result in a large error in the equilibrium constant. Fig. 1 contains also the data of Mooney and Ludlam and it will be observed that not their high temperature constants, but only those obtained in the low range fall on the continuation of the straight line obtained in the present work. It appears thus that some source of error which Mooney and Ludlam failed to avoid distorted the measurements in the upper temperature range. We are uncertain as to how this error crept into their measurements, but a formation of solid solutions of iodine and ethylene iodide present in their experiments seems to be not out of the question, although it is doubtful whether in this way the entire discrepancy can be accounted for.

The heat of the reaction obtained from our measurements is found to be 13.4 kcal. and if one includes the low temperature determinations of Mooney and Ludlam in deciding upon the slope of the line in Fig. 1, the estimated error is

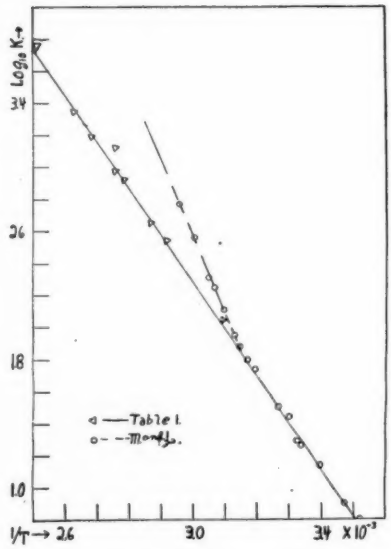

FIG. 1.

of the order of 0.5 kcal. The new measurements alone give a considerably larger error, because of the shorter temperature range covered.

The heat of dissociation here presented is in good agreement with Berthelot's figure from the combustion data, which, upon correcting to gaseous state of all participants,[1, 7] is found to be 15.5 kcal. The use of Mixter's data for the heat of combustion of ethylene, which leads to a value of more than 20 kcal. for the heat of dissociation, is certainly not justified because, in conjunction with reliable values for the heat of combustion of ethane, it gives a decidedly wrong heat of hydrogenation of ethylene.[9]

Also the results of Polissar are consistent with the present determination, considering the errors involved, and it appears thus that no well founded objections to the value of 13.4 kcal. can be found in the literature. The method described in this contribution is capable of being used with higher homologues of ethylene, no stable diiodides of which are known. It should be of some interest to determine whether the decreased stability is due to a lower heat of dissociation or to the less favorable entropy change in reaction. Such work is being planned now.

[9] Kistiakowsky *et al.*, J. Am. Chem. Soc. **57**, 65 (1935).

Electronic Structures of Molecules

XIII. Diborane and Related Molecules

ROBERT S. MULLIKEN, *Ryerson Physical Laboratory, University of Chicago*

(Received July 29, 1935)

The electronic structure of diborane (B_2H_6), which is known to have a nuclear arrangement similar to that of ethane but which has two less electrons, is determined. It is shown that there must be eleven low energy electron states (some singlet, some triplet), belonging to three electron configurations. To account for the colorless diamagnetic character of B_2H_6, it must be that all or most of these eleven states fall within an energy range of 1.5 volts or less, with the lowest state, somewhat accidentally, probably of $^1A_1$ type. Derivatives of B_2H_6 have similar structures. According to the present method there is nothing particularly anomalous about these structures. The structures here arrived at are in general agreement with the suggestions of Sidgwick and Pauling that the three H atoms in each BH_3 in B_2H_6 are held by two electron-pair bonds and one one-electron bond, although according to the present method one would say that the H atoms are held by two $[s]$ and three $[\pi]$ bonding electrons, a total of five, shared equally by the three H's. The present method shows clearly that in, e.g., $B_2H_2(CH_3)_4$, there is no reason to suppose that the B−H bonds have fewer electrons per bond than the B−C bonds, the number being 5/3 in each case. Equal energy for B_2R_6 and 2 BR_3 would mean equal effective strength of B−R and B−B bonds. It is noted that the B−B bond is a remarkably strong one. Reasons why BCl_3 does not form B_2Cl_6 are discussed. The desirability of magnetic susceptibility and perhaps molecular weight determinations, if possible at elevated temperatures, for some of the types BR_3 and B_2R_6 is pointed out.

I. DIBORANE

THE electronic structure of the boron hydrides has long been a puzzling problem. It will be shown below, by fitting empirical data into the framework of the present theoretical method, that a completely satisfactory explanation can be obtained of the existence and main properties of such compounds, in particular B_2H_6 (diborane).[1, 2]

X-ray crystal structure investigation of solid diborane[3] shows that the arrangement of the atoms must be similar to that in C_2H_6, but with a B−B distance of roughly 1.85A, about 20 percent larger than the C−C distance in C_2H_6. This is just about what might be expected, because of the lower Z_{eff} and correspondingly larger size of the B atom orbitals, if the B−B bond in B_2H_6 is essentially a single bond of the same type as the C−C bond in C_2H_6.[4] The quantity ξ (cf. Table I of IX of this series[4]) comes out 1.14 for the B−B distance in B_2H_6 as compared with 1.19 for the C−C distance in C_2H_6. Compared with C_2H_6, B_2H_6 has two less electrons; we can expect then to get at its electronic structure by considering the removal of two electrons from the normal C_2H_6 structure (cf. (4) and (4*a*) of IX).

While considering the normal state of B_2H_6, it is necessary also to determine what excited states of low energy are expected. This will prove imperative because there are probably several states which are close competitors for the position of normal state, and because the structures assigned for the normal and excited states must be in agreement with the fact that B_2H_6 (gaseous and solid) is colorless. The electron configurations must also be consistent with the fact that B_2H_6 at room temperature is diamagnetic.[5]

[1] For a preliminary account of the subject of the present paper, cf. R. S. Mulliken, Phys. Rev. **43**, 765(L) (1933). Here it was predicted that B_2H_6 should probably, but not certainly, be paramagnetic. This prediction fortunately stimulated research which has shown B_2H_6 to be diamagnetic.[5] This result is of great value for the present paper in permitting more definite conclusions to be reached than would otherwise be possible.

[2] For earlier discussions of the nature of the binding in B_2H_6 cf. among others A. Stock, Ber. der deutschen Chem. Ges. **A54**, 142 (1921); **A59**, 2226 (1926), etc.; N. V. Sidgwick, *Electronic Theory of Valency* (London, 1929), p. 103; M. Dunkel, Zeits. f. physik. Chemie **B7**, 81; **B10**, 434 (1930); G. Glockler, Science **68**, 305 (1928); G. Herzberg, Leipziger Vorträge, 1931, p. 167 (S. Hirzel, Leipzig); L. Pauling, J.Am. Chem. Soc. **53**, 3225 (1931); R. S. Mulliken, Chem. Rev. **9**, 347 (1931).

[3] H. Mark and E. Pohland, Zeits. f. Kryst. **62**, 103 (1925).

[4] R. S. Mulliken, J. Chem. Phys. **3**, 517 (1935): IX of this series.

[5] L. Farkas and H. Sachsse, Trans. Faraday Soc. **30**, 331 (1934) show by an indirect method that the normal state must be diamagnetic, and that any excited states of paramagnetic character must be at least 0.13 volt higher. Direct measurements in the Chemistry Department of this University also show diamagnetism at room temperature, but perhaps somewhat weaker than would be expected if there were no paramagnetic excited states.

For the normal and lowest excited states only the following possibilities need be considered (1s boron electrons are omitted):

$$[sa_1]^2[sa_1]^2[\sigma+\sigma, a_{1g}]^2[\pi e]^3[\pi e]^3, \quad {}^3A_{2g}, {}^1E_g, {}^1A_{1g}, {}^1A_{1u}, {}^3E_u, {}^3A_{2u}, \quad (1)$$

$$[sa_1]^2[sa_1]^2[\sigma+\sigma, a_{1g}][\pi e]^4[\pi e]^3, \quad {}^3E_g, {}^3E_u, {}^1E_g, {}^1E_u, \quad (2)$$

$$[sa_1]^2[sa_1]^2[\pi e]^4[\pi e]^4, {}^1A_{1g}. \quad (3)$$

The orbitals $[sa_1]$ and $[\pi e]$ are BH_3 radical orbitals giving strong B−H bonding. Symmetry C_{3v} is assumed for each radical (cf. discussion of corresponding CH_3 orbitals in C_2H_6).[4] The orbital $[\sigma+\sigma, a_{1g}]$ is primarily a B−B bonding orbital.

Symmetry D_{3d} (a center of symmetry) is assumed in (1)–(3) for B_2H_6. This keeps the H atoms, other things being equal, as far apart as possible, and presumably corresponds to the position of minimum energy, as in C_2H_6. For most purposes, however, it is probably more nearly correct to assume free rotation, the symmetry then being D_3 except at special rotation angles which make it D_{3d} or D_{3h}. The formulations (1), (2), (3) are unchanged for symmetry D_3 except that all subscripts g, u are dropped. Designations for symmetry D_{3h} are as follows, the symbols being given in the same order as the corresponding symbols in (1)–(3): a_1' instead of a_{1g}; then ${}^3A_2'$, ${}^1E'$, ${}^1A_1'$, ${}^1A_1''$, ${}^3E''$, ${}^3A_2''$ in (1); ${}^3E''$, ${}^3E'$, ${}^1E''$, ${}^1E'$ in (2); ${}^1A_1'$ in (3).

The correctness of the electron *states* given above for the *configurations* in (1)–(3) will be justified at the end of this section. It will be advisable now to mention the relations of these configurations and states to those of two separated BH_3 radicals. The free BH_3 radical[6] is very probably of plane form (symmetry D_{3h}), with a diamagnetic normal state

$$1s_B^2[sa_1']^2[\pi e']^4, {}^1A_1' \quad (4a)$$

and with lowest excited states

$$1s_B^2[sa_1']^2[\pi e']^3[\sigma a_2''], {}^1, {}^3E''. \quad (5a)$$

It appears likely (see below) that the BH_3 radical becomes pyramidal when it enters into combination to form B_2H_6. For pyramidal BH_3 (symmetry C_{3v}), the symbolism (4a), (5a) needs to be somewhat altered, although there is of course no great change in the forms of the orbitals unless the pyramids become high. We then have

$$1s_B^2[sa_1]^2[\pi e]^4, {}^1A_1, \quad (4)$$

$$1s_B^2[sa_1]^2[\pi e]^3[\sigma a_1], {}^1, {}^3E. \quad (5)$$

Schemes (4a), (5a) may be considered as special cases of (4), (5).

If two pyramidal BH_3 radicals are brought together with the pyramid-apices (B atoms) pointing toward each other and the pyramid axes coincident, it can be shown that two ${}^1A_1$ radicals both in state (4) tend to give B_2H_6 in state (3). [These and the results stated in the next paragraph will be justified at the end of this section.] According to Heitler-London theory, since ${}^1A_1$ of BH_3 is a closed-shell state, state (3) of B_2H_6 should not be stable.

In a similar manner, if two BH_3 are brought together head on, one in state (4), the other in state ${}^3E$ of (5), they tend to give B_2H_6 in one of the two states ${}^3E_g$ or ${}^3E_u$ of (2). If two BH_3 each in ${}^3E$ of (5) are brought together head on, the possibilities for the resulting state of B_2H_6 which they tend to give include all the states of (1), together with some quintet states which will not interest us. Other possible combinations (${}^3E$ plus ${}^1E$, ${}^1E+{}^1E$, etc.) will not be of interest here.

As noted above, Heitler-London theory indicates that (3) should be unstable. Examining (3), one sees that it contains no B−B bonding electrons, but only closed BH_3 shells which should tend to produce a net repulsion. Configuration (2), however, contains one $[\sigma+\sigma]$ electron, and configuration (1) two $[\sigma+\sigma]$ electrons, of strongly B−B bonding character. Besides B−B bonding, each $[\sigma+\sigma]$ should also give a little B−H bonding within each BH_3 radical, at least if the latter is pyramidal. [Cf. the analogous $[\sigma+\sigma]$ orbitals in C_2H_6.[4]]

The $[\pi e]$ electrons in (1) and (2), in case those in the two BH_3 groups should interact strongly, would offer a possibility of more or less additional B−B bonding, since the $[\pi e]$ shells are not entirely closed. This effect should be stronger in (1) than in (2). *If* this $[\pi]$ bonding should be *strong* (but see below), we would do well to replace the $[\pi e]$ orbitals of the BH_3 radicals by whole-molecule orbitals $[\pi+\pi, e_u]$ and $[\pi-\pi, e_g]$. The former would be

[6] Cf. R. S. Mulliken, J. Chem. Phys. 1, 492 (1933): V. Table I and pp. 500–503.

B−B bonding, the latter B−B antibonding, but both would also retain strong B−H bonding properties for H's at both ends of the molecule. Using $[\pi\pm\pi]$, (2) would break up into

$$\cdots[\pi+\pi, e_u]^4[\pi-\pi, e_g]^3, {}^{3,1}E_g \quad \text{and} \quad \cdots[\pi+\pi, e_u]^3[\pi-\pi, e_g]^4, {}^{3,1}E_u. \quad (2a)$$

The derivation of this result can be seen from the discussion of a very similar case for C_2H_6 (reference 4, page 521). In the ${}^{3,1}E_g$ there would be a net B−B bonding effect, in the ${}^{3,1}E_u$ a net B−B antibonding effect, from the $[\pi\pm\pi]$ groups.

Similarly (1) would break up into

$$\cdots[\pi+\pi, e_u]^4[\pi-\pi, e_g]^2, {}^3A_{2g}, {}^1E_g, {}^1A_{1g} \quad \text{and} \quad \cdots[\pi+\pi, e_u]^3[\pi-\pi, e_g]^3, {}^1A_{1u}, {}^3E_u, {}^3A_{2u}. \quad (1a)$$

[The configuration $\cdots[\pi+\pi]^3[\pi-\pi]^3$ would also give additional states ${}^3A_{1u}$, ${}^1E_u$, ${}^1A_{1u}$, but these do not correspond to any of the states of $\cdots[\pi]^3[\pi]^3$ in (1).] The formulation corresponding to (3) but using whole-molecule orbitals is

$$\cdots[\pi+\pi, e_u]^4[\pi-\pi, e_g]^4, {}^1A_{1g}. \quad (3a)$$

If we reckon each net pair of B−B bonding electrons (B−B antibonding electrons being counted negatively) as one B−B bond, then the numbers of B−B bonds corresponding to (1), (1*a*), (2), (2*a*), (3), (3*a*) are, respectively, 1,2, $\frac{1}{2}$, 1, 0,0. In the case of (1*a*), this refers only to the $_g$ states; for the $_u$ states there is only 1 net bond.

At this point it may be noted that the states (1*a*) would be very closely related to low energy, mostly well-known, states of the O_2 molecule, while (2*a*) and (3*a*) would be similarly related to high energy states of O_2 which are not yet known experimentally. The lowest energy states of O_2 are

$$2s^22s^2(\sigma+\sigma, \sigma_g)^2(\pi+\pi, \pi_u)^4(\pi-\pi, \pi_g)^2, {}^3\Sigma^-_g, {}^1\Delta_g, {}^1\Sigma^+_g, \quad (6)$$

with ${}^3\Sigma^-_g$ as the normal state. If we could split each O nucleus in O_2 into nuclei of B+3H, then the respective states ${}^3\Sigma^-_g$, ${}^1\Delta_g$, and ${}^1\Sigma^+_g$ of (6), it can be shown,[7] would go over continuously into ${}^3A_{2g}$, ${}^1E_g$, and ${}^1A_{1g}$ of (1*a*) or (1). The probably next lowest group of states of O_2, of which the ${}^3\Sigma^-_u$ and perhaps also the ${}^3\Delta_u$ or ${}^3\Sigma^+_u$ or both are known experimentally, are

$$2s^22s^2(\sigma+\sigma, \sigma_g)^2(\pi+\pi, \pi_u)^3(\pi-\pi, \pi_g)^3, {}^1\Sigma^-_u, {}^3\Delta_u, {}^3\Sigma^+_u, {}^3\Sigma^-_u, {}^1\Delta_u, {}^1\Sigma^+_u. \quad (7)$$

These are related continuously to the respective states ${}^1A_{1u}$, ${}^3E_u$, ${}^3A_{2u}$ given in (1*a*) or (1) and the additional states ${}^3A_{1u}$, ${}^1E_u$, and ${}^1A_{2u}$ mentioned following (1*a*).

The most important difference between the orbitals $(\pi\pm\pi)$ of (6) and (7) and the analogous orbitals $[\pi\pm\pi]$ of B_2H_6 in (1*a*) is that in the former only O−O bonding or antibonding is involved, while in the latter there is strong B−H bonding in addition to B−B bonding or antibonding. Because of this *competition* between B−H and B−B bonding, neither can be as strong as it would otherwise be. In other words, any B−B bonding power which the $[\pi+\pi]$ orbitals may have is partly at the expense of their B−H bonding power.

A similar competition does not exist or is unimportant in the case of the $[\sigma+\sigma]$ orbitals in B_2H_6, since these have little if any B−H bonding power anyway. Nevertheless, any B−B bonding produced by an electron in a $[\sigma+\sigma]$ orbital is ultimately at the expense of B−H bonding, since it can be secured only by first removing the electron from a B−H bonding $[\pi]$ or $[\pi\pm\pi]$ orbital in order to put it into $[\sigma+\sigma]$.

From the foregoing discussion it will be seen that in seeking to determine the nature of the normal and the low energy excited states of B_2H_6, we have inevitably to deal with a somewhat complicated system of possibilities. In order to clarify the situation, we may formulate three questions. (*A*). Is it a better approximation, for the molecular dimensions which exist in the actual normal state of B_2H_6, to use formulations (1), (2), (3) or to use (1*a*), (2*a*), (3*a*)? (*B*). *If* formulations (1), (2), (3) are better, which of these configurations gives the lowest mean energy, for the actual dimensions of the actual normal state? This is equivalent to asking whether $[\sigma+\sigma]$ or $[\pi]$ in (1)–(3) is the more firmly bound. If formulations (1*a*), (2*a*), (3*a*) are better, we ask an analogous question. (*C*). Having decided (*B*), what particular electron state of the lowest energy electron configuration is the normal state?

The answer to question (*A*) depends largely on the degree of overlapping of the $[\pi]$ orbitals of the two BH_3 radicals occurring in (1), (2), (3). If this is large, then there is strong interaction between them, and (1*a*), (2*a*), (3*a*) should be better; if small, (1), (2), (3) should be better. The decision depends on the effective ξ value for the $[\pi]$ groups of the two BH_3 (cf. discussion of ξ values for $[\pi]$ groups of CH_3 in C_2H_6, reference 4, p. 520). If the BH_3 radicals are still plane in B_2H_6, the ξ is that given at the beginning of this paper, a value which (cf. Table I and discussion in reference 4) would mean considerable overlapping and interaction of the $[\pi]$'s, although less than if the $[\pi]$'s did not have strong B−H bonding power. More probably, however, the BH_3 radicals are pyramidal for essentially the same reason that the CH_3 radicals are pyramidal in C_2H_6. Each B atom would then be surrounded by four other atoms in approximately a tetra-

[7] R. S. Mulliken, Phys. Rev. **43**, 293–4 (1933): Tables III and IV.

hedral arrangement. In this case, the effective ξ would certainly be so large (cf. discussion of $[\pi]$'s of CH_3 in reference 4) that there would be little overlapping and (1), (2), (3) would be preferable. Accepting the existence of this state of affairs tentatively (cf. justification near the end of this section), it will be noted that, among other things, the possibility of a really double-bonded B=B structure (1*a*) analogous to (6) of O_2 is eliminated. Nevertheless there remains a more or less formal resemblance or at any rate a formal correlation of energy levels with those of O_2.

Next we have to decide between configurations (1), (2) and (3) for the lowest state of B_2H_6. As noted above, Heitler-London theory shows that (3) must be unstable. Hence, for the observed B−B distance $r_e = 1.85$A in B_2H_6, (3) must have a higher energy than $2BH_3$, although not necessarily much higher (perhaps 1 volt or less). The chemical existence of B_2H_6, however, shows that the normal state of the latter must have a lower energy than $2BH_3$, by perhaps 1 volt or at least 0.5 volt. Hence the normal state must apparently belong to configuration (1) or (2), more probably the former, since the mean energy of (2) should be intermediate between those of (1) and (3).

Thus it appears that the energy increases in the order (1), (2), (3), although overlapping of the groups of energy levels associated with the three configurations is possible. The energy differences between (1), (2), and (3) need not, in fact must not, be great, however; roughly, the energies of (1), (2), (3) may be about equal. [It is even not absolutely certain, in view of the existence of a "resonance" (see below) between (3) and the $^1A_{1g}$ state of (1), that the order may not be (3), (2), (1); this could be possible if the resonance is very strong, but is not at all probable.]

The foregoing conclusions imply that $[\sigma+\sigma]$ must be as firmly bound, or a little more firmly bound, than $[\pi]$ in B_2H_6. It may be recalled that in the case of C_2H_6 we concluded[4] that $[\sigma+\sigma]$ is at least two volts *less* firmly bound than $[\pi]$. Can we account for such a difference between C_2H_6 and B_2H_6? One important factor tending in the right direction is the charge-transfer effect. The considerable negative charging of the C atoms in C_2H_6 was estimated to decrease the ionization potential I for $[\sigma+\sigma]$ by 1 or 2 volts, while in B_2H_6 the positive charging of the B atoms should tend in the opposite direction, since C is more but B less electronegative than H.

The I's of $[s]$, $[\pi]$, and $[\sigma+\sigma]$ in B_2H_6 may be predicted by the methods of VIII of this series[8] (cf. the examples discussed in IX[4]). The results are: $[s]$, $I>14.45$ volts; $[\sigma+\sigma]$, $I>8.63$ volts; $[\pi]$, $I>11.08$ volts. No allowance for charge-transfer effects has been included. From these predictions, it would at first seem that $[\pi]$ should be more firmly bound than $[\sigma+\sigma]$. If, however, the inequality sign represents a sufficiently larger value for $[\sigma+\sigma]$ than for $[\pi]$, this need not be true. Although the necessary difference is surprisingly large, it must be accepted as empirically required by the observed stability of B_2H_6. It is also found that the necessary difference is not beyond credibility. For instance, the following set of I's would be credible: $[s]$, $I=17$ volts; $[\sigma+\sigma]$, 13.0 volts; $[\pi]$, 12.6 volts. The inequality sign would then represent 4.4 volts for $[\sigma+\sigma]$ and 1.5 volts for $[\pi]$. Of the 4.4 volts, perhaps 1.2 volts might be attributed to charge-transfer, leaving 3.2 volts as a measure of the strength of the bonding in $[\sigma+\sigma]$, as compared with 1.5 volts for $[\pi]$. While little significance should be attached to these precise figures, it is clear that the existence of B_2H_6 must be in part a result of the possession of unusual strength by the B−B bond (cf. also section II below).

As we have seen, the energy must probably increase in the order (1), (2), (3). The spacings (2)–(1) and (3)–(2) are presumably about equal, using for the electron configurations (1) and (2) the centers of gravity of the two groups of electron levels associated with them. Another point of importance is this: since we have decided that the interaction is small between the two groups $[\pi]^3$ in (1), the various energy levels of (1) should be close together in energy, very likely within a total range of half a volt or less. As for the *order* of the various levels within the group, a comparison of (1), or better (1*a*), with the analogous case of O_2 in (6), (7) indicates that the order of increasing energy should be that given in (1), with $^3A_2$ (analogous to $^3\Sigma^-_g$ of O_2) the lowest. This last cannot be correct, however,

[8] R. S. Mulliken, J. Chem. Phys. 3, 514 (1935): VIII.

since $^3A_2$ would give paramagnetic properties,[1] contrary to the observed diamagnetism of B_2H_6. As will be seen below, there is a specific disturbing factor which can well account for this discrepancy. Besides, the comparison with O_2 is not entirely conclusive as to the order of the levels of (1). Furthermore, since the levels should all be close together, the exact order is easily subject to disturbance by minor factors.

Consideration of (2) from the same point of view indicates that the E_u-E_g intervals should be small, since they arise from the weak $[\pi]$, $[\pi]$ interactions. The intervals $^1E_u-^3E_u$ and $^1E_g-^3E_g$ should be larger (presumably as much as a volt, with the singlet levels higher), since they depend on interactions between $[\pi]$ and $[\sigma+\sigma]$, which should be fairly strong.

As we have seen, the normal state of B_2H_6 must apparently belong to configuration (1),—or possibly (2). Further, the diamagnetic character of this state immediately excludes all the triplet states of (1) and (2) as possibilities. Since the singlet states of (2) should lie above the triplet states, they are also excluded. This leaves only ^1E_g, $^1A_{1g}$, $^1A_{1u}$ of (1). We concluded above that these should lie close together, although $^1A_{1u}$ should be somewhat above the others if the $[\pi]-[\pi]$ interactions are at all appreciable. The ^1E_g is also doubtful, since it is analogous to the paramagnetic $^1\Delta_g$ of O_2 and should probably be strongly paramagnetic, although this is uncertain without calculations. [It is a question of the extent to which the resultant angular momentum along the symmetry axis, present in $^1\Delta_g$ of O_2, is preserved or has meaning in ^1E_g of B_2H_6.]

It seems probable that the normal state is $^1A_{1g}$ of (1), somewhat modified. Referring to (1), (2), (3), it will be noted that there are altogether two $^1A_{1g}$ states, one from (1) and one from (3). Now, as we have seen earlier, the $^1A_{1g}$ of (3) corresponds to a state where two unexcited BH_3 radicals ($^1A_1$ of (4)) are repelling each other. The $^1A_{1g}$ of (1), on the other hand, corresponds to a state where two excited BH_3 radicals (^3E of (5)) are attracting each other strongly. That is, $^1A_{1g}$ of (3) should have a potential energy curve, for variation of the B—B distance r, which rises as r decreases, while $^1A_{1g}$ of (1) should have a curve descending strongly as r decreases. According to this, the $^1A_{1g}$ curves of (1) and (3) should most probably cross, or at least come close together.

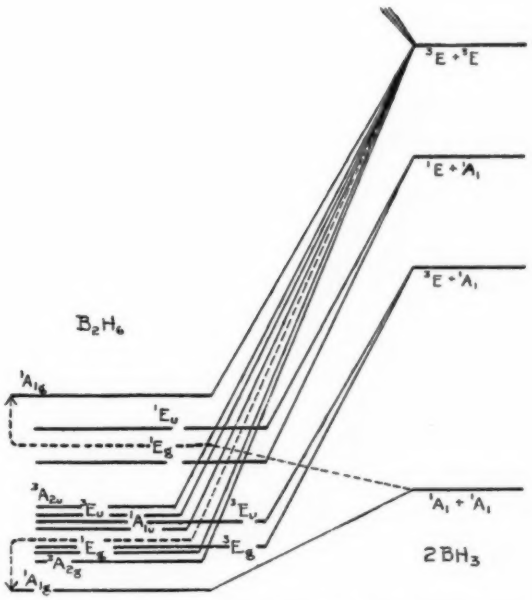

FIG. 1. Low energy electron levels of B_2H_6 (approximate, estimated). B_2H_6 levels (full horizontal lines at left) are all for a fixed nuclear configuration the same as that of the normal state. Longest horizontal lines are states of $[\sigma+\sigma][\pi]^4[\pi]^3$,—cf. (2) of text. Remaining horizontals of B_2H_6 are states of $[\sigma+\sigma]^2[\pi]^3[\pi]^3$ and of $[\pi]^4[\pi]^4$,—cf. (1) and (3) of text. Dotted horizontals represent estimated positions of two $^1A_{1g}$ states if they did not interact with each other; mutual perturbation pushes them apart, as indicated by arrows, to give normal state and probable highest state of group. Dissociation correlations are indicated by slanting lines, assuming symmetry D_{3d} preserved during dissociation, and assuming no predissociation nor breakdown in separability of electronic and vibrational wave functions. Dotted slanting lines show correlations for the two $^1A_{1g}$ states *if they did not interact* with each other; actual interaction causes crossing of these correlation lines to be avoided, with upper $^1A_{1g}$ now going to $^3E+{}^3E$, lower to $^1A_1+{}^1A_1$. The scale may be judged by the following (very uncertain) estimates used in the figure: $^3E-{}^1A_1=2.0$ volts for BH_3; dissociation energy of lowest B_2H_6 state $=0.9$ volt.

Perturbation theory shows, however, that the wave functions of the two $^1A_{1g}$ states should mix more or less, especially near the probably expected crossing point. If the mixing tendency is strong, as is perfectly reasonable (see below), two new curves should result, the lower one with a considerably lower energy minimum than the original curve of (1) but dissociating to two unexcited BH_3 like the original curve of (3). This pushing down of the $^1A_{1g}$ curve of (1) by admixture with (3),—or possibly *vice versa* if the two

original "unperturbed" curves do not cross,—serves to explain the at first rather unexpected[1] fact that the paramagnetic ${}^3A_{2g}$ state of (1) is not the normal state. The ${}^3A_{2g}$ and other states of (1) and (2) must, however, be not far above the normal state (see below).

A plausible estimate of the positions of the "original" (unperturbed) and the final resulting curves is shown diagrammatically in Fig. 1, the former by dotted lines, the latter by full lines. A crossing of the unperturbed ${}^1A_{1g}$ curves is shown, although the correctness of this is of course not absolutely certain. Curves corresponding to the remaining states of (1) and (2) are also shown diagrammatically in Fig. 1. The horizontal straight lines for B_2H_6 show estimated positions of the various energy levels *for vertical excitation* from the ${}^1A_{1g}$ normal state (*unchanged B—H and B—B distances*). The estimates are based on the considerations advanced previously as to positions of energy levels, and are merely illustrative so far as their detailed arrangement is concerned. Their dissociation-correlations should, however, be essentially correct, at least for dissociation processes in which the original symmetry is preserved throughout the dissociation, and neglecting possible predissociation short-cuts. If the figure were modified to show the minimum energy, in each case, instead of the vertical energy relative to the normal state nuclear configuration, all the excited levels would be lowered more or less, since adiabatic excitation processes would in each case surely involve more or less change in the equilibrium B—B and B—H distances. For instance, the B—B equilibrium distance would surely be increased for the states of electron configuration (2).

It may possibly be that the stability of the normal state of B_2H_6 is critically determined by the above-discussed "resonance" of the two ${}^1A_{1g}$ states. At any rate, it is advisable to justify somewhat more fully the existence of the assumed rather strong resonance. Of the eleven states of configurations (1)–(3), for symmetry D_{3d}, there are six whose types (${}^1A_{1g}$, ${}^1E_g$, ${}^3E_u$) are alike in pairs (cf. (1), (2), (3)). For symmetry D_3 there are *more* duplications of type, since the $_g$, $_u$ distinctions are lost. For symmetry D_{3h} there are again three pairs of types ${}^1A_1'$, ${}^1E'$, ${}^3E''$. On examining the correlation of states between symmetries D_{3d} and D_{3h}, however (cf. paragraph following (3)), it is found that of the three pairs of states which agree in type for D_{3d}, only one pair still agrees for D_{3h}, and *vice versa*. This one pair comprises the ${}^1A_{1g}$ states of (1) and (3), which both become ${}^1A_1$ for D_3 and ${}^1A_1'$ for D_{3h}. Without such agreement in type for all angles of rotation, one could not expect a strong mutual perturbation; in view of the existence of such agreement in the case of the ${}^1A_{1g}$ of (1) and (3), our assumption of rather strong resonance between these two states becomes tenable.

The nature of the normal state of B_2H_6 being thus fairly accurately determined, it is of interest to consider the excited states shown by (1)–(3) and in Fig. 1. The positions of these, taken in connection with electronic selection rules, must be consistent with the colorlessness of B_2H_6. This lack of color shows that any absorption must be confined to the infrared and ultraviolet. From the ${}^1A_1$ normal state, the electronic selection rules (cf. IV of this series,[7] p. 290) permit transitions to the following among the various states of (1)–(3).

Sym. D_{3d}:	From	${}^1A_{1g}$	to			${}^3E_u$,	${}^3A_{2u}$,	${}^3E_u$,	${}^1E_u$.
" D_3:	"	${}^1A_1$	"	${}^3A_2$,	${}^1E$,	${}^3E$,	${}^3A_2$,	${}^3E$,	${}^1E$, ${}^1E$.
" D_{3h}:	"	${}^1A_1'$	"		${}^1E'$,		${}^3A_2''$,	${}^3E'$,	${}^1E'$.

We may expect transitions which are not allowed for all angles of rotation (i.e., not for all the possible symmetries), as well as all transitions to triplet states, to be relatively very weak. This leaves only the transition to the ${}^1E_u$ of (2) as a probably fairly intense one. The possibility that this lies in the ultraviolet can be immediately excluded, since that would require that configurations (1) and (2) should differ far too much in energy, while (3), higher in energy than (2), would correspond to far too strong a repulsion. Hence the transition to ${}^1E_u$ of (2) must lie in the infrared, i.e., at a wave-length not less than say about λ8000, which corresponds to 1.55 volts. Since it is probable from the theory that ${}^1E_u$ is the highest level of (2), and is higher than any level of (1), we conclude that all the levels of (1) and (2) are probably crowded into a space of not more than about 1.5 volts on the energy level diagram (for vertical excitation, but even less for adiabatic excitation). The level (3) can be higher; absorptive transitions to it are, however, rigor-

ously forbidden for all the possible symmetries. Fig. 1 has been constructed in accordance with the foregoing results and other considerations discussed earlier. It is of course only qualitative and diagrammatic.

It was tentatively assumed at one point in the foregoing discussion, and thenceforward, that the BH_3 radicals in B_2H_6 are of pyramidal form. If so, $[\pi]$, $[\pi]$ interactions are small. Conversely, the absence of visible absorption and the consequent limitations on Fig. 1 are found on examination to indicate that the $[\pi]-[\pi]$ interactions cannot in fact be very large; hence they constitute empirical evidence that the BH_3 radicals really are pyramidal in B_2H_6. For if the $[\pi]-[\pi]$ interactions were large, the states of (1) and (2) would spread out, and probably the $^3A_{2g}$ of (1) or perhaps the ^3E_g of (2) would come very near or below the $^1A_{1g}$ and make B_2H_6 paramagnetic. Without calculations, the argument is not entirely conclusive, however. A further argument in favor of small $[\pi]-[\pi]$ interactions and pyramidal BH_3 is that the observed B—B distance[2] in B_2H_6 is about what would be expected for a single B—B bond. If there were a real double bond (strong $[\pi]-[\pi]$ interactions, and (1*a*) better than (1)), the B—B distance should be smaller. Nevertheless quite possibly the BH_3 pyramids in B_2H_6 are considerably flatter than for tetrahedral angles, with *some* $[\pi]-[\pi]$ bonding and *some* tendency toward (1*a*). On the whole, however, there appears to be little doubt that (1), (2), (3), modified by resonance between the $^1A_{1g}$ of (1) and (3), and with more or less free rotation around the B—B bond, give a reasonably accurate description of the normal and low-energy excited states of B_2H_6.

It now remains to justify, as promised above, the nature of the electron states associated with electron-configurations (1)–(3), and their correlations with corresponding states for symmetry D_{3h}; and also to justify certain correlations given above between states of B_2H_6 and those of $2BH_3$. These problems are all, or can be reduced to, examples of a type of correlation problem similar to that solved by Wigner and Witmer for diatomic molecules.[9] It will be better to postpone a detailed discussion for a separate paper dealing generally with this subject, but something of the method will be outlined here.

Configurations and states (1), (2), (3) can be imagined as obtained from certain corresponding states (8), (9), (10) of O_2 by a continuous process in which each O nucleus is split into B+3H. Omitting $2s^22s^2$ in each case, we have

$$(\sigma+\sigma, \sigma_g)^2 2p\pi^3 2p\pi^3,\ ^3\Sigma^-_g,\ ^1\Delta_g,\ ^1\Sigma^+_g,\ ^1\Sigma^-_u,\ ^3\Delta_u,\ ^3\Sigma^+_u, \quad (8)$$

$$(\sigma+\sigma, \sigma_g) 2p\pi^4 2p\pi^2,\ ^3\Pi_g,\ ^3\Pi_u,\ ^1\Pi_g,\ ^1\Pi_u, \quad (9)$$

$$2p\pi^4 2p\pi^4,\ ^1\Sigma^+_g. \quad (10)$$

The symmetry here for O_2 is $D_{\infty d}$. Depending on the arrangement of the resulting B and H nuclei, the symmetry may be reduced on splitting the O nuclei to D_{3d}, D_3, D_{3h}, or some other type. Definite rules[7] show how the states for symmetry $D_{\infty d}$ must go into those of D_{3d} or D_{3h} (or of D_3, which may be obtained from either D_{3h} or D_{3d} by further reducing the symmetry).

By comparing the list of states for symmetry $D_{\infty d}$ with those respectively obtained for D_{3h} and D_{3d}, it is possible to establish a set of correlations showing how the classification type of each actual electronic state varies during rotation as the symmetry goes successively through D_{3d}, D_3, and D_{3h}. It must be noted, however, that this set of correlations is not a universal one, but is applicable in its details only to the particular electron configurations here considered. For instance, state ^1E_g of (1) becomes a ^1E for symmetry D_3, which becomes a $^1E'$ for symmetry D_{3h}; but ^1E_g of (2), after becoming a ^1E for D_3, then becomes a $^1E''$ for D_{3h}. In general, a state X of symmetry D_3 may be correlated with either an X_g or an X_u of D_{3d}, and with either an X' or an X'' of D_{3h}. The actual correlations depend on the particular case.

The configurations (8), (9), (10) for O_2 respectively correspond, as is easily seen, to (1), (2), (3) of B_2H_6. Really, the use of $2p\pi$ O atomic orbitals as in (8)–(10) does not represent a good approximation for the actual O_2 molecule; instead molecular orbitals ($\pi\pm\pi$) would be better (cf. the three states of (6) and the first three states of (7), which together correspond to the six states of (8)). This does not matter, however, since our argument depends (within limits) only on formal correlations. The use of (8)–(10) is equivalent to using the Heitler-London-Pauling-Slater mode of description for the π electrons of O_2, although still retaining one molecular orbital ($\sigma+\sigma$).

Our B_2H_6 problem is thus reduced to the problem of proving the correctness of the electron states given for the somewhat artificial O_2 electron configurations in (8)–(10). This can be done by a consideration of the wave functions, best systematically after the manner of Wigner and Witmer. Electrons in closed shells can be disregarded. For the remainng electrons, only the resultant state or states of groups of equivalent electrons are important. In (8)–(10) only the two groups of π electrons, one on each atom, matter. The group π^4 would give a $^1\Sigma^+$ resultant state, π^3 a $^2\Pi$ state. Hence the determination of the resultant states of (8), (9), (10), is equivalent to finding those of the state-pairs $^2\Pi+^2\Pi$, $^2\Pi+^1\Sigma^+$, $^1\Sigma^++^1\Sigma^+$, respectively, for the case of two systems with identical nuclear force-fields (here those of atoms, but the results would apply equally to any pair of like radicals each of symmetry $C_{\infty v}$ or $D_{\infty d}$). Once the problem is stated in this form, there is no difficulty in solving it along the lines of

[9] E. Wigner and E. E. Witmer, Zeits. f. Physik **51**, 859 (1928).

the Wigner-Witmer method,[9] the results being those given in (8)–(10).

The problem of finding the states of B_2H_6 obtained by bringing together two BH_3 radicals in specified electronic states can be solved in a similar way. One considers the system O+O with O atoms in specified states, and notes the resulting O_2 states. Then one imagines each O split into a BH_3 and its states changed into BH_3 states, and simultaneously one imagines O_2 split into B_2H_6 and its states changed into those of the latter. By comparison, the desired correlations between BH_3 states and B_2H_6 states are obtained, the results being those given (in part) above. These results are strictly applicable only insofar as predissociation short-cuts resulting from electronic-vibrational interactions do not occur.

II. Valence in Diborane and Related Molecules

Diborane and related molecules and derivatives will now be discussed from the standpoint of valence theory. We shall also consider why some molecules B_2R_6 are stable while others do not occur but are represented by 2 BR_3. Here R is supposed to represent any monovalent atom or radical, and formulas BR_3 and B_2R_6 are supposed to stand also for cases where not all the R's are alike.

Empirically, B_2R_6 molecules such as the following are known: B_2H_6, B_2H_5Cl, $B_2H_5CH_3$, $(H_3C)_2BH \cdot BH_3$, $(H_3C)_2BH \cdot BH_2CH_3$, $(H_3C)_2BH \cdot BH(CH_3)_2$.[10] On the other hand, we have BCl_3, $B(CH_3)_3$, $C_6H_5BH_2$, $(CH_3O)_2BH$.[10] From an inspection of this list it is obvious that there must often be a close competition between B_2R_6 and 2 BR_3 as to which is the more stable; also that the probability of B_2R_6 is increased if some of the R's are H atoms. The occurrence of various more complex boron hydrides, e.g., B_4H_{10}, B_5H_{11}, $B_{10}H_{14}$, may also be noted.[10]

The analysis in Part I shows that by the present method, which is not fettered by the requirements of ordinary valence theory, it has been possible to arrive at a perfectly natural, unmysterious, and definite explanation of the electronic structure of B_2H_6. The results may be described essentially as follows. Suppose we start from 2 BH_3, where for each BH_3 there are six B–H bonding electrons, i.e., one pair of electrons per ordinary B–H chemical bond (cf. (4*a*)). The structure of BH_3 in this, its normal, state is certainly of a saturated, closed-shell, diamagnetic type. There exists, however, the possibility of withdrawing one electron from B–H bonding and putting it into a state where it is capable of forming a new bond. The molecule BH_3 is then in a low energy excited state (cf. 5*a*) with only five B–H bonding electrons and one free valence electron. If one requires to know how many B–H bonds there then are, one may reply that there are $2\frac{1}{2}$, distributed, however, equally among all the three H atoms. More accurately, one might say that there are one $[s]$ bond and $1\frac{1}{2}$ $[\pi]$ bonds, the former type, incidentally, being less polar than the latter.

Two of the excited BH_3 can now come together, each with its free valence electron, to form between them a strong B–B bond of the electron-pair type. The total number of bonds in the resulting B_2H_6 is then $2\frac{1}{2}+1+2\frac{1}{2}=6$, just the same number as for two free BH_3 each in its normal state. Hence the question of whether B_2H_6 is more stable than 2 BH_3 is essentially one of the relative stability of B–B and B–H bonds. The existence of B_2H_6 indicates empirically that the B–B bond is slightly the more stable.

We may next ask why B_2H_6, with only five instead of the normal six electrons to hold the three H atoms to each B, is not unstable with respect to $B_2H_4+H_2$. B_2H_4 is not known experimentally; if it were, it would have one B–B bond and four B–H bonds, each bond with the normal quota of two electrons. It is to be noted that the total number of bonding electrons (twelve) is the same in $B_2H_4+H_2$, B_2H_6 and 2 BH_3. The observed greater stability of B_2H_6 as compared with 2 BH_3 and $B_2H_4+H_2$ then merely indicates that the effective strengths of bonds are in the order B–B > B–H > H–H, which is not incredible, although the great strength thus indicated for the B–B bond (greatest of all known homopolar bond strengths) is remarkable. The doubtless comparatively small margin of stability of B_2H_6 over 2 BH_3 indicates that the inequalities just stated are small, hence subject to upset under the impact of comparatively minor factors. This delicate balance suffices in a qualitative way to make understandable the existence of the various hydrides

[10] Cf. A. Stock, *Hydrides of Boron and Silicon* (Cornell University Press, Ithaca, N. Y., 1933); H. I. Schlesinger and A. B. Burg, J. Am. Chem. Soc. **53**, 4321 (1931); **55**, 4020, 4025 (1933); **56**, 499 (1934); **57**, 621 (1935).

B_2H_6, B_4H_{10}, B_5H_{11}, $B_{10}H_{14}$ etc. No attempt will be made here, however, to explore in detail the electronic structures of these.—In connection with the above reference to the unknown B_2H_4, the fact that B_2Cl_4 is experimentally well established[10] should be mentioned.

The foregoing discussion of the relative strengths of B−B and B−H bonds needs minor qualification, or explanation, in some respects. For one thing, the stability of the normal state of B_2H_6, as we have seen in Part I, is greater than it would otherwise be because of an interaction between the $^1A_{1g}$ states of electron configurations (1) and (3). The resulting extra stability increases the effective strength of the B−B bond in B_2H_6, and probably in its derivatives, although really the extra strength does not inherently belong to this bond. It may even be that this resonance effect is a decisive factor in making these compounds more stable than 2 BR_3.

Another point is that the B−B bond in B_2H_6 must have *some* tendency, although probably small (see Part I) to be a double bond. This no doubt increases the effective strength of the bond at least a little.

Still a further qualification in our discussion arises from the fact that the B−H bonding electrons in B_2H_6 and BH_3 are of two types, $[sa_1]$ and $[\pi e]$. The B−H bond strength defined in the ordinary chemical manner really corresponds to a weighted average of strengths due to $[s]$ and $[\pi]$. Our statement that the bond strengths are in the order B−B>B−H>H−H should then really be modified to say that the effective B−B bond strength (cf. two preceding paragraphs) exceeds the effective strength of *the* $[\pi]$ *type* of B−H bonds, while this in turn exceeds the H−H bond strength. For it is just the $[\pi]$ type of B−H bonding electrons which are sacrificed if B_2H_6 or $B_2H_4+H_2$ is formed from 2 BH_3. The relation B−B>B−H>H−H might possibly not be true if the bond strengths were measured according to ordinary chemical definitions; it is, however, doubtful whether data are available for testing this point.

In seeking further to understand the stability of molecules of the type B_2R_6, a comparison with the case of NR_3 may be instructive. Here there is no tendency to form N_2R_6. This is intimately connected with the fact that the outer shell of the N atom is full with $[s]^2[\pi]^4[\sigma]^2$ in NR_3, while the two $[\sigma]$ places are vacant in BR_3, or at least in BH_3. In the case of BH_3, one $[\pi]$ electron can be withdrawn from the B−H bonding and put into the vacant low energy $[\sigma]$ state (cf. 5*a*). Then it is capable of forming a strong $[\sigma+\sigma]$ B−B bond with another BH_3 in the same condition, so that there is no net change in number of bonds in going from 2 BH_3 to B_2H_6. With NH_3, however, there is no excited state of as low energy as the ^3E of (5*a*) for BH_3. The lowest excited state is probably $[\sigma]^{-1}3s$, $^3A_1$ (cf. VII of this series). Here, to be sure, there is a certain advantage over the BH_3 case in that the $[\sigma]$ electron excited is of little value for the N−H bonding, but this is balanced by the fact that the $(3s+3s)$ N−N bond, which the excited 3ξ electrons of two $[\sigma]^{-1}3s$ molecules of NH_3 could form, would be very weak.

The present method is in general agreement with the conclusion of Sidgwick[2] that in B_2R_6, one R on each B is held by a one-electron bond, the others by ordinary electron-pair bonds. Nevertheless the description in terms of one-electron bonds tends to be rather misleading (cf. Pauling[2]) unless one thinks of each such bond as circulating exceedingly rapidly among the three R's, so that no one of them is disfavored. The present method, by describing the situation in a way which does not require the localization of bonding electrons between particular atom-pairs, makes this point clear at once. Thus it shows that in each BR_3 in B_2R_6 there are five B−R bonding electrons shared equally by three R's if the latter are alike, or nearly equally if they are not too unlike.

The present method shows that it is not correct, even in a molecule such as $(CH_3)_2BH \cdot BH(CH_3)_2$, to suppose that, e.g., the CH_3 radicals are held by electron-pair bonds and the H atoms by one-electron bonds. On the contrary, it shows that the five bonding electrons within each group $(CH_3)_2BH$ must be distributed fairly equally in the service of the B−H and the two B−C bonds, i.e., one may speak of a 5/3-electron bond to each C and to the H. This does not of course imply that the *strength* of the B−H bond is precisely the same as that of the two B−C bonds, but only that the distribution of bonding electricity is fairly symmetrical with respect to these three bonds.

To make the matter clearer, it may be advisable to give the electronic structure of $B_2H_2(CH_3)_4$. Assuming the substance to be diamagnetic, the normal state should be closely analogous to B_2H_6, which is given essentially by $^1A_{1g}$ of (1). The structure may be written approximately, omitting 1*s* electrons, as

$$[sa_1]^{2\times4}[s]^2 \quad [s]^2 \quad [\pi e]^{4\times4}[\sigma+\sigma]^2 \; [\pi]^3 \; [\pi]^3, \; {}^1A. \qquad (11)$$
$$CH_3 \; BHC_2 \; BHC_2 \quad CH_3 \; B-B \; BHC_2 \; BHC_2$$

Since the molecule as a whole, as well as the $(CH_3)_2BH$ groups within it, are probably without symmetry, the usual representation symbols have been omitted, except those for the orbitals $[sa_1]$ and $[\pi e]$ of the four CH_3 radicals. In (11), the orbital $[s]$ within each $BH(CH_3)_2$ connects the B with the H and the two C's, just as in B_2H_6 the $[sa_1]$ of each BH_3 connects the B with the three H's. Similarly, the $[\pi]$'s of the $BH(CH_3)_2$ also connect the B with the H and two C's. Thus the substitution of the four CH_3's for H's does not essentially alter the bonding action of the B atom. (Cf. discussion in VII and others of this series in regard to minor complications caused by substitutions.)

If we consider the series B_2H_6, $\cdots$, $B_2H_2(CH_3)_4$, $B_2(CH_3)_6$, we have evidently an increasing tendency to split at the B—B bond, a tendency which is actually realized in the last compound. This can be understood if the effective strength of the B—C $[\pi]$ bonds in $B_2(CH_3)_6$ is slightly greater than that of the B—B bond, so that the molecule splits, but that in B_2H_6 the effective strength is appreciably weaker for the $[\pi]$ bonds than for the B—B bond. Similarly the nonoccurrence of B_2Cl_6 suggests greater effective strength for B—Cl bonds of $[\pi]$ type than for B—B bonds. Can these variations be understood?

In the first place, we recall (see above), that the *effective* strengths of bonds are often affected by more or less accidental minor factors which may turn the scales one way or the other. It would hardly be possible without detailed analysis and computation to estimate the net effect of all such minor factors. We may nevertheless ask if there are any obvious new factors which enter when CH_3 or Cl is substituted for H, and which would tend to produce a relative decrease in the effective strength of the B—B bond. Of course for one thing, the B—C and B—Cl $[\pi]$ bonds might directly be stronger than the B—H $[\pi]$ bond, but this is not easily proved or disproved theoretically.

Another possibility is a sort of "steric hindrance,"—not to be interpreted too literally, however. In $(CH_3)_3B$, each CH_3 radical contains a set of closed shells $1s^2[s]^2[\pi]^4$,—cf. (11). If the closed shells, particularly the $[\pi]$ shells, of the CH_3 groups attached to one B atom came too close to those attached to a second B atom in a molecule $(CH_3)_3BB(CH_3)_3$, a considerable repulsion would result which has no counterpart in B_2H_6. This might be a sufficient factor, especially if, for the strongest B—B bonding, the BH_3 or BC_3 pyramids in B_2H_6 or $B_2(CH_3)_6$ are relatively flat, to throw the balance of stability in favor of 2 $B(CH_3)_3$.

When Cl is substituted for CH_3, there is a set of closed shells, $\cdots s^2p\pi^4$ for each Cl atom, analogous to $\cdots [s]^2[\pi]^4$ of the CH_3 radicals. Since it has been possible to carry Cl substitution in B_2H_6 probably only as far as B_2H_5Cl, while CH_3 substitution has been carried as far as $B_2H_2(CH_3)_4$, it would appear that the Cl atom closed shell repulsions are even more potent than those of CH_3 radicals.[11] However, there are also other possibilities. In fact there is one very definite factor tending to stabilize molecules like BCl_3, which can hardly be so effective for $B(CH_3)_3$. This factor is a bonding action which should exist between the B atom and the three $(p\pi)^4$ shells of the Cl atoms. Such action is completely analogous to a similar action in the molecules $BO_3^{=}$, $CO_3^{=}$, NO_3^{-}, SO_3, etc., and which may be considered as a determining factor for the stability of the latter. This action, which may be called "cap-bonding," has been mentioned briefly in the end of I and in II (p. 56) of this series, and will be discussed more fully in a later paper.

Whatever may be the detailed explanations, it can be predicted that energy level diagrams similar to Fig. 1 are applicable to all molecules BR_3 and B_2R_6, with changes only in the relative positions and spacings of the energy levels. Strong cap-bonding would raise very considerably, relative to the normal level of BR_3, the energies of the B_2R_6 and the excited BR_3 levels which correspond to levels in Fig. 1. If the form B_2R_6 is the stable form, that means that the lowest energy on the diagram is that of some B_2R_6 level,

[11] In conversation, Dr. A. B. Burg has informed the writer of unpublished evidence tending to indicate the existence of higher chlorine derivatives, presumably including $B_2H_4Cl_2$ at least.

probably a $^1A_{1g}$ as in Fig. 1 in most if not all cases. A study of magnetic properties of various B_2R_6 at various temperatures would help to decide this.

If 2 BR_3 is more stable than B_2R_6, this means that the lowest B_2R_6 energy is close to or higher than the energy of 2 BR_3. In case the difference is not large, as is probably often true, then, if it is feasible to heat the substance sufficiently, a fraction of the molecules should go over into (one or more of the states of) B_2R_6. Similarly on heating a substance of the type B_2R_6, a fraction of the molecules should of course go over into BR_3. Other fractions should also go into some of the low excited states of B_2R_6 appearing in Fig. 1. Since some of these are paramagnetic, the substance should begin to show paramagnetism if the temperature can be raised sufficiently without decomposition.

Measurements of magnetic susceptibilities of substances of the B_2R_6 and even perhaps some of those of the BR_3 type (e.g., B $(CH_3)_3$) should give interesting results, especially if temperatures can be raised. Studies leading to determinations of the splitting energies of B_2R_6 into 2 BR_3 would naturally also be of interest. An investigation of the photographic infrared absorption spectrum of B_2H_6, in order to look for the probably expected $^1A_{1g} \rightarrow {}^1E_u$ bands, is being undertaken at this University.

The writer is indebted to Professor H. I. Schlesinger and Dr. A. B. Burg for helpful and interesting discussions.

OCTOBER, 1935 JOURNAL OF CHEMICAL PHYSICS VOLUME 3

The Structure of Potassium Hexachlorothalliate Dihydrate

J. L. HOARD AND LEONARD GOLDSTEIN, *Department of Chemistry, Stanford University*

(Received July 22, 1935)

Potassium hexachlorothalliate dihydrate is shown from x-ray data to possess a body centered tetragonal unit of structure with $a_0 = 15.841 \pm 0.020$A, $c_0 = 18.005 \pm 0.020$A containing 14 $K_3TlCl_6 \cdot 2H_2O$. A structure with nineteen determinable parameters is developed from $D_{4h}^{17} - I\,4/mmm$, and accounts satisfactorily for observed intensity data. $TlCl_6^{3-}$ ions occur as well-defined groups. 24 of the 42 K^+ ions are closely surrounded by 8 Cl^-, 16 K^+ by 7 Cl^- and 2 H_2O, and the remaining 2 K^+ by 6 H_2O; these $K(H_2O)_6^+$ groups are situated in regions of definitely negative potential. The structure is very compact, but has quite satisfactory interatomic distances throughout. The evidence from this and from a previous structural determination of $Cs_3Tl_2Cl_9$ shows that thallic thallium tends to form six stable covalent bonds with chlorine with a Tl-Cl separation of about 2.55A, in agreement with the covalent radii of Pauling and Huggins. It is shown also that a compound of empirical formula $Rb_3TlBr_6 \cdot (8/7)H_2O$ probably possesses essentially the same type of structure as $K_3TlCl_6 \cdot 2H_2O$; dimensional relations in the bromothalliate permit the alkali ions of 2(*b*) to coordinate eight rather than six molecules of water.

INTRODUCTION

THE coordination and bonding properties of such heavy metal forming elements as thallium and lead, lying in the B subgroups of the periodic system, have as yet been comparatively little studied. With a view toward elucidating the characteristic structural properties of trivalent thallium, we have undertaken x-ray studies of a number of its complex salts. The results of one such investigation, dealing with cesium enneachlorodithalliate, $Cs_3Tl_2Cl_9$, have already been reported;[1] we describe in the present paper the structure of potassium hexachlorothalliate dihydrate, $K_3TlCl_6 \cdot 2H_2O$, and summarize briefly our present knowledge of the structural properties of thallic thallium.

Good crystals of $K_3TlCl_6 \cdot 2H_2O$, from one to two mm on an edge, were prepared without difficulty according to the directions of Meyer.[2] In habit and in general appearance the crystals seemed to agree closely with the description of Groth,[3] who lists them as tetragonal bipyramidal, $c/a = 0.7913$. Laue and oscillation photographs were used as a source of x-ray data.

DETERMINATION OF THE STRUCTURE

The smallest tetragonal unit of structure is one with $a_0 = 15.841 \pm 0.020$A, $c_0 = 18.005$

[1] Hoard and Goldstein, J. Chem. Phys. **3**, 199 (1935).

[2] Meyer, Zeits. f. anorg. allgem. Chemie **24**, 321 (1900).

[3] Groth, Chemische Krystallographie, Engelmann, Leipzig, **1**, 424 (1908).

± 0.020A, $c_0/a_0 = 1.137$, to be compared with $\sqrt{2} \cdot 0.7913 = 1.119$. This unit accounts for both the oscillation and the numerous Laue data, and may be confidently accepted as the true one.

All of the x-ray data agree with a body centered lattice; the unit must then contain an even number of molecules. Placing 14 $K_3TlCl_6 . 2H_2O$ within a unit of this size leads to a calculated density of 2.89 g/cm³, whereas the reported density[4] is 2.859 g/cm³, and our experimentally determined value, using the flotation method, is 2.90 ± 0.10 g/cm³. We conclude, therefore, that the body centered unit contains fourteen, and a primitive unit contains the rather extraordinary number of seven molecules of $K_3TlCl_6 . 2H_2O$. This conclusion is supported also by x-ray and density data obtained from the apparently isomorphous compound, $Rb_3TlBr_6 . (8/7)H_2O$, which we discuss briefly in the last paragraph of this section.

The symmetry indicated by the x-ray data is that of D_4^h. All space groups based upon a body centered lattice with special criteria which could give rise to x-ray data of this symmetry are eliminated by the appearance of "forbidden" reflections.[5] We assume the holohedral space group, $D_{4h}^{17} - I\,4/mmm$, in preference to the remaining possibilities which lack centers of symmetry since (1) the face development of the crystals is in agreement with this view, and (2) an experiment designed to test for pyroelectricity performed[6] upon a rather large specimen of $Rb_3TlBr_6 . (8/7)H_2O$ gave a negative result.

Within the tetragonal cell we must place 14 Tl, 42 K, 84 Cl, and 28 O; evidently we must deal with a many-parameter structure. We find, however, that the x-ray data suffice to fix the positions of thallium, following which the introduction of a few reasonable assumptions suggested by chemical and structural considerations permits of the complete elucidation of a structure which leads to satisfactory agreement between calculated and observed intensities of x-ray reflections.

Without giving the argument in detail, the relatively very strong intensities observed for all reflections from (001) and (100) with $n/4$ integral seem to require the following arrangement[7] of thallium atoms: 2 Tl in $2(a)$, 000; etc., 4 Tl in $4(c)$, $0\frac{1}{2}0$, $\frac{1}{2}00$; etc., 8 Tl in $8(f)$, $\frac{1}{4}\frac{1}{4}\frac{1}{4}$; $\frac{1}{4}\frac{3}{4}\frac{1}{4}$; $\frac{3}{4}\frac{1}{4}\frac{1}{4}$; $\frac{3}{4}\frac{3}{4}\frac{1}{4}$, etc. Except for the unoccupied positions $00\frac{1}{2}$; $\frac{1}{2}\frac{1}{2}0$, the thallium atoms are arranged at the points of a body centered tetragonal lattice with $a_0' = (15.84/2)$A, $c_0' = (18.005/2)$A.

The ratio of the univalent radii,[8] $r_{Tl^{+++}}/r_{Cl^-}$, is 0.635, indicating a coordination number toward chlorine for thallium of six, or possibly of eight. The symmetry of the positions in question in every case rules out the structurally improbable coordination number of seven. The thallium atoms are placed too far apart to permit of sharing of polyhedron elements, so that a coordination number of eight can occur throughout only if water in addition to chlorine is coordinated. Symmetry requirements make this at least very improbable, and the evidence strongly indicates that $TlCl_6^{3-}$ octahedra are structural units.

In $Cs_3Tl_2Cl_9$, thallium shows a coordination number toward chlorine of six. The existence of the $Tl_2Cl_9^{3-}$ complex together with the Tl−Cl separations which are found therein seem to show definitely that the Tl−Cl linkage is primarily covalent rather than ionic in character. In $K_3TlCl_6 . 2H_2O$ we assume the existence of regular $TlCl_6^{3-}$ octahedra with Tl−Cl = 2.55A. This is obtained by adding the "octahedral" radius[9] of Tl^{III} to the "normal" radius of Cl; this value we regard as more reliable than either of the experimentally determined values, 2.54 and 2.66A, obtained from $Cs_3Tl_2Cl_9$, because of the shared face in the $Tl_2Cl_9^{3-}$ complex. The sum of the ionic radii, 2.76A, is 0.21A larger than the covalent Tl−Cl separation which we use here.

The $TlCl_6^{3-}$ octahedra of $2(a)$ and $4(c)$ are required by the symmetry of those positions to assume one of two discrete orientations which differ by a rotation of 45° about c. The octahedra of $8(f)$ may in addition have an arbitrary rotation about the twofold axes which are perpendicular to {110}. These restrictions are sufficient to permit us to select reasonable positions not only

[4] Int. Crit. Tab. **1**, 156 (1926).
[5] Astbury and Yardley, *Tabulated Data for the Examination of the 230 Space Groups by Homogeneous X-Rays*, Phil. Trans. **224**, 221–57 (1924).
[6] See A. J. P. Martin, Min. Mag. **22**, 519 (1931).
[7] R. W. G. Wyckoff, *The Analytical Expression of the Results of the Theory of Space Groups*, second edition (Carnegie Inst. of Wash., 1930), p. 99.
[8] Linus Pauling, J. Am. Chem. Soc. **49**, 765 (1927).
[9] Pauling and Huggins, Zeits. f. Krist. **87**, 205 (1934).

for the potassium ions but also for the water molecules, leading ultimately to the complete determination of the structure. The parameter values given are the result of careful consideration of the many interatomic distances involved, and lead to satisfactory agreement between calculated and observed intensities.

The octahedra with centers in 2(*a*) have
4 Cl_I in 4(*e*): 00*u*; etc., with $u_I = 0.142$.
8 Cl_{II} in 8(*i*): *u*00; etc., with $u_{II} = 0.161$.
The octahedra with centers in 4(*c*) have
8 Cl_{III} in 8(*g*): $0\frac{1}{2}u$; etc., with $u_{III} = 0.142$.
16 Cl_{IV} in 16(*l*): *uv*0; etc., with $u_{IV} = 0.386$, $v_{IV} = 0.114$.
The octahedra with centers in 8(*f*) have
16 Cl_V in 16(*m*): $u\bar{u}v$; etc., with $u_V = 0.181$, $v_V = 0.362$.
16 Cl_{VI} in 16(*m*): $u\bar{u}v$; etc., with $u_{VI} = 0.160$, $v_{VI} = 0.163$.
16 Cl_{VII} in 16(*k*): *u*, $u+\frac{1}{2}$, $\frac{1}{4}$; etc., with $u_{VII} = 0.364$.
Potassium positions are
2 K_I in 2(*b*): $00\frac{1}{2}$; $\frac{1}{2}\frac{1}{2}0$.
8 K_{II} in 8(*h*): *xx*0; etc., with $x_{II} = 0.214$.
16 K_{III} in 16(*n*): 0*xy*; etc., with $x_{III} = 0.295$, $y_{III} = 0.132$.
16 K_{IV} in 16(*n*): 0*xy*; etc., with $x_{IV} = 0.293$, $y_{IV} = 0.376$.
Oxygen positions are
4 O_I in 4(*e*): 00*t*; etc., with $t_I = 0.347$.
8 O_{II} in 8(*j*): $s0\frac{1}{2}$; etc., with $s_{II} = 0.173$.
16 O_{III} in 16(*n*): 0*st*; etc., with $s_{III} = 0.157$, $t_{III} = 0.276$.
The structure is seen to have nineteen determinable parameters.

In Table I we present the comparison between calculated and visually estimated intensities for several groups of reflections. The *f* values employed are those of Pauling and Sherman.[10] No correction is included either for the decrease in intensity arising from the thermal vibrations of the atoms within the lattice or for absorption by the crystal; the latter is large enough so that only reflections with quite substantial structure factors are observed.

The agreement between calculated and observed intensities is quite generally satisfactory. For a structure of this complexity the calculated intensities are not much affected by rather substantial variations in the positions of the lighter atoms. We shall show, however, that this atomic arrangement is structurally very satisfactory; this fact together with the intensity data make it highly probable that the suggested structure is the true one.

One point about the intensity comparisons seems worthy of special mention. We notice that reflections from (001) and (100) with $n/4$ half-integral, e.g., (006) and (0·0·14), are observed to be weaker relative to reflections with $n/4$ integral than a comparison of their calculated intensities would indicate. The structure factor contains $14f_{Tl}$ for $n/4$ integral, but only $2f_{Tl}$ for $n/4$ half-integral; the main contributions to $S_{(006)}$ and $S_{(0\cdot0\cdot14)}$ are from chlorine and potassium. The decrease in atomic scattering powers arising from thermal agitation is very large for this structure, and, moreover, evidently should be much more marked for potassium and chlorine than for thallium atoms. Apparent discrepancies of the type observed are thus to be anticipated.

TABLE I. *Comparison of calculated with observed intensities.**

(*hkl*)	Intensity Observed	Intensity Calculated	(*hkl*)	Intensity Observed	Intensity Calculated
002	<1	0.35	800	12	19.1
004	6	7.5	10·0·0	<1	3.9
006	3	7.5	12·0·0	4	7.6
008	45	60.0	14·0·0	0	2.2
0·0·10	0	0.1	16·0·0	2	8.2
0·0·12	6	11.3	18·0·0	0	2.0
0·0·14	<1	4.4	20·0·0	1	5.8
0·0·16	7	18.0	101	†	0.10
0·0·18	0	0.3	202	8	9.7
0·0·20	2	6.7	303	0	0.01
0·0·22	0	2.4	404	<1	0.73
0·0·24	2	8.9	505	0	0.07
0·0·26	0	0.03	606	4	13.0
0·0·28	0	4.4	707	0	0.42
200	<1	0.21	808	3	10.4
400	8	12.6	909	0	0 04
600	4	18.7	10·0·10	1.5	5.0

* Temperature factor not included.
† Not observed.

Crystals of $Rb_3TlBr_6 \cdot (8/7)H_2O$ were prepared according to the directions of Pratt.[11] Laue and oscillation data show the unit cell to be body centered tetragonal with $a_0 = 16.95$, $C_0 = 19.45$A, about, with D_{4h}^{17} as the probable space group. With 14 $Rb_3TlBr_6 \cdot (8/7)H_2O$ within the unit cell, the calculated density is 3.97 g/cm³, to be compared with the experimental[4] value 4.07 g/cm³. Upon the basis of quite meager analytical data, Pratt assigns the formula $Rb_3TlBr_6 \cdot H_2O$ to this compound, requiring the placing of 14 H_2O within the unit cell. Since his analysis actually indicates a somewhat higher proportion of water, and since, moreover, symmetry conditions do not permit of the placing of 14 H_2O within the structure which we have developed, we have decided

[10] Pauling and Sherman, Zeits. f. Krist. **81**, 1 (1932).

[11] J. H. Pratt, Am. J. Sci. **149**, 397 (1895).

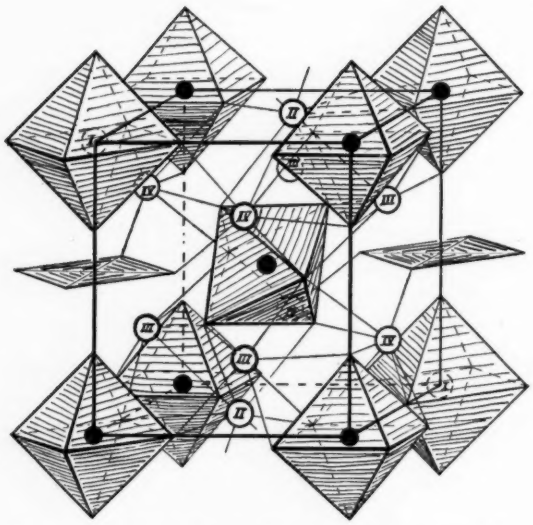

FIG. 1. One-eighth of the tetragonal unit cell of $K_3TlCl_6 \cdot 2\ H_2O$. Thallium atoms are represented by closed blackened circles at the centers of octahedra whose vertices show the positions of chlorine atoms. Potassium ions are represented by open circles, the two larger octahedra being $K(H_2O)_6^+$. Water molecules of 16(n) are represented by the corners of the two squares (shown in perspective). Crystallographically distinct kinds of potassium ions and their coordination properties are indicated, respectively, by the attached labels and by the lines connecting circles with vertices of various polyhedra.

that the unit cell contains 16 H_2O (or perhaps more). This is discussed in detail later.

Using regular $TlBr_6^{3-}$ octahedra with a Tl–Br separation of 2.70A, the following assignment of parameter values leads to generally satisfactory interatomic distances:

The octahedra with centers in 2(a) have
4 Br_I in 4(e): $00u$; etc., with $u_I = 0.139$.
8 Br_{II} in 8(i): $u00$; etc., with $u_{II} = 0.159$.
The octahedra with centers in 4(c) have
8 Br_{III} in 8(g): $0\frac{1}{2}u$; etc., with $u_{III} = 0.139$.
16 Br_{IV} in 16(l): $uv0$; etc., with $u_{IV} = 0.387$, $v_{IV} = 0.113$.
The octahedra with centers in 8(f) have
16 Br_V in 16(m): $u\bar{u}v$; etc., with $u_V = 0.181$, $v_V = 0.360$.
16 Br_{VI} in 16(m): $u\bar{u}v$; etc., with $u_{VI} = 0.161$, $v_{VI} = 0.165$.
16 Br_{VII} in 16(k): u, $u+\frac{1}{2}$, $\frac{1}{4}$; etc., with $u_{VII} = 0.363$.
Rubidium positions are
2 Rb_I in 2(b): $00\frac{1}{2}$; $\frac{1}{2}\frac{1}{2}0$.
8 Rb_{II} in 8(h): $xx0$; etc., with $x_{II} = 0.214$.
16 Rb_{III} in 16(n): $0xy$; etc., with $x_{III} = 0.295$, $y_{III} = 0.132$.
16 Rb_{IV} in 16 (n): $0xy$; etc., with $x_{IV} = 0.293$, $y_{IV} = 0.366$.
Oxygen positions are
16 O_I in 16(n): $0st$; etc., with $s_I = 0.122$, $t_I = 0.400$.

Our intensity data are inadequate to permit of the detailed testing of this structure through a comparison of calculated and observed intensities of x-ray reflections.

Discussion of the Structure

The essential nature of the structure can be readily understood by reference to a pseudo unit (Fig. 1) of 1/2 the axial lengths and 1/8 the volume of the true tetragonal cell. Each face of this prism lies in a plane of symmetry; the other seven parts of the true unit may then be visualized without difficulty.

This pseudo unit, containing $1\frac{3}{4}$ molecules, is comparable with the two molecule body centered tetragonal unit of the ammonium fluoferrate structure.[12]

In the $K_3TlCl_6 \cdot 2\ H_2O$, as opposed to the $(NH_4)_3FeF_6$ structure, two octahedra [2(b)] are missing, two octahedra [2(a)] are rotated through 45° about c, and 8 octahedra are rotated through 37.5° about the twofold axes perpendicular to {110}. The coordination around potassium ions in $K_3TlCl_6 \cdot 2\ H_2O$ is very different from that around the analogous ammonium ions in $(NH_4)_3FeF_6$. Whereas in the latter structure $\frac{2}{3}$ of the NH_4^+ ions are closely surrounded by 12 F^- and the remaining $\frac{1}{3}$ by only 6 F^-, in $K_3TlCl_6 \cdot 2H_2O$ 24 of the 42 K^+ ions are closely surrounded by 8 Cl^-, 16 K^+ by 7 Cl^- and 2 H_2O, and the remaining 2 K^+ by 6 H_2O. The structural relations to their surroundings of 40 of the 42 K^+ ions are entirely satisfactory, and, although less

TABLE II. *Interatomic distances in $K_3TlCl_6 \cdot 2\ H_2O$.*

Atom	Neighbors	Separation	Atom	Neighbors	Separation
K_I	2 O_I, 4 O_{II}	2.75A	K_{IV}	1 O_{II}	2.90A
K_I	8 O_{III}	4.73	K_{IV}	1 O_{III}	2.80
K_I	8 Cl_V	4.75	Cl_I	4 Cl_{VI}	3.60
K_I	8 K_{IV}	5.15	Cl_I	4 O_{III}	3.46
K_{II}	2 Cl_{II}	3.49	Cl_{II}	4 Cl_{VI}	3.94
K_{II}	2 Cl_{IV}	3.16	Cl_{II}	2 Cl_{IV}	4.00
K_{II}	2 Cl_V	3.42	Cl_{III}	1 Cl_{III}	3.90
K_{II}	2 Cl_{VI}	3.18	Cl_{III}	4 Cl_{VII}	3.62
K_{III}	1 Cl_{II}	3.20	Cl_{IV}	2 Cl_V	4.20
K_{III}	1 Cl_{III}	3.26	Cl_{IV}	2 Cl_{VI}	4.80
K_{III}	2 Cl_{IV}	3.31	Cl_{IV}	2 Cl_{VII}	4.60
K_{III}	2 Cl_{VI}	3.34	Cl_V	2 O_{II}	3.80
K_{III}	2 Cl_{VII}	3.21	Cl_V	2 O_{III}	3.28
K_{IV}	1 Cl_{III}	3.29	Cl_{VI}	2 O_{III}	3.25
K_{IV}	2 Cl_{IV}	3.23	Cl_{VII}	1 Cl_{VII}	3.96
K_{IV}	2 Cl_V	3.37	O_I	4 O_{II}	3.90
K_{IV}	2 Cl_{VII}	3.31	O_I	4 O_{III}	2.80

[12] R. W. G. Wyckoff, *The Structure of Crystals*, second edition (Chemical Catalog Co., New York, 1931), p. 307.

favorably placed, the remaining 2 K^+ are also in regions of negative potential. Each K^+ of 2(*b*) is surrounded by 6 H_2O at 2.75A, 8 H_2O at 4.73A, 8 Cl^- at 4.75A, 8 K^+ at 5.15A, and 10 Cl^- at still larger distances.

Our assignment of parameter values necessarily places each Tl at the center of a regular $TlCl_6$ octahedron with Tl−Cl=2.55A, Cl−Cl=3.61A. The closest distance of approach of two thallium atoms is 7.17A. All other interatomic distances which bear directly upon the question of the stability of this structure are given in Table II.

The K−Cl separation varies from 3.16 to 3.49 with an average value of 3.30A, closely that to be expected for a coordination number of eight. Other interatomic distances are in equally good agreement with theory and past experience. Considered as a whole, the most striking feature of the structure is its compactness. Having first adjusted the values of potassium and chlorine parameters so as to make all K−Cl separations satisfactory, it turns out that the potassium ions of 2(*b*) can coordinate no more than 6 H_2O, and, moreoever, that the 28 H_2O can be placed in only one way; there is no room in the structure for additional water. The apparently accurate chemical analysis[2] is entirely consistent with this finding.

Since dimensional relations within the structure permit the coordination of no more than 6 H_2O by K^+, we may not conclude that this represents the normal degree of hydration of the potassium ion. In general, and especially in the crystalline state, a higher degree of hydration is to be anticipated.

The assumption of regular $TlCl_6^{3-}$ octahedra with Tl−Cl=2.55A leads to Cl−Cl=3.61A, just the ionic diameter of Cl^-. Small departures from regularity in the octahedra, not materially affecting interatomic distances throughout, are not improbable.

If the Tl−Cl separation were from 0.1 to 0.2A larger than that assumed, we should find the problem of adjusting parameter values so as to obtain generally satisfactory interatomic distances definitely embarrassing, and probably impossible. As already pointed out,[1] the existence in $Cs_3Tl_2Cl_9$ of $Tl_2Cl_9^{3-}$ double octahedra with shared faces constitutes convincing evidence that the bond type is largely covalent rather than ionic in character. The structures of both $Cs_3Tl_2Cl_9$ and $K_3TlCl_6 . 2\ H_2O$ indicate that thallic thallium tends to form six stable covalent bonds with chlorine. It is probable that the Tl−Cl separation in the $TlCl_6^{3-}$ group does not vary from the value 2.55A by more than a few hundredths of an Angstrom unit.

Values of the Rb−Br separation in $Rb_3TlBr_6 . (8/7)H_2O$ range from 3.40 to 3.70A, the average being 3.54A. The only critical contacts between bromine atoms of different octahedra are 3.90A for $Br_I - Br_{VI}$ and 3.93A for $Br_{IV} - Br_{VII}$, to be compared with 3.90A for the ionic diameter. In $K_3TlCl_6 . 2\ H_2O$ it is dimensionally impossible for the potassium ions of 2(*b*) to coordinate more than 6 H_2O, but in the bromothalliate each rubidium of 2(*b*) can coordinate at least 8 H_2O. We find $Rb_I - O_I = 2.86$A, $Rb_{IV} - O_I = 2.97$A, $O_I - O_I = 2.92$ and 3.89A, $O_I - Br_V = 3.31$A. With some variations from the parameter values given, it might be possible to add either 4 H_2O in 4(*e*) or 8 H_2O in 8(*h*) to give rubidium effectively a coordination number of either ten or twelve, respectively. The latter possibility appears the more probable from a dimensional standpoint.

Except for the degree of hydration of the alkali ions of 2(*b*), crystals of $K_3TlCl_6 . 2\ H_2O$ and $Rb_3TlBr_6 . (8/7)H_2O$ are truly isomorphous.

LETTERS TO THE EDITOR

This section will accept reports of new work, provided these are terse and contain few figures, and especially few halftone cuts. The Editorial Board will not hold itself responsible for opinions expressed by the correspondents. Contributions to this section must reach the office of the Managing Editor not later than the 15th of the month preceding that of the issue in which the letter is to appear. No proof will be sent to the authors. The usual publication charge ($3.00 per page) will not be made and no reprints will be furnished free.

The Structure of Cyanuric Triazide

Some months ago I published in this Journal[1] a description of a crystal structure for cyanuric triazide which was based upon visual estimates of the x-ray reflection intensities. Since there were ten parameters to evaluate, a Fourier method was used although such a procedure is not customary when quantitative measurements are not available. Approximations and graphical methods were introduced to reduce the labor of the method to a level warranted by the accuracy of the data. The limit of error placed upon the resulting parameters was consequently large compared with that usually ascribed to Fourier analyses. It was estimated from the agreement between calculated and estimated structure factors that the average error would not exceed one-one hundredth of the edge of the unit cell *a*.

Miss I. E. Knaggs has now published[2] details of her very careful examination of the same crystal, including a Fourier analysis based upon absolute quantitative measurements. In recent letters[3] Miss Knaggs has pointed out the differences between our structures. I should like to point out that my parameters agree with Miss Knaggs' more accurate ones within the limits cited in my paper, as is shown by Table I. Column 1 indicates the parameters using Miss Knaggs' atomic designations. The second column gives her parameters reduced to fractions of the cell edge while the third gives my corresponding values. The final column records the differences. It will be observed that the average value is considerably less than 0.010 and that only one difference is notably greater than 0.010.

It would seem that my structure was sufficiently accurate for the purpose at hand, which was to confirm the chain form found for the azide group by Brockway and Pauling.

Comparison of my estimated structure factors with the quantitative measurements shows that as relative values they are not excessively bad. The average difference for seventy-five reflections was found to be about 16 percent. It is my opinion that the differences in results are due more to my omission of less important Fourier amplitudes than to errors in estimating the amplitudes and that my data really warranted more careful analysis than I thought appropriate at the time. If all observed reflections had been included in the Fourier series it is probable that the accuracy obtained would have been sufficient for most purposes and I feel that one would be justified in repeating this qualitative method for similar structures if quantitative measurements could not be made. I am not so certain however how valuable such an analysis would be in locating atoms of low atomic number in crystals containing heavy atoms or in locating the centers of atoms which "overlap" badly in the projection.

TABLE I.

Atom		K	H	Δ
x	A	0.214	0.208	0.006
	B	.386	.385	.001
	C	.458	.455	.003
	D	.342	.325	.017
	E	.242	.240	.002
y	A	.485	.480	.005
	B	.552	.560	.008
	C	.442	.433	.009
	D	.281	.270	.011
	E	.137	.125	.012
				Mean .0074

EDWARD W. HUGHES

Cornell University,
Ithaca, N. Y.,
August 21, 1935.

[1] Hughes, J. Chem. Phys. **3**, 1 (1935).
[2] Knaggs, Proc. Roy. Soc. **A150**, 576 (1935).
[3] Knaggs, Nature **135**, 268 (1935); J. Chem. Phys. **3**, 241 (1935).

Raman Spectrum of Methyl Deuteride

We report on the vibrational frequencies of CH_3D observed in the Raman effect. A theory of the isotope effect for such pentatomic molecules has been developed by Rosenthal[1] in terms of a five constant potential energy function. Dennison and Johnston[2] using the observed frequencies of CH_4[3,4] and the value of the rotational-vibrational interaction[5] have calculated the five force constants of the Rosenthal development, and the normal frequencies of the four deutero-methanes. Barker and Ginsburg[6] have observed the infrared absorption spectrum of CH_3D.

The methyl deuteride was prepared from methyl iodide and pure deuterium oxide with an aluminum-mercury couple. CH_3I and D_2O were vacuum distilled on to dry aluminum-mercury couple. The mixture was then allowed

TABLE I.

Molecule	Vibration[8]	Calculated	Observed	Intensity	Differences
CH_4	ω_1	2914.8[4]	2914.2	4	− 0.6
CH_3D	ω_{4ab}	1300	1330.1	2	+30.1
	ω_{3ab}	2183	2199.0	2	+16.0
	$2\omega_{4c}$	2302	2314.8	10	+12.8
	$2\omega_2$	2920	2921.7	4	+ 1.7

to heat up and react until the pressure was atmospheric. At this point, the gas was bled off and collected over mercury. This method produces 10–15 percent D_2. The small amount of CH_4 evidently present may come from exchange or adsorbed H_2 on the couple. The Raman spectrum was obtained at a pressure of three atmospheres using Hg2537 as the exciting line.[7] Exposure time was 120 hours. Four vibrational lines of CH_3D and one of CH_4 were obtained. Their values in cm^{-1} in vacuum and a comparison with the calculated values of Dennison and Johnston[2] are given in Table I. No rotational structure was observed.

GEORGE E. MACWOOD
H. C. UREY

Department of Chemistry,
Columbia University,
August 29, 1935.

[1] J. Rosenthal, Phys. Rev. **45**, 538 (1934).
[2] D. Dennison and M. Johnston, Phys. Rev. **47**, 93 (1935).
[3] J. Cooley, Astrophys. J. **62**, 73 (1925).
[4] Dickinson, Dillon and Rasetti, Phys. Rev. **34**, 582 (1929).
[5] E. Teller, Hand- und Jahrbuch d. Chem. Physik **9**, 125 (1934).
[6] E. Barker and N. Ginsburg, J. Chem. Phys. **2**, 299 (1934).
[7] Spectrograph and accessories are completely described in a paper by G. Teal and G. MacWood to appear shortly.
[8] J. Rosenthal, Phys. Rev. **46**, 730 (1934).